Voltage Stability Analysis with High Distributed Generation (DG) Penetration

by

Rashid Al-Abri

A thesis
presented to the University of Waterloo
in fulfillment of the
thesis requirement for the degree of
Doctor of Philosophy
in
Electrical and Computer Engineering

Waterloo, Ontario, Canada, 2012

AUTHOR'S DECLARATION

I hereby declare that I am the sole author of this thesis. This is a true copy of the thesis, including any required final revisions, as accepted by my examiners.

I understand that my thesis may be made electronically available to the public.

Abstract

Interest in Distributed Generation (DG) in power system networks has been growing rapidly. This increase can be explained by factors such as environmental concerns, the restructuring of electricity businesses, and the development of technologies for small-scale power generation. DG units are typically connected so as to work in parallel with the utility grid; however, with the increased penetration level of these units and the advancements in unit's control techniques, there is a great possibility for these units to be operated in an autonomous mode known as a microgrid.

Integrating DG units into distribution systems can have an impact on different practices such as voltage profile, power flow, power quality, stability, reliability, and protection. The impact of the DG units on stability problem can be further classified into three issues: voltage stability, angle stability, and frequency stability. As both angle and frequency stability are not often seen in distribution systems, voltage stability is considered to be the most significant in such systems. In fact, the distribution system in its typical design doesn't suffer from any stability problems, given that all its active and reactive supplies are guaranteed through the substation. However, the following facts alter this situation:

- With the development of economy, load demands in distribution networks are sharply increasing. Hence, the distribution networks are operating more close to the voltage instability boundaries.
- The integration of distributed generation in distribution system introduces possibility of encountering some active/reactive power mismatches resulting in some stability concerns at the distribution level.

Motivated by these facts, the target of this thesis is to investigate, analyze and enhance the voltage stability of distribution systems with high penetration of distributed generation. This study is important for the utilities because it can be applied with Connection Impact Assessment (CIA[1]). The study can be added as a complement assessment to study the impacts of the installation of DG units on voltage stability.

In order to accomplish this target, this study is divided into three perspectives: 1) utilize the DG units to improve the voltage stability margin and propose a method to allocate DG units for this purpose, 2) investigate the impact of the DG units on proximity to voltage stability 3) conduct harmonic

[1] Connection Impact Assessment (CIA) assesses the impact of projects on the electrical system, as well as provide the specific details of what is required to connect the projects, how much they will cost and how long they will take to connect.

resonance analysis to visualize the impacts of both parallel and series resonance on the system's stability. These perspectives will be tackled in Chapter 3, Chapter 4, and Chapter 5, respectively.

Chapter 3 tackles placing and sizing of the DG units to improve the voltage stability margin and consider the probabilistic nature of both the renewable energy resources and the load. In fact, placement and sizing of DG units with an objective of improving the voltage stability margin while considering renewable DG generation and load probability might be a complicated problem, due to the complexity of running continuous load flow and at the same time considering the probabilistic nature of the load and the DG unit's resources. Therefore, this thesis proposes a modified voltage index method to place and size the DG units to improve the voltage stability margin, with conditions of both not exceeding the buses' voltage, and staying within the feeder current limits. The probability of the load and DG units are modeled and included in the formulation of the sizing and placing of the DG units.

Chapter 4 presents a model and analysis to study the impact of the DG units on proximity to voltage instability. Most of the modern DG units are equipped with power electronic converters at their terminals. The power electronic converter plays a vital role to match the characteristics of the DG units with the requirements of the grid connections, such as frequency, voltage, control of active and reactive power, and harmonic minimization. Due to the power electronics interfacing, these DG units have negligible inertia. Thus, they make the system potentially prone to oscillations resulting from the network disturbances. The main goal of this chapter is to model and analyze the impact of distributed generation DG units on the proximity of voltage instability, with high penetration level of DG units.

Chapter 5 studies the harmonic resonance due to the integration of DG units in distribution systems. Normally, the harmonic resonance phenomenon is classified as a power quality problem, however, this phenomenon can affect the stability of the system due to the parallel and series resonance. Thus, the main goal of this chapter is to study and analyze the impact of the integration of distributed generation on harmonic resonance by modeling different types of DG units and applying impedance frequency scan method.

Acknowledgements

Firstly, all my gratitude and thanks to Allah almighty who guided and aided me to bring forth this thesis.

I wish to express my deepest thanks and gratitude to my supervisor, Prof. Ehab F. El-Saadany, Department of Electrical and Computer Engineering, University of Waterloo, for his constructive guidance, advice, comments, support and discussions throughout the development of my PhD studies.

I would like to thank my doctoral committee members Prof. Medhat M. Morcos (external examiner), Prof. Ramadan El-shatshat, Prof. Kankar Bhattacharya, and Prof. Jatin Nathwani for their insightful comments and suggestions.

I would like also to thank my colleagues for being extremely supportive. Special thanks goes to Dr. Yasser A.-R Mohamed from University of Alberta, Dr. Yasser Attwa, Eng. Aboelsood Ali Zidan, Dr. Mohammed Albadi and Dr. Mohammed Bait-Suwailam.

Finally, I would like to thank my parents, my wife, and my children for their understanding, encouragement and continuous support

Dedication

To my parents, my wife (Azhaar), and my children

Table of Contents

List of Figures

List of Tables

Chapter 1
Introduction and Objectives

1.1 General

A traditional electrical generation system consists of large power generation plants, such as thermal, hydro, and nuclear. Because these plants are located at significant distances from the load centers, the energy must be transported from the power plants to the loads through transmission lines and distribution systems. These plants, transmission lines, and distribution systems are currently being utilized to their maximum capacity, but the load demand is growing. This increase in load demand requires that new generation power plants be built and that the transmission and distribution systems be expanded, neither of which is recommended from an economic or environmental perspective, especially when many countries are trying to meet the targets set in the Kyoto Protocol in order to reduce greenhouse gas emissions [1, 2]. Therefore, interest in the integration of distributed generation (DG) into distribution systems has been rapidly increasing [3]. Distributed generation is loosely defined as small-scale electricity generation fueled by renewable energy sources, such as wind and solar, or by low-emission energy sources, such as fuel cells and micro-turbines.

DG units are typically connected so that they work in parallel with the utility grid, and they are mostly connected in close proximity to the load. DG units have not so far been permitted without a utility grid. However, the economic advantages of utilizing DG units, coupled with the advancements in techniques for controlling these units, have led to the definite possibility of these units being operated in an autonomous mode, or what is known as a microgrid. Hence, distribution systems with embedded DG units can operate in two modes: grid-connected and autonomous.

In grid-connected mode, although the voltage and frequency are typically controlled by the grid and the DG units are synchronized with the grid, integrating DG units can have an impact on the practices used in distribution systems, such as the voltage profile, power flow, power quality, stability, reliability, and protection. Since DG units have a small capacity compared to central power plants, the impact is minor if the penetration level is low (1%-5%). However, if the penetration level of DG units increases to the anticipated level of 20%-30%, the impact of DG units will be profound. Furthermore, if the DG units operate in autonomous mode, as a microgrid, the effects on power stability and quality are expected to be more dramatic because of the absence of the grid support.

1.2 Research Motivations

With the integration of DG units in distribution systems, these systems are expected to face problems in stability. Some of these problems are as follows:

- Normally, the voltage stability is studied in power system networks (on transmission level). The distribution system in its typical design doesn't suffer from any stability problems, given that all its active and reactive supplies are guaranteed through the substation. However, the integration of distributed generation in distribution systems alters this situation, and introduces some probability of encountering some active/reactive power mismatches resulting in stability concerns at the distribution level. Two types of distributed generation are available: rotary type (directly connected to the grid using induction generators or synchronous generators), and static type (indirect interfacing using power electronics converters). The DG units that are equipped with a directly-connected induction motor can affect the voltage stability margin negatively due to their reactive power consumption. In order to decrease the reactive consumption of these DG units, reactive power compensators (such as a capacitor, with sizes ranging about 1/3 of the DG unit rating) are installed at the terminals of the DG units. However, the reactive power consumption increases due to the increase of the power generation, as can be seen in the Figure 1-1. This increased consumption might result in overloading the system, in turn resulting in a decrease in the voltage stability margin. On the other hand, the DG units that are equipped with converters can have positive impacts on the voltage stability margin of the system, since these DG units can be controlled to operate at unity power or can be adjusted to inject fixed amount of reactive power to the system.

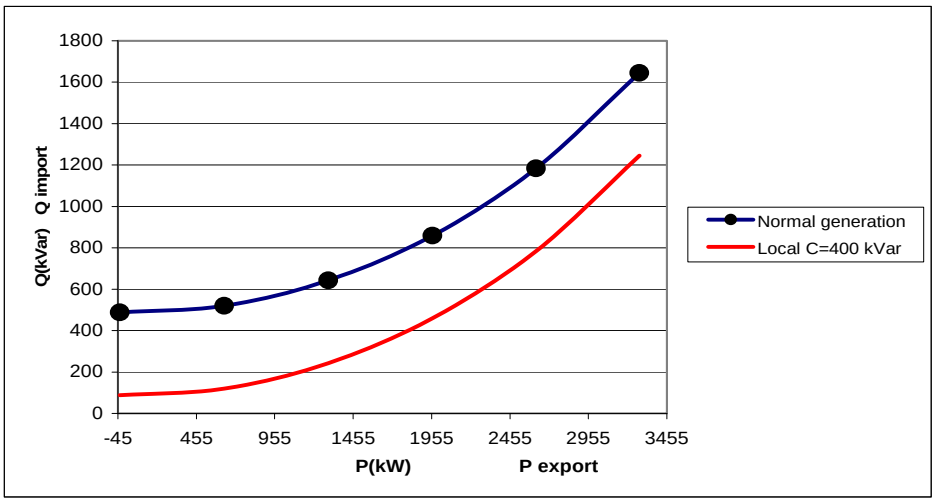

Figure 1- 1:P-Q relation of an induction generator[2]

With the expected high penetration levels of DG units in the distribution system, the investigation of both the DG effects on distribution system's voltage stability, and of the utilization of such units to improve the voltage stability margins, are required. Moreover, in the near future, it is expected to allow parts of the distribution system to operate as isolated microgrids (grid-disconnected mode). This will make the system more prone to voltage instability, compared to grid-connected mode.

- In the near future, it is expected that many power electronic converter-based DG units will make their way into the distribution systems. The power electronic converter plays a vital role to match the characteristics of the DG units and the requirements of the grid connections, such as frequency, voltage, control of active and reactive power, and harmonic minimization. Due to the power electronics interfacing, these DG units have negligible inertia, which makes the system potentially prone to oscillation resulting from the network disturbances. These oscillations could affect system stability.

- The integration of DG units in distribution systems can have impacts on the system power quality, among which harmonic resonance is the most significant. The DG units can have impacts on the system resonance behaviour due to their harmonic injection and due to the

[2]More information can be found in appendix A

changes of the equivalent impedance of the system. In addition, reactive power compensators are normally attached to some types of DG units, such as directly connected induction generators. These compensators can change the equivalent impedance of the system, thus shifting the system resonance to higher or lower frequencies, which might change the system resonance characteristics. Harmonic resonance affects system stability by increasing the voltage beyond the typical limits of 1±0.05 p.u due to parallel resonance, or increasing the current beyond feeder's thermal capacity due to the series resonance. Therefore, this harmonic resonance could affect system stability.

1.3 Thesis Objectives

Motivated by the above problems, the ultimate goal of this research is to enhance the voltage stability of distribution systems that have high DG penetration. Moreover, this research is targeting the following objectives:

- Analyze the impacts of the DG units on voltage stability.
- Introduce a guide to place and size the DG units to improve the voltage stability margin in a distribution system.
- Tackle the probabilistic nature of the distributed generation and the load.
- Model and investigate the impact of grid-connected mode DG units on the proximity of voltage instability with high penetration level of DG units. This goal is achieved by stressing the system incrementally until it becomes unstable, and then at each operating point small-signal analysis and modal analysis are applied.
- Evaluate the impact of the integration of distributed generation on harmonic resonance by modeling different types of DG units and applying impedance frequency scan methods. This research investigates important issues related to the impact of the DG units on harmonic resonance, such as, the change of the load demand, DG units' disconnections, and the arrangement of the DG units in a wind farm.

1.4 Outline of the Thesis

The remainder of this thesis is organized as follows:

Chapter 2 presents a literature survey on Distributed Generation (DG) and system stability. In the distributed generation part, different definitions, types of DG units, types of interfacing and the impact of the DG units on power system are discussed. The second part of the survey is dedicated to system stability beginning with introducing the power system stability and its types. The impacts of DG units on system stability are presented in this part. Also, it provides a survey on proximity to voltage instability and harmonic resonance.

Chapter 3 proposes a method to place and size DG units to improve the voltage stability margin in a distribution system. The chapter starts by introducing a method to select candidate buses for the DG units' installation. Then it formulates an optimization method to sit and size DG units. This will be conducted taking the probabilistic nature of both DG units and the load into consideration.

Chapter 4 presents a model and analysis to study the impact of DG units on the proximity to voltage instability. It starts by introducing a small signal model for the system with integrated DG units. Then, different case studies are presented to analyze the impacts of the DG units on proximity to voltage instability.

Chapter 5 studies the harmonic resonance due to the integration of DG units in distribution systems. It begins by explaining the modeling of the system. Then, it demonstrates the results with different scenarios to reveal the impact of the DG units on harmonic resonance.

Chapter 6 presents the thesis summary, and contributions.

Chapter 2
Literature Survey

This chapter presents the state-of-the-art and literature survey on distributed generation, voltage stability and harmonic resonance.

2.1 Distributed Generation

Based on the literature, there is no consistent definition of Distributed Generation (DG), but generally they are small-scale generation units located near or at loads. However, the definition can be diversified based on voltage level, unit connection, type of prime-mover, generation not being dispatched, and maximum power rating [4].

IEEE [5] defines DG as "the generation of electricity by facilities that are sufficiently smaller than central generating plants so as to allow interconnection at nearly any point in a power system." IEEE compared the size of the DG to that of a conventional generating plant. A more precise definition is provided by the International Council on Large Electric Systems (CIGRE) [6] and The International Conference on Electricity Distribution (CIRED) [7], which defines DG based on size, location, and type. CIGRE defines distributed generation as "all generation units with a maximum capacity of 50 MW to 100 MW, that are usually connected to the distribution network and that are neither centrally planned nor dispatched." CIRED defines DG to be "all generation units with a maximum capacity of 50 MW to 100MW that are usually connected to the distribution network." Chambers [8] looks into the economic side in his definition. He defines distributed generation as "the relatively small generation units of 30MW or less that are sited at or near customer sites to meet specific customer needs, to support economic operation of the distribution grid, or both". Dondiet [9] defines distributed generation as "a small source of electric power generation or storage (typically ranging from less than a kW to tens of MW) that is not a part of a large central power system and is located close to the load." He includes the storage facilities on his definition. Ackermann [4] defines a distributed generation source as "an electric power generation source connected directly to the distribution network or on the customer side of the meter." Ackermann's definition is the most generic one, because there is no limit on the DG size and capacity. The definition covers the location of the DG.

2.2 Types of Distributed Generation Sources

Based on this research, two main types of DG sources are used in distribution systems: dispatchable and non-dispatchable. They are shown in Figure 2-1 and discussed as follows:

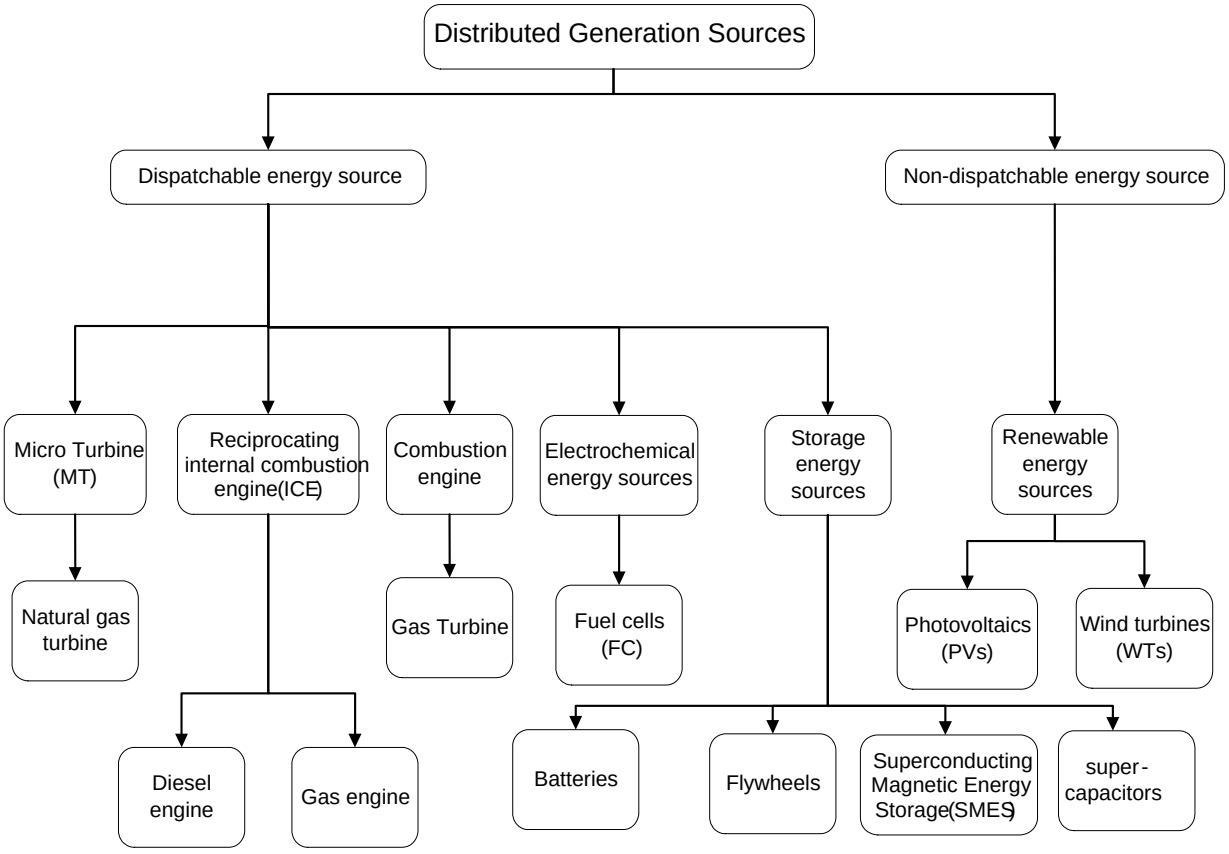

Figure 2-1: Distributed Generation sources

2.2.1 **Wind turbines**

Wind energy is the most widely used DG source in the world. A wind turbine is a rotating machine that converts the kinetic energy of wind into mechanical energy, and then into electrical energy, using ac generators such as induction and synchronous types. These generators are attached to the wind turbine. The wind turbine consists of turbine blades, a rotor, a shaft, a coupling device, a gear box, and a nacelle. A cluster of wind turbines installed in a specific location is called a wind farm. A wind

farm should be installed in a windy place, because its electric capacity is limited by the amount of wind. The overall efficiency of the wind turbine is between 20-40%, and its power rating varies between 0.3 to 7 MW [10]. The advantages of wind energy are that it is a clean power source, and the cheapest technology compared to other types of renewable energies. Wind turbines are classified into four types : A, B, C, and D as shown in Figure 2-2 [11].

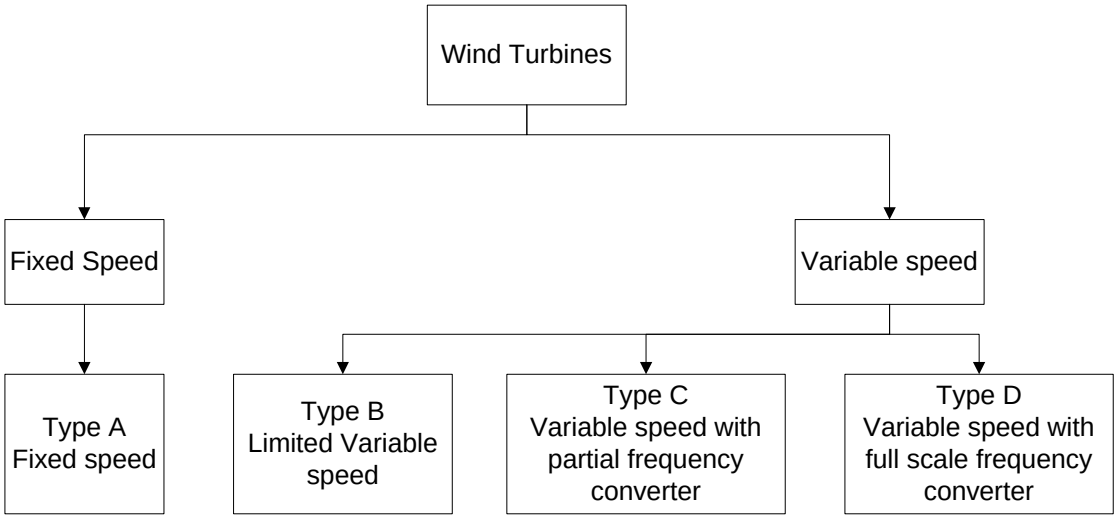

Figure 2-2: Types of wind turbines

Type A uses a fixed speed wind turbine with a Squirrel Cage Induction Generator (SCIG) connected to the grid via a transformer. In this type, fluctuations in wind speed are converted to electrical power fluctuations and consequently into voltage fluctuations if the grid is weak [11]. Thus, since the microgrid is considered a weak grid, fluctuation in winds yields fluctuation in voltage.

Type B uses a Wound Rotor Induction Generator (WRIG). In this type, the slip is typically controlled from 0 to -0.1, meaning that the speed of the generator could be increased up to 10% above the synchronous speed.

Type C uses a technology called the Doubly Fed Induction Generator (DFIG) with a wound rotor induction generator (WRIG) and a partial scale frequency converter on the rotor circuit.

Type D uses a full variable speed wind turbine with an induction or a synchronous generator, connected to the grid through a full load frequency converter. The induction generator is a WRIG

machine. However, the synchronous generator could be a Wound Rotor Synchronous Generator (WRSG) or a Permanent Magnet Synchronous Generator (PMSG).

2.2.2 **Photovoltaic**

Solar cells represent the basic component of a photovoltaic system, and are made from semiconductor materials such as monocrystalline and polycrystalline silicon. Solar cells have much in common with other solid-state electronics devices such as diodes, transistors, and integrated circuits [12]. Solar cells are assembled to form a panel or module. A typical PV module is made up of about 36 or 72 cells. The modules are then connected in series/parallel configurations to form a solar array that is used to generate electrical energy from the sunlight. The photovoltaic rating can be found in small solar cells of 0.3 kW and all the way up to multi-megawatt in large system [13]. Compared with that of wind turbines, the efficiency of photovoltaic generation is still low, less than 20%. The photovoltaic module lifetime can reach more than 25 years. However, the efficiency decreases with aging, to 75-80% of the nominal value [14].

Photovoltaic DG units are interfaced to the power system by using power electronic converters with Maximum Power Point Tracking (MPPT) [15]. Many techniques are used to operate photovoltaic generators with MPPT, such as voltage feedback, the perturb and observe method, linear line approximation, fuzzy logic control, neural network method, and practical measure method [16].

2.2.3 **Fuel cells**

A fuel cell is one of the existing DG technologies. It is an electrochemical device that can be used to convert chemical energy to electrical and thermal energy, without combustion [17]. A fuel cell is considered similar to a battery: it is made of two electrodes with an ion-conductive electrolyte sandwiched between them. However, it is unlike a battery in that it does not need to be charged for the consumed materials during the electrochemical process since these materials are continuously supplied to the cell. The efficiency of these cells is significantly high, about 40-60% when used for electricity production. Moreover, when the exothermic heat is combined with electrical power (CHP), the overall efficiency can reach more than 80% [14]. Fuel cell capacities vary from 1kW to a few MW depending on the application and whether it is a portable or stationary application. References [18, 19] have presented different types and applications of fuel cells. The advantages of fuel cells are

their relatively small footprint, noiseless operation, and absence of harmful emissions during operation. A typical fuel cell's energy density is 200 Wh/l, more than ten times that of a battery [14]. Fuel cells are considered as a dispatchable DG source because they are fueled by a variety of hydrogen-rich fuel sources such as natural gas, gasoline, or propane. Since the output voltage of fuel cells is low dc voltage, these cells require a power electronic interface (dc-dc 'boost converter', then dc-ac inverter) in order to condition their output [14].

2.2.4 **Reciprocating Internal Combustion Engine (ICE)**

A reciprocating engine is one that uses one or more pistons to convert pressure into a rotating motion. It is also known as a piston engine. ICE is the most commonly applied DG technology and the least expensive one [20]. The most common interface of the reciprocating engine is a synchronous or an induction generator. A synchronous generator is commonly used for ratings higher than 300kW, and an induction generator for ratings lower than 300kW. This type of DG unit can be connected directly to the grid without any power electronics interfacing.

2.2.5 **Micro-turbines**

Micro-turbines are basically a combination of a small generator and a small turbine. These types of generators are normally fueled by natural gas. The capacity of the micro-turbines can range from several kilowatts to megawatts [21]. They are unlike the conventional combustion turbines in that they rotate at very high speed, in the range of 50,000-120,000 rpm [22]. In addition, they run at lower pressure than conventional combustion turbines. The advantages of micro-turbines are that they are small in size, so they can fit in a small area; they also have high efficiency, low noise, low gas emission, and low installation and maintenance costs. Due to the high speed rotation, micro-turbines generate a very high frequency power (1500–4000 Hz) compared to the nominal power frequency, which is 50Hz or 60 Hz [22]. Therefore, the turbines require power electronics converter (ac-dc-ac converter) to interface them to the grid or to operate them in parallel with other types of DG sources [21].

Because micro-turbines operate on natural gas, they can be considered dispatchable sources. As a result, they do not cause intermittent generation problems. This point adds extra merit to the turbines and makes them promising type of DG units that can be used in microgrid systems.

2.2.6 **Storage Devices**

In power systems, storage devices are used to improve stability, power quality, and reliability of supply [23]. In DG systems, storage devices are used to pick up fast load changes and enhance the reliability of the system, and to flatten the generation profile of non-dispatchable DG sources. The common types among them are batteries, flywheels, super-capacitors, and superconducting magnetic energy storage. These devices are interfaced to the power system network via power electronics converters.

2.3 DG Grid Interfacing

The interface of DG units to the grid can be divided into two types [24]:

a. Direct grid-connected DG units

   Direct-connected DG units are achieved either by means of synchronous generator or induction generator. The prime mover operates at a constant speed to drive these generators.

b. Indirect grid-connected DG units

   Indirect grid interfacing is used when the output of the source is DC such as photovoltaic systems and fuel-cells, high frequency AC source such as micro-turbines, and variable frequency such as wind turbines (type C and D). In this case, power electronics converters are used.

2.4 Impacts of DG units on power system

Although the integration of the DG units in electric systems has multifarious benefits, they increase the complexity [25]. Therefore, the DG units have impacts on the system performance such as voltage profile, power flow, system losses, power quality, stability, reliability, and protection. The main target of this research is to study the voltage stability and harmonic resonance due to the high penetration of the DG units [26-29]. Thus, the next part of this chapter presents the impact of the DG units on system stability and harmonic resonance.

2.4.1 **System Stability**

In the operation of a power system, at any given time, there must be a balance between the electricity supply and the demand. A power system should, therefore, be able to maintain this balance under both normal conditions (steady-state) and after disturbances (transient). The stability of a power system is defined as "a property of a power system that enables it to remain in a state of equilibrium under normal operating conditions and to regain an acceptable state of equilibrium after being subjected to a disturbance" [30].

The operating condition of a power system is described according to physical quantities, such as the magnitude and phase angle of the voltage at each bus, and the active/reactive power flowing in each line. If these quantities are constant over time, the system is in steady state; if they are not constant, the system is considered to be in disturbance [31]. The disturbances can be small or large depending on their origin and magnitude. For instance, small variations in load and generation are types of small disturbances, but faults, large changes in load, and loss of generating units are types of large disturbances [31]. The stability of a power system can be classified as shown in Figure 2-3into [32]: rotor angle stability, voltage stability, and frequency stability.

In basic terms, distribution system networks are designed to receive power from the transmission line and then distribute it to customers. Thus, real power and reactive power both flow in one direction. However, when DG units are installed in distribution systems, the directions of the real and reactive power may be reversed. Therefore, the penetration of DG units into distribution systems affects the stability of the system, and as the penetration level increases, stability becomes a significant issue. Any fault occurring in the distribution system might cause voltage and angle instability [33].
In distribution systems with embedded DG units, the main factors that influence stability are the control strategies of the DG units, the energy storage systems, the types of load in the system, the location of faults, and the inertia constant of the motor [34].

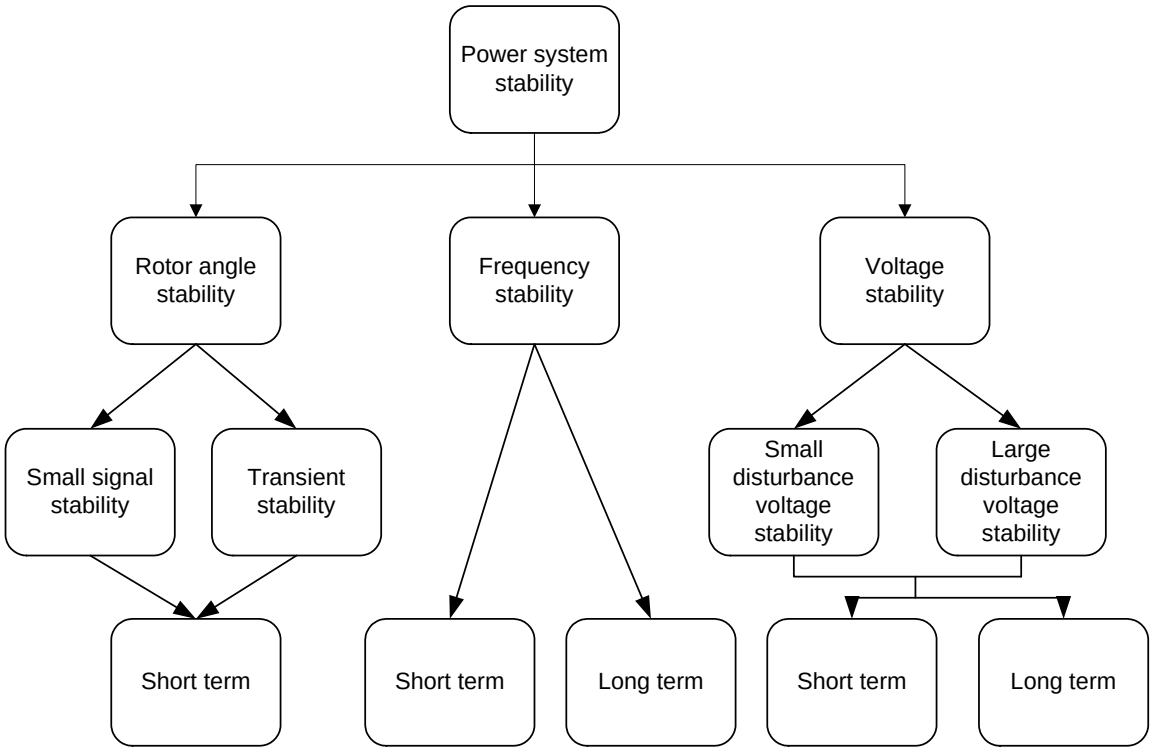

Figure 2-3: Classification of types of power system stability

2.4.1.1 Rotor angle and frequency stability

Rotor angle stability is "the ability of interconnected synchronous machines in a power system to remain in synchronism under normal operating conditions and after being subjected to a disturbance" [32]. Instability occurs in the form of increasing angular swings of some generators, which leads to the loss of synchronism. Therefore, machine characteristics and modeling are helpful in the study of the rotor angle stability [32].

In distributed generation, rotor angle stability has been studied in both transmission and distribution systems. Reference [35] investigated the impact of high penetration levels of DG units on the transient stability of a transmission power system. The researchers examined transient stability by making scenarios of faults in all possible branches, and concluded that the penetration level of the units affects the power flow in the transmission lines, and hence, the transient stability of the transmission. The author of [36] studied the impact of distributed generation technology (such as

inverter-based and rotating-based DG units) on the transient stability of a power system. This study found that transient stability is strongly dependent on the technology used in the DG units.

With respect to distribution systems, reference [37] studied the transient stability of a system during its transition from grid-connected mode to a microgrid. This study was based on the time domain simulation method and focused on the transients of a microgrid in cases of both planned and unplanned grid disconnection. The researchers used two DG units: inverter-based and direct-connected synchronous. The inverter-based DG was assumed to be dispatchable in order to control the real and reactive power during the transition from grid-connected to autonomous mode. The results showed that interfaced DG units can effectively enhance power quality and also maintain angle stability. However, the microgrid was assumed to be a balanced system; i.e., no single-phase loads or unbalanced three-phase loads were considered. In addition, the time constants of both DG units were noticeably different and hence did not cause a dynamic interaction during the transient.

Frequency stability is the ability of a power system to maintain the frequency within an acceptable range following a system upset that results in a significant imbalance between generation and load [32]. Analyzing rotor angle and frequency stability are not in the scope of this thesis.

2.4.1.2 Voltage stability

Voltage stability refers to the ability of a power system to maintain steady and acceptable voltages at all buses in the system after being subjected to a disturbance from a given initial operating condition. The main factor causing voltage instability is inability to meet the reactive power demand [30]. Voltage stability can be classified as small or large based on the disturbance type. Small voltage stability refers to the ability of the system to control the voltage when small perturbations occur, such as changes in the loads. Large voltage stability refers to the ability of the system to control the voltage after being subjected to large disturbances such as load outages, faults, and large-step changes in the loads.

Voltage stability can be evaluated by two different methods of analysis: static and dynamic, the details of which are presented in the following subsection.

1. Static analysis

This method examines the viability of the equilibrium point represented by a specified operating condition of the power system. This method allows the examination of a wide range of system conditions. The electric utility industry depends on P-V and Q-V curves in order to determine stability at selected buses. The static method is evaluated by means of a variety of techniques such as:

a) P-V and Q-V curves

P-V and Q-V curves are generated by executing a large number of power flows using power flow methods. In this case, a power system is typically modeled with non-linear differential algebraic equations [38].

$$\dot{x} = f(x, \lambda) \tag{2.1}$$

where

$x \in R^n$ represents a state vector, including the bus voltage magnitude (V) and angles (δ).

$\lambda \in R^m$ is a parameter vector that represents the real and reactive power demand at each load bus.

The parameter vector λ is subject to variations due to variations in the load. Therefore, the power flow solution varies as λ varies. The power system's power flow is represented by [38].

$$0 = f(x, \lambda) \tag{2.2}$$

The following example depicts the P-V curve:

Consider a single-machine PV bus as shown in Figure 2-4. This bus supplies a PQ load of constant power factor through a transmission line. The state vector x in equation (2.2) represents the voltage (V), and the power angle (δ) and parameter vector λ represent the real and reactive power. At low loading, the power flow of equation (2.2) gives two equilibrium solutions: one with a high voltage value and the other with a low voltage value. The solution

with the higher voltage value is the stable solution [39]. As the loading increases, the higher voltage solution values decrease and the lower voltage increases. These solution points continue moving on a P-V curve until they coalesce into a critical loading power and then disappear. The load flow after this critical value diverges.

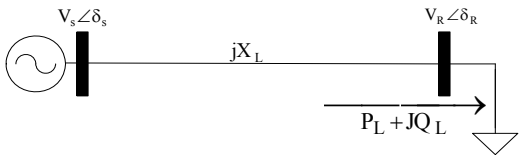

Figure 2- 4: Single-machine PV bus supplying a PQ load bus

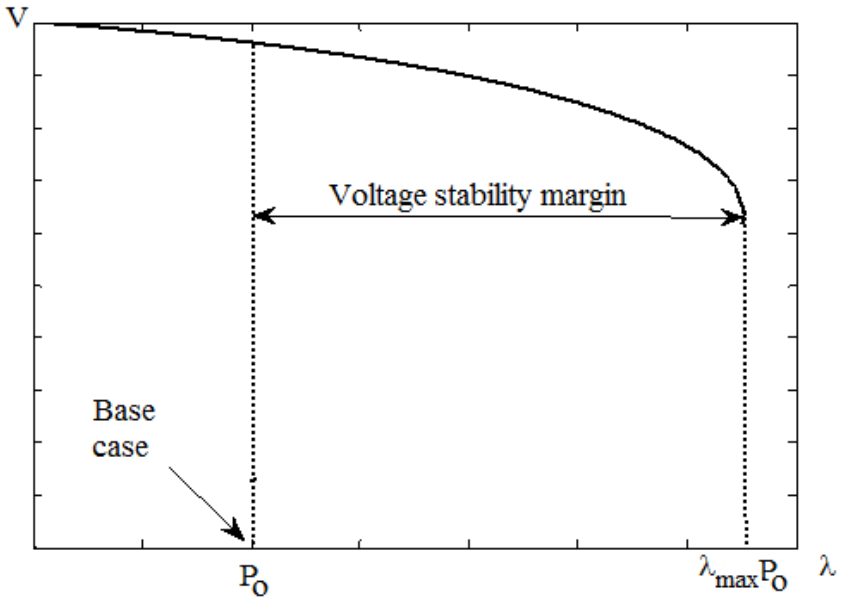

Figure 2- 5: P-V curve or nose curve

b) V-Q sensitivity analysis

In this method, the network is represented by a power flow equation that can be linearized, as given in equation (2.3) [40].

$$\begin{bmatrix} \Delta P \\ \Delta Q \end{bmatrix} = \begin{bmatrix} J_{P\theta} & J_{PV} \\ J_{Q\theta} & J_{QV} \end{bmatrix} \begin{bmatrix} \Delta\theta \\ \Delta V \end{bmatrix} \tag{2.3}$$

where

ΔP : the incremental change in bus real power

ΔQ : the incremental change in bus reactive power

ΔV : the incremental change in bus voltage magnitude

$\Delta\theta$: the incremental change in bus voltage angle

J : the Jacobian matrix.

With the assumption of the real load power (P) being constant, the incremental change in the bus real power ΔP equals to zero. Then, using the partial inversion of equation (2.3) gives

$$\Delta Q = (J_{QV} - J_{Q\theta} J_{P\theta}^{-1} J_{PV}) \Delta V \tag{2.4}$$

or

$$\Delta V = (J_{QV} - J_{Q\theta} J_{P\theta}^{-1} J_{PV})^{-1} \Delta Q \tag{2.5}$$

The V-Q sensitivity can be calculated by solving equation (2.4). The V-Q sensitivity at a bus represents the slope of the Q-V curve (Figure 2-6) at a given operating point. A positive V-Q sensitivity is indicative of stable operation, and a negative sensitivity is indicative of unstable operation [30].

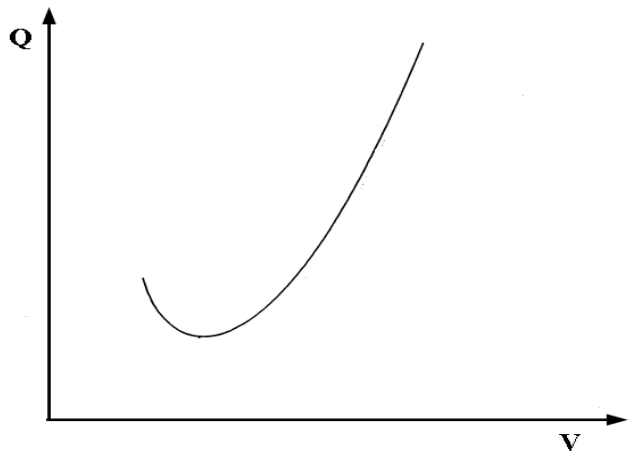

Figure 2- 6: Q-V characteristic curve [30]

2. Dynamic Analysis

Dynamic analysis can show the real behaviour of the system such as loads (dynamic and static), DG units, automatic voltage and frequency control equipment, and the protection systems. The overall power system is represented by a set of first order differential equations, as given in equation (2.6).

$$\dot{X} = f(x, V) \tag{2.6}$$

and a set of algebraic equations

$$I(x, V) = Y_N V \tag{2.7}$$

with a set of known initial conditions (X_0, V_0)

where

X: state vector of the system

V: bus voltage vector

I: current injection vector

Y_N: network node admittance matrix

Equations (2.6) and (2.7) can be solved in a time domain using numerical integration methods. This study provides time domain results; therefore, the system can be modeled and simulated with the help of different simulation software such as MATLAB.

Voltage instability in distribution systems has been understood for decades and was referred to as load instability [41]. For example, a voltage instability problem in a distribution network, which was widespread to a corresponding transmission system, caused a major blackout in the S/SE Brazilian system in 1997 [42].

With the development of economy, load demands in distribution networks increase sharply. Hence, the distribution networks are operating closer to the voltage instability boundaries. The decline of voltage stability margin is one of the most important factors which restricts the increase of load served by distribution companies [43]. Therefore, it is necessary to consider voltage stability with the integration of DG units in distribution systems. The literature has covered this impact from different points of view. For example, [44-47] studied the impact of induction generators due to small and large disturbances. The authors of [35, 36] investigated the impact of distributed generation technology such as synchronous, induction generators, and high or low speed generators that are grid

coupled through a power electronic converter. A practical investigation of the impacts of DG units on system stability can be found in [48]. Reference [49] presented an assessment of the impact of the DG units' size and location under a change in the loading conditions due to a contingency on unbalanced distribution systems. In [50], the effect of DG units' capacity and location on voltage stability enhancement of distribution networks was also investigated. The DG units were allocated and sized based on minimizing overall cost.

This paper ([50]) recommended considering the voltage stability as an objective function when dealing with optimum locations of DG units. References, [51, 52] proposed methods to locate distributed generation units to improve the voltage profile and voltage stability of a distribution system. The author in [51] placed DG units at the buses most sensitive to voltage collapse, and resulted in improvement in voltage profile, as well as decline in the power losses. The author in [52] developed the work in [51] further to maximize the loadability conditions in normal and contingency situations.

Reference [53] studied the voltage and frequency stability of a distribution system in grid-connected mode and in a microgrid. The study considered the imbalance of loads and sources, and was divided into two parts: simulation with storage DG units only and then simulation with storage and renewable energy units operating in parallel. However, it was a time domain simulation study and the renewable energy DG units were assumed to supply the system with constant power.

2.5 Proximity to voltage instability

As mentioned before, the static technique can be analyzed by using the relation between the receiving power (P) and the voltage (V) at a certain bus in a system, which is known as a P-V curve or nose curve (Figure 2-5). The P-V curve is obtained by applying the continuous power flow method [54]. The critical point λ_{max} (saddle-node bifurcation point) in the P-V curve represents the maximum loading of a system. This point corresponds to a singularity of the Jacobian of the power flow equations. The stability margin can be defined by the MW distant from the operating point to the critical point. The penetration of the DG units in a distribution system can increase or decrease the voltage stability margin depending on their operation at unity, lead or lag power factors as well as their location. Figure 2-5 illustrates a P-V curve of an electrical system. The x-axis represents λ, which is the scaling factor of the load demand at a certain operating point (Equation (2.8)). λ varies from zero to the maximum loading (λ_{max}).

$$P_i = \lambda P_{o,i}$$
$$Q_i = \lambda Q_{o,i} \tag{2.8}$$

However, static analysis cannot determine the control action and the interaction between the integrated DG units in the system. Proximity to the voltage instability method can be used to determine those issues.

The impacts of the DG unit's dynamics using small-signal stability analysis have analyzed in the literature. Small-signal stability analysis in power systems is achieved in frequency domain using eigenvalue analysis. It is carried out by linearizing the mathematical model of the system and then solving for the eigenvalues and eigenvectors of the linearized model. The authors in [55] presented a small-signal model of inverter DG units in a microgrid. [56] also modeled the microgrid with small-signal and included a mix of inverter-based and conventional DG units. In [37, 57] the small-signal model to investigate the dynamic behaviour of the system was utilized and the control parameters of the DG units were selected. In addition, they used small-signal analysis to improve the control of the DG units, as well as studying the mode of control when the DG system is moved from grid-connected to a micro-grid mode.

2.6 Harmonic resonance

Harmonic distortion is one of the power quality problems which is produced in distribution systems due to the presence of some non-linear elements. These elements include power electronic devices, transformers, non-linear load, and recently distributed generators which are fully or partially interfaced to the grid-network through power electronics inverters. When harmonics exceed a certain level, it negatively impacts customer equipment as well as the network components. These impacts appear as a reduction in the efficiency of network components, and malfunction of the network devices [58]. The harmonics' levels are obtained by calculating the voltage and current harmonic distortions and compare them to the limits set by standards. These standards are set by different entities such as IEEE, IEC, EN, and NORSOK [59].

Normally, the distribution system consists of inductive and capacitive elements. The reactance values of these elements depend on the frequency. Thus, the harmonic components affect the system and cause series or parallel resonance phenomenon. This phenomenon occurs when the inductive and the capacitive reactances are equal. In the parallel resonance, the system impedance is high and a small exciting current can develop large voltage. However, in series resonance, the system impedance is

low and a small exciting voltage can develop high current. The resonance phenomena are an important issue in distribution systems, since the system consists of distributed non-linear loads, shunt capacitors, and distributed generation. The literature has studied the resonance in order to design reactive power compensation or filter design, and several techniques have been proposed to study the resonance, such as using analytical expressions, conducting harmonic power flow studies, or applying frequency scan techniques [60, 61].

The impact of the grid connected wind farm is studied in [58]. This study was conducted in a power system with a wind farm of 200 MVA. In terms of resonance analysis, the study focused on the impact of the changes of the shunt capacitor which is connected in the substation of the wind farm. Reference [62] analyze harmonics in power systems with an integrated 10 MVA wind farm. In terms of resonance, this study covered the impact of the capacitance of the submarine cable which is connected between the wind-farm and the power system. In [63] , the impact of wind DG units on resonance and harmonic distortion was studied. This study ([63]) covered the impact of the size of power factor capacitor bank which is located in the system network, DG unit shunt capacitor bank, and the capacitance of the collector cable which connects the DG units to the system.

2.7 Discussion

In this chapter, a literature survey on Distributed Generation (DG) and system stability was presented. In the distributed generation part, different definitions, types of DG units, types of interfacing and the impact of the DG units on power system were discussed. The second part of the survey is devoted to system stability. It starts by introducing the power system stability and its types. The impacts of DG units on system stability were presented in this part. Furthermore, it provides survey on proximity to voltage instability and harmonic resonance.

On the impact of DG units on voltage system stability (section 2.4), the problem of voltage stability was tackled with the assumption that all connected DG units are dispatchable. Yet, this thesis introduces the probabilistic nature of both the renewable energy resources and the load demand as vital factors to be considered for improving the voltage stability. Therefore, this thesis will tackle placing and sizing of the DG units to improve the voltage stability margin, and consider the probabilistic nature of the renewable energy resources and the load. It proposes a modified voltage index method to place and size the DG units to improve the voltage stability margin, with conditions of both not exceeding the buses' voltage, and staying within the feeder current limits. In addition, the

probability of the load and DG units are modeled and included in the formulation of the sizing and placing of the DG units.

In section 2.5, literature focused on analyzing microgrid systems, but they did not cover grid-connected mode analysis. In addition, voltage stability along with small-signal stability, which is known as proximity to voltage instability analysis, has not been covered yet. Thus, this thesis presents this method, and it is accomplished by loading the system in steps of λ until the system become unstable, or the maximum loadability is reached. In each step of loading, small-signal stability analysis and sensitivity analysis are applied. Thus, the aims of this study are: 1) to model, investigate, and analyze the impact of grid-connected mode DG units in terms of small-signal analysis and with the voltage stability P-V curve, and 2) to examine the impact of the DG size and location in small signal stability.

Based on the literature in section 2.6 , the following impacts of the DG units integration on harmonic resonance have not been tackled yet: I) the impact of the changes of the load demand , II) the impact of placing more than one DG unit in different locations, III) the impact of the load and line disconnection, IV) the impact of the DG units' disconnection, and V) the impact of the DG units arrangement. This thesis will conduct a case study to tackle these issues.

2.8 Summary

It can be concluded that the installation of DG units can impact the distribution system by either improving or degrading the system stability. The literature studied the impact of the DG units on voltage stability, however, the presented work only focused on dispatchable DG units with pre-defined capacities and constant load representation. Yet utilizing DG units to improve the voltage stability margins while considering the probabilistic nature of both generation units and loads has not been tackled. In addition, the impacts to the proximity of voltage stability using small signal analysis are not investigated. The placement of the DG units can cause resonance in the distribution system. This resonance can affect the stability of the system. Thus, it is recommended to study this issue with the integration of distributed generation. Therefore, the next chapters will tackle these issues.

Chapter 3

Distributed Generation placement and sizing method to improve the voltage stability margin in a distribution system

3.1 Introduction

Recently, integration of Distributed Generation (DG) in distribution systems has increased to high penetration levels, and the impact of DG units on the voltage stability margins has become significant. Optimization techniques are tools which can be used to locate and size the DG units in the system, so as to utilize these units optimally within certain limits and constraints. Thus, the impacts of DG units on several important issues, such as voltage stability and voltage profile, can be analyzed effectively. The ultimate goal of this chapter is to propose a method of locating and sizing DG units so as to improve the voltage stability margin.

Figure 3-1 summarizes the proposed method. It starts by selecting candidate buses into which to install the DG units on the system, prioritizing buses which are sensitive to voltage variation and thus improving the voltage stability margin. Then, model the load and the DG generation with the consideration of the probabilistic nature of both the renewable DG units and the load. After that, conduct placement and sizing is formulation using mixed integer non-linear programming (MINLP), with an objective function of improving the stability margin. MINLP is solved by an outer approximation method using GAMS software. The stability margin can be defined by the MW distant from the operating point to the critical point.

The allocation problem will be subjected to several system constraints in order to make sure that the normal operating practices of the distribution system are not violated. The constraints considered in this study are the system voltage limits, feeders' capacity, and the limits for the DG penetration level.

The chapter is arranged as follows: Section 3.2 presents the impact of the DG units on voltage stability, Section 3.3 carries out a method to select the most suitable candidate buses for DG units installation, Section 3.4 formulates a method to sit and size DG units, Section 3.5 describes the system under study, and Sections 3.6 and 3.7 demonstrate the results and discussion, respectively.

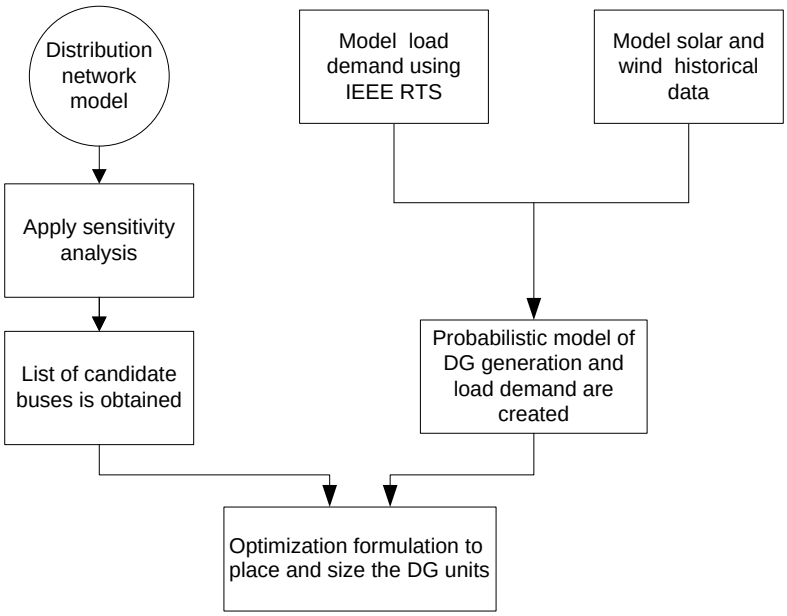

Figure 3- 1: A diagram providing a brief description about the placement and sizing of the DG units to improve the voltage stability margin

3.2 Impact of the DG size on voltage stability

Currently, most installed DGs are connected to operate at unity power factor to avoid interference with the voltage regulation devices connected to the system [64, 65]. For this reason, this study assumes that all the DG units are operating at unity power factor. In addition, some utilities allow the DG units to operate in fixed power factor mode, ranging from 0.95 lagging to 0.95 leading; a case study representing this condition is also considered.

Figure 3-2 visualizes the impact of a DG unit on voltage stability margin and maximum loadability. The x-axis represents λ, which is the scaling factor of the load demand at a certain operating point (Equation (2.8)). λ varies from zero to the maximum loading (λ_{max}). Due to real power injection of a DG unit, the normal operating point of the voltage increases from V_1 to V_2, and at the same time the maximum loadability increases from λ_{max1} to λ_{max2}.

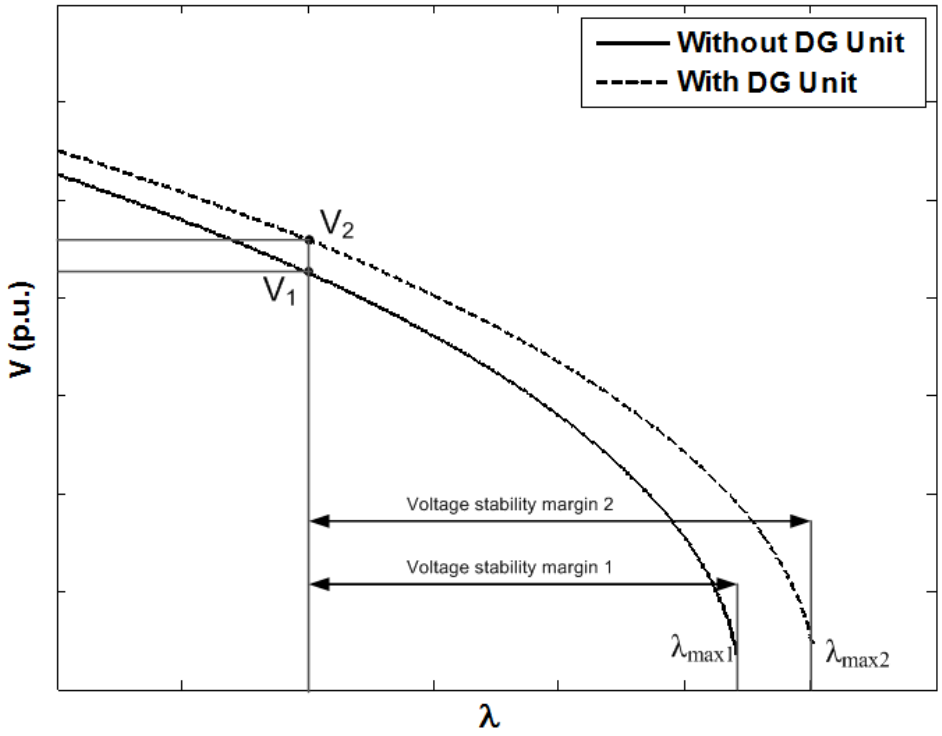

Figure 3- 2: Impact of a DG unit on maximum loadability and voltage stability margin

3.3 Selection of the Candidate buses

In the literature, the candidate buses for the DG installation can be selected randomly, by recommended location, or by selecting sensitive buses to the voltage profile. Because this study is focusing on improving the voltage stability of the system, it uses voltage sensitivity analysis to select the candidate buses. In addition, the candidate buses should be located on the main feeders of the system. The method is conducted by testing the voltage sensitivity to the change of the DG injected power, and can be explained as follows.

Power systems are typically modeled with non-linear differential algebraic equations [38]. The system model can be linearized as in (2.3). With the assumption that the reactive load power (Q) is constant, the incremental change in bus reactive power ΔQ equals to zero. Then, using the partial inversion of (2.3) gives:

$$\Delta P = (J_{PV} - J_{P\theta} J_{Q\theta}^{-1} J_{QV}) \Delta V \tag{3.1}$$

or,

$$\Delta V = (J_{RPV})^{-1} \Delta P \tag{3.2}$$

Where J_{RPV} is a reduced Jacobian matrix, which gives the voltage magnitude variations due to DG active power injection variations. If the buses are modeled as PQ buses, $J_{Q\theta}^{-1}$ is a feasible and square matrix. Therefore, this situation normally occurs in distribution systems where the slack bus is the only bus that keeps the voltage magnitude at a fixed point.

This study focused on radial distribution systems. The load buses are considered as PQ. Yet, for the DG unit placement, there are three types of DG control, namely PV control, current control, and PQ control. For the DG with PV controller, the connected bus can be modeled as a PV bus. Further, for DG units equipped with either a current or a PQ controller, the connected bus is modeled as a PQ bus. Yet, the IEEE P1547 Standard [5] specified that the DG units should not regulate distribution system voltages. Any attempt by a DG unit to regulate the distribution system voltage can conflict with the existing voltage regulation schemes applied by the utility to regulate the same or a nearby point to a different voltage reference [64]. Thus, DG units with a PV controller are not recommended. Therefore, this research focused on modeling DG units buses' as PQ buses. It is worth mentioning that modeling DG units as PQ busses with controlled reactive power injection might be valid for electronically-coupled DG units where reactive power contribution is independent from the interface bus voltage. Since the most dominant type of DG units in the market are electronically coupled, such as type C and type D for the wind turbines [66], and solar PV units, this thesis assumes the DG units are electronically interfaced (inverter-based DG). However, for fixed and semi-variable-speed wind units (namely Type-A and Type-B [66]), this assumption is not valid, since the reactive power requirements of these two units depend on the value of the voltage at the interface bus. Usually, the RX model, instead of the PQ model, is used to address these two points.

In this case, Equation (3.2) can be used to study the impact of the DG units on voltage profile. This equation is valid if the DG units are operating at unity power factor, otherwise the V-Q sensitivity should be considered. Therefore, the system load values at an operating point can be analyzed using Equation (3.2) to determine the buses most sensitive to the voltage profile. The most sensitive buses should be selected as the candidate buses for the DG installation.

3.4 DG placement problem formulation

After the candidate buses are selected in Section 3.3, allocating DG units within the system requires investigation in terms of DG resources and their uncertainties. It also requires modeling the types of load and their criticality at each bus. In addition, placing the DG units in the most sensitive buses might violate the voltage limits or the capacity of the feeders, depending on the size of the DG units and the load demand of the system. Accordingly, this section proposes a method to place DG units with an objective of improving the voltage stability of the system. This study is demonstrated in five scenarios.

- *Scenario 1: is a reference scenario, in which no DG units are connected to the system (base case)*
- *Scenario 2: only dispatchable (non-renewable) DG units are connected.*
- *Scenario 3: only wind-based DG units are connected.*
- *Scenario 4: only PV DG units are connected.*
- *Scenario 5: a mix of dispatchable, wind-based and PV DG units are connected.*

In this formulation, the following assumptions are considered.

- More than one type of DG can be installed at the same candidate bus.
- The DG units are assumed to operate at unity power factor. In addition, a simulation for DG units that operates between 0.95 lagging and leading power factor is presented.
- All buses in the system are subjected to the same wind speed and solar irradiance. This assumption greatly simplifies the analysis.
- The penetration level is equal or less than 30%; referring to Ontario's standard program, the maximum penetration level is 30% of the maximum load [67].

The selected wind turbine is 1.1 MW, and the photovoltaic module is 75W, however, other wind and PV ratings can be considered without loss of generality. The utilized DG units' ratings and characteristics are obtained from [68]. The annual capacity factor (CF) of the wind turbine is found to be 0.22, while that of the PV module generator is found to be 0.174. Capacity Factor (CF) is defined as the ratio of the average output power to the rated output power over a certain period of time.

$$CF = \frac{P_{ave}}{P_{rated}} \tag{3.3}$$

The hourly average output power of a wind turbine or a PV module is the summation of the output power at all possible states[3] for an hour, multiplied by the corresponding probability of each state. Once the average output power is calculated for each time segment, the average output power is calculated for the typical day in each season, and hence, the annual average output power.

The annual capacity factor is only used to formulate the maximum penetration level as given in Equation (3.27). The characteristics of both types of DG units are given in Appendix (B). The total penetration of the wind turbines will be an integer multiple of the selected rating. For example, if the result shows the penetration level at a certain bus is 6.6 MW, it means six turbines of 1.1 MW are recommended to be installed at this bus. On the other hand, solar generators can be modeled using photovoltaic modules (PV modules). Since the ratings of PV modules are small, they are unlike wind turbines, and the solar generators can be modeled to the required sizes. For example, if the required size of the solar generator is 1.55 MW, it requires 206667 modules of 75W. The dispatchable DG unit is selected to be 0.5 MW. It is assumed to generate a constant power at its rating. For example, if the required size is 4.5 MW, it requires nine dispatchable DG units. Since, the dispatchable generator generates constant power during the year, it does not have uncertainty, and hence its annual capacity factor is 1.

The DG placement method is carried out as follows.

3.4.1 **Step 1: load and DG units modeling**

This study uses the models proposed in [68, 69]. The load is modeled by the IEEE-RTS system. It is modeled by hourly load and the load profile is shown in Table 3-1. These data are percentages of the annual peak load. The annual peak load demand is 16.18 MVA and the annual load demand is shown in Figure 3-3. For the renewable DG units, three years of historical data have been provided from the site under study. These data are used to model the solar irradiance and wind speed by Beta and Weibull probability distribution functions, respectively.

[3] The Beta and Weibull probability density functions are divided into states (periods) to incorporate the output power of the solar DG and wind-based DG units (see Section 3.4.1.2).

Table 3- 1: Load data for the system under study

Hour	Winter	Spring	Summer	Fall
12-1 am	0.4757	0.3969	0.64	0.3717
1--2	0.4473	0.3906	0.6	0.3658
2--3	0.426	0.378	0.58	0.354
3--4	0.4189	0.3654	0.56	0.3422
4--5	0.4189	0.3717	0.56	0.3481
5--6	0.426	0.4095	0.58	0.3835
6--7	0.5254	0.4536	0.64	0.4248
7--8	0.6106	0.5355	0.76	0.5015
8--9	0.6745	0.5985	0.87	0.5605
9--10	0.6816	0.6237	0.95	0.5841
10--11	0.6816	0.63	0.99	0.59
11--12pm	0.6745	0.6237	1	0.5841
12--1	0.6745	0.5859	0.99	0.5487
1--2	0.6745	0.5796	1	0.5428
2--3	0.6603	0.567	1	0.531
3--4	0.6674	0.5544	0.97	0.5192
4--5	0.7029	0.567	0.96	0.531
5--6	0.71	0.5796	0.96	0.5428
6--7	0.71	0.6048	0.93	0.5664
7--8	0.6816	0.6174	0.92	0.5782
8--9	0.6461	0.6048	0.92	0.5664
9--10	0.5893	0.567	0.93	0.531
10--11	0.5183	0.504	0.87	0.472
11--12am	0.4473	0.441	0.72	0.413

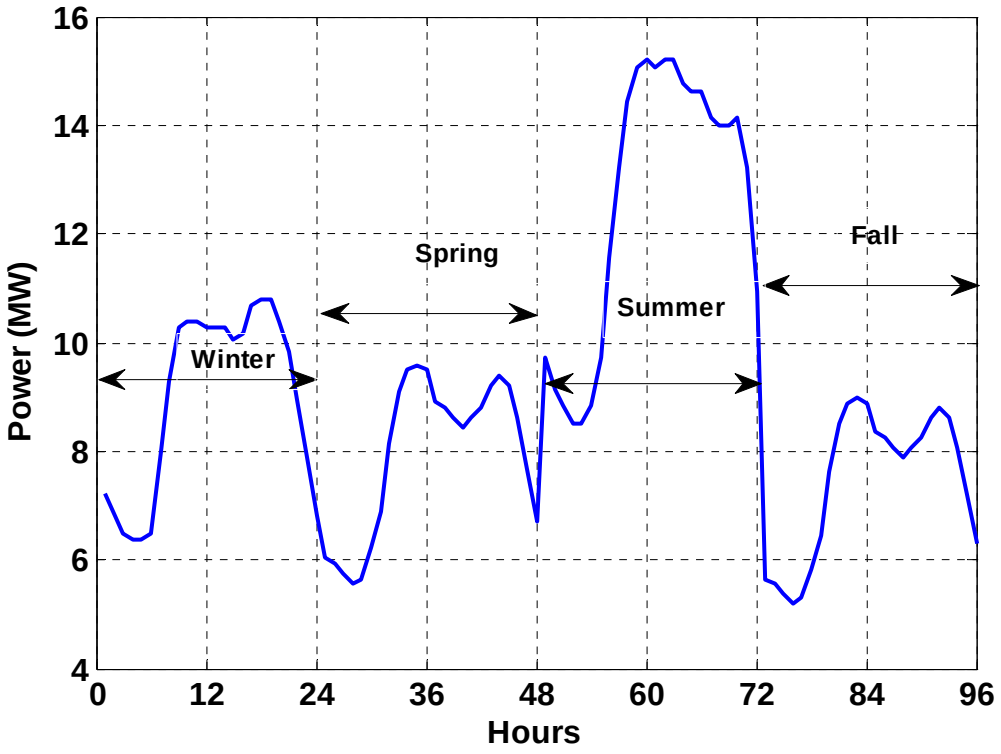

Figure 3- 3: Annual load demand of the system under study (each season is represented by one typical day)

3.4.1.1 Beta and Weibull probability distribution functions

Beta distribution function

Beta probability distribution function is a model that can be used to describe the random behaviour of the solar irradiance. Usually, for the same hour of a typical day in a season, the irradiance data have a bimodal distribution function. The data are divided into two groups, each group having a unimodal distribution function [68, 70, 71]. It is expressed as follows:

$$f_b(s) = \begin{cases} \dfrac{\Gamma(\alpha+\beta)}{\Gamma(\alpha)\Gamma(\beta)} * s^{(\alpha-1)} * (1-s)^{(\beta-1)} & for\ 0 \le s \le 1, \alpha \ge 0, \beta \ge 0 \\ 0 & otherwise \end{cases} \quad (3.4)$$

where,

$f_b(s)$: is the Beta distribution function of s. α, β are the parameters of the Beta distribution function

s: is the solar irradiance kW/m^2.

In order to find the parameters of the Beta distribution function, the mean (μ) and standard deviation (σ) of the random variable*s* are calculated as follows:

$$\beta = (1-\mu) * (\frac{\mu * (1+\mu)}{\sigma^2} - 1) \tag{3.5}$$

$$\alpha = \frac{\mu * \beta}{1-\mu} \tag{3.6}$$

Weibull distribution function

Wind speed variations can be described by the Weibull function shown in Equation (3.7) [72, 73].

$$f_w(v) = \frac{k}{c}\left(\frac{v}{c}\right)^{k-1} \exp\left[-\left(\frac{v}{c}\right)^k\right] \tag{3.7}$$

Where k is called the shape index, and c is called the scale index. When the shape index k equals 2, the pdf is called a Rayleigh pdf ($f_r(v)$) as given in Equation (3.8). This pdf mimics most wind speed profiles; therefore, it is used in this study to model the wind speed for each time segment.

$$f_r(v) = \left(\frac{2v}{c^2}\right) \exp\left[-\left(\frac{v}{c}\right)^2\right] \tag{3.8}$$

The Rayleigh scale index c can be calculated using the following approximation:

$$c \approx 1.128 v_m \tag{3.9}$$

3.4.1.2 DG units modeling

The model is conducted as follows:

1. Each year is divided into four seasons, and each season is represented by any day within that season. For each season, these data are used to generate a typical day's frequency distribution of wind speed and irradiance measurements. Furthermore, the day which represents a season is divided into 24 hours of segments (time segments). Each segment refers to a particular hourly interval of the entire season. As a result, there are 96 time segments for the year (24 for each season). Consider a month to be 30 days, each segment has 270 wind speed and irradiance level data points (3 years x 30 days per month x 3 months per season).
2. The mean and standard deviation for each time segment are calculated
3. The Beta and Weibull probability density functions are generated for each hour using the mean and standard deviation for each segment.

   Figure 3-4 summarizes the steps 1 to 3.

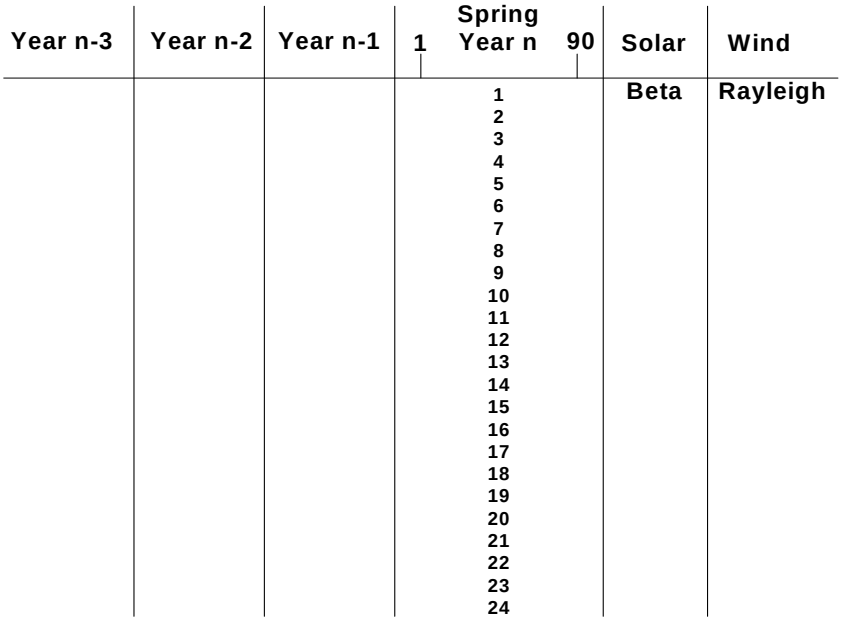

Figure 3- 4: Modeling of renewable resources from three years of historical data

4. The Beta and Weibull probability density functions are divided into states (periods) to incorporate the output power of the solar DG and wind-based DG units. The number of states is chosen carefully, as a small number of states will affect the accuracy, while a large number will increase the problem's complexity. In this , the state is adjusted to be 0.1 kW/m^2 for solar irradiance, and 1m/s for wind speed.
5. The corresponding output power of the PV module and wind turbine in each state are

calculated using the PV module characteristics and wind turbine power performance curve.

3.4.1.3 PV module output power

After the implementation of Beta probability density functions and division it into states (as in step 4), the PV output power can be obtained from the PV module. An example of a PV module characteristic is shown in Figure 3-5. It can be calculated using the following equations:

$$Tc_y = T_A + s_{ay}\left(\frac{N_{OT} - 20}{0.8}\right) \tag{3.10}$$

$$Iy = s_{ay}[I_{sc} + K_i(Tc - 25)] \tag{3.11}$$

$$V_y = V_{oc} - K_v * Tc_y \tag{3.12}$$

$$P_{Sy}(s_{ay}) = N * FF * V_y * I_y \tag{3.13}$$

$$FF = \frac{V_{MPP} * I_{MPP}}{V_{oc} * I_{sc}} \tag{3.14}$$

where

T_{cy}	is the cell temperature ^{o}C during state *y;*
T_A	is the ambient temperature ^{o}C.K_v;
K_i	is the current temperature coefficient A/^{o}C. of cell in ^{o}C;
K_v	is the voltage temperature coefficient V/^{o}C;
N_{OT}	is the nominal operating temperature;
FF	is the fill factor;
I_{sc}	is the short circuit current in A;
V_{oc}	is the open-circuit voltage in V;
I_{MPP}	is the current at maximum power point in A;
V_{MPP}	is the voltage at maximum power point in V;

P_{Sy} is the output power of the PV module during state *y*;

s_{ay} is the average solar irradiance of state *y*.

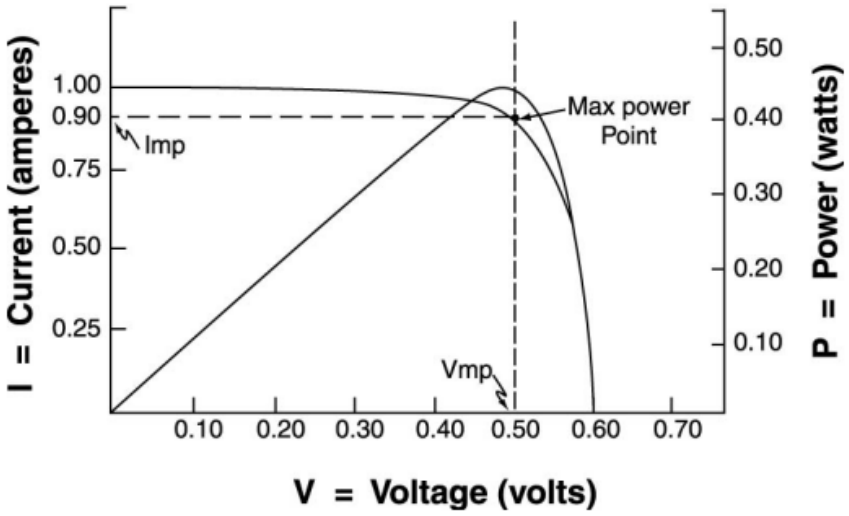

Figure 3- 5: An example of typical current and power characteristics of a solar cell [74]

3.4.1.4 Wind turbine output power

After the implementation of the Weibull probability density functions and division it into states (as in step 4), the wind turbine output power can be obtained from the wind turbine power performance curve. An example of a typical wind turbine power performance curve is illustrated in Figure 3-6. The output power can be calculated using Equation (3.15).

$$P_{Vw}(v_{aw}) = \begin{cases} 0 & 0 \le v_{aw} \le v_{ci} \\ P_{rated} * \dfrac{(v_{aw} - v_{ci})}{(v_{aw} - v_{ci})} & v_{ci} \le v_{aw} \le v_r \\ P_{rated} & v_r \le v_{aw} \le v_{co} \\ 0 & v_{co} \le v_{aw} \end{cases} \quad (3.15)$$

where,

v_{ci} is the cut-in speed of the wind turbine;

v_r is the rated speed of the wind turbine;

v_{co} is the cut-off speed of the wind turbine;

P_{Vw} is the output power of the wind turbine during state *w;*

v_{aw} is the average wind speed of state *w.*

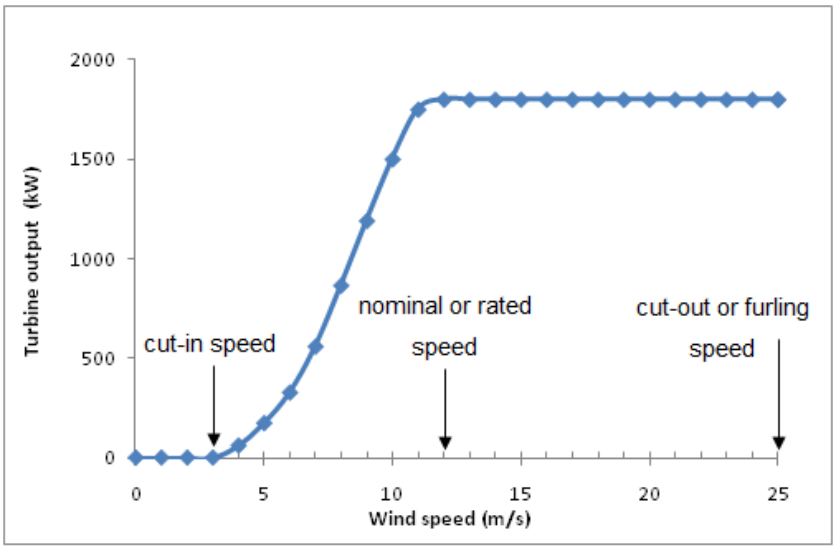

Figure 3- 6: An example of typical power output curve wind turbine (Vestas V90-1.8 MW)

3.4.2 **Step 2: Optimization**

The proposed method starts by reading the input data which are probabilistic generation-load model, candidate buses list, and distribution network data. Then, the procedure of the proposed optimization is illustrated in a flow chart in Figure 3-7.

3.4.2.1 Objective function

Based on Section 3.3, the DG placement and sizing, with an objective of increasing the voltage stability margin, can be formulated by increasing the voltage of the system using DG units. Equation (3.16) is obtained from [75] and is used to improve the voltage profile of the system, thus, it can be used to improve the voltage stability margin of the system. This equation is modified to include the

probabilistic nature of the DG generation as in Equation (3.17).

$$V_n = \frac{V_{P,with\ DG}}{V_{P,without\ DG}} \tag{3.16}$$

where,

$V_{P,with\ DG}$ The voltage profile of the system with DG units;

$V_{P,without\ DG}$ The voltage profile of the system without DG units;

V_P $= \sum_{i=1}^{m} V_i L_i k_i$

V_i The voltage magnitude at bus i;

L_i The load demand at bus i;

k_i The weighting factor for load bus i;

m The total number of load buses in the distribution system.

$$Maximize \qquad V_{index} = \frac{(\sum_{n=1}^{N} V_n\ pr_n)}{96} \qquad n = 1, 2, ...N \tag{3.17}$$

Where,

N The number of load and DG generation combination;

Pr_n The probability of each combination;

96 Time segments (hours) for the year (24 for each season);

The highest V_{index} implies the best location for the installation of the DG units in term of improving the voltage profile. The following attributes show the impact of the DG units.

$$V_{index} \begin{cases} < 1: \text{ DG units will worsen the voltage profile} \\ = 1: \text{ DG units will not impact on the voltage profile} \\ > 1: \text{ DG units will improve the voltage profile} \end{cases} \tag{3.18}$$

A weighting factor k_i is chosen based on the importance and criticality of different loads. In this thesis, the weighting factor is designed to be a ratio of the load demand at a specific bus to total demand as in Equation (3.19). This means the bus that has highest load demand will have the highest k_i factor. The rationale behind this design is to improve the voltages in the buses that have high power demand, and consequently improve the voltage stability margin.

$$k_i = \frac{p_{i,n}}{p_{TD,n}} \tag{3.19}$$

where,

$p_{i,n}$ The power demand at bus i at state n;

$p_{TD,n}$ The total power demand of the system at state n.

Starting with a set of equal weighting factors, modifications can be made and, based on an analysis of the results, the set that will lead to the most acceptable voltage profile on a system-wide basis can be selected. It should be noted that if all the load buses are equally weighted, the value of k_i is given as $k_1=k_2=k_3=K_m = 1/m$ [75]. This voltage profile expression allows the important load to have a strong impact, because the weighting factor can be based on the important bus.

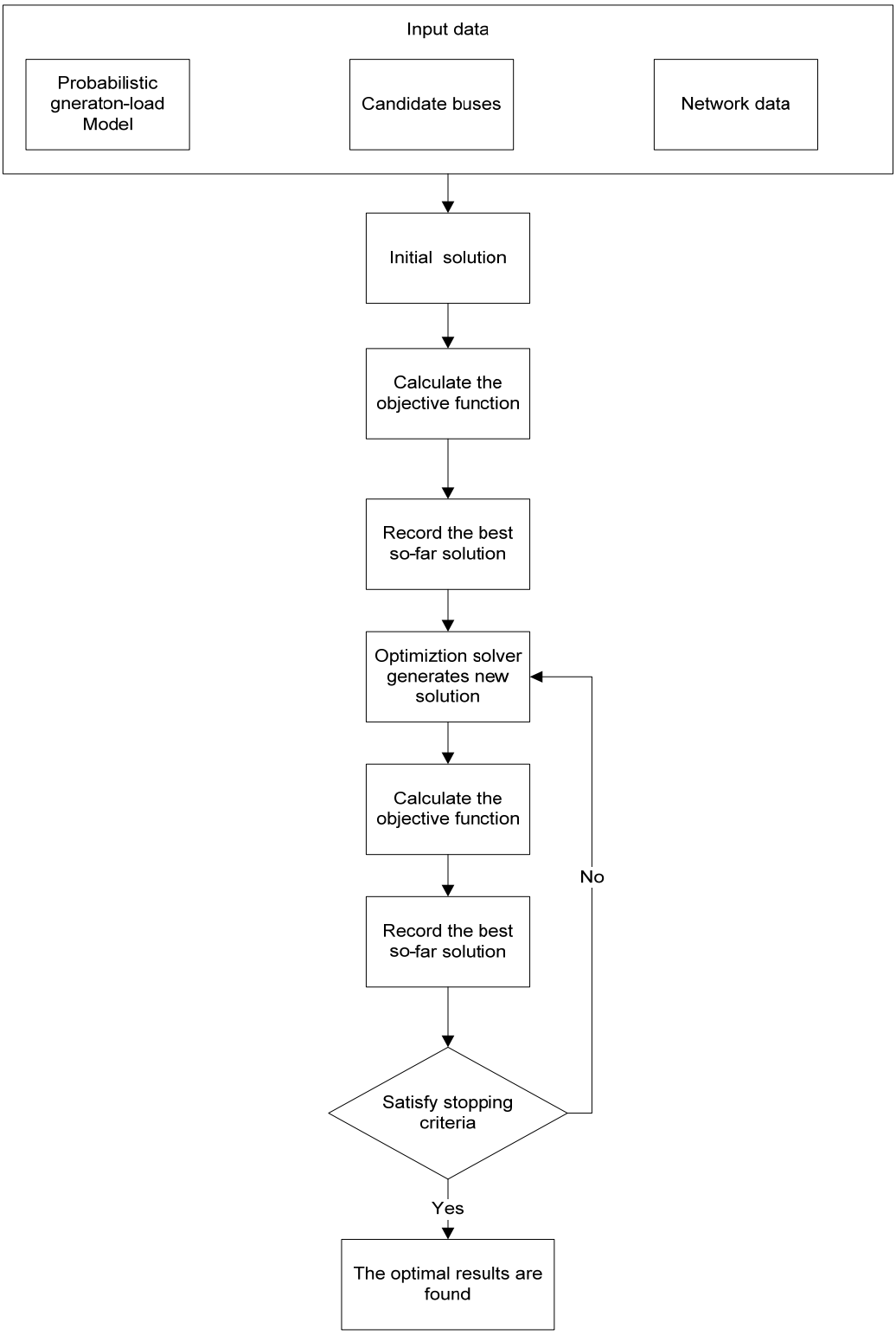

Figure 3- 7: A flow chart illusitrates the proposed optimization method

3.4.2.2 Constraints

- Power flow equations:

$$P_{G_{n,1}} + C(n,1) * P_{DGD_i} + C(n,2) * P_{DGW_i} + C(n,3) * P_{DGS_i} - C(n,4) * P_{D_i} = \sum_{j=1}^{m} V_{n,i} * V_{n,i} * Y_{ij} * \cos(\theta_{ij} + \delta_{n,j} - \delta_{n,i}) \ \forall i,n \quad (3.20)$$

$$Q_{G_{n,1}} - C(n,4) * Q_{D_{n,i}} = -\sum_{j=1}^{m} V_{n,i} * V_{n,i} * Y_{ij} * \sin(\theta_{ij} + \delta_{n,j} - \delta_{n,i}) \quad \forall i,n \quad (3.21)$$

where

P_{G1}	The substation active power injected;
Q_{G1}	The substation reactive power injected;
P_{DGDi}	The rated power of the dispatchable DG connected at bus *i;*
P_{DGWi}	The rated power of the wind-based DG connected at bus *i;*
P_{DGSi}	The rated power of the solar DG connected at bus *i;*
Q_{DGDi}	The rated reactive power of the dispatchable DG connected at bus *i;*
Q_{DGWi}	The rated reactive power of the wind-based DG connected at bus *i;*
Q_{DGSi}	The rated reactive power of the solar DG connected at bus *i;*
P_{Di}	The peak active load at bus *i;*
Q_{Di}	The peak reactive load at bus *i;*
Vn,i	The voltage at bus i during state n;
C	A matrix of 4 columns that include all possible combinations of the wind output power states, solar output power states, and load states (i.e., column 1,2 and 3 represent the output power of the dispatchable DG, wind-based DG and the solar DG as a percentage of their rated power, and column 4 represents the different load levels;

- Branch current equation:

$$I_{n,ij} = \left|Y_{ij}\right| * \left[(V_{n,i})^2 + (V_{n,j})^2 - 2 * V_{n,i} * V_{n,j} * \cos(\delta_{n,j} - \delta_{n,i})\right]^{1/2} \quad \forall n, i, j \tag{3.22}$$

where,

$I_{n,i,j}$: The current in the feeder connecting buses *i* and j during state *n*.

- Slack bus voltage and angle (the slack in this system is assumed to be bus 1:

$$V_{n,1} = 1.025$$
$$\delta_{n,1} = 0.0 \tag{3.23}$$

- Voltage limits at the other buses:

$$0.95 \le V_{n,i} \le 1.05 \quad \forall\, i \notin substation\, bus,\ n \tag{3.24}$$

- Feeder capacity limits:

$$0 \le I_{n,ij} \le I_{ij_{\max}} \qquad \forall i, j, n \tag{3.25}$$

- Maximum penetration on each bus:

$$P_{DGD_i} + P_{DGW_i} + P_{DGS_i} \le 10MW \tag{3.26}$$

The maximum penetration of DG capacity should not exceed 10 MW at each bus of the candidate buses.

- Maximum penetration of DG units on the system:

$$\sum_{i=1}^{m} P_{DGD_i} + \sum_{i=1}^{m} CF_w P_{DGW_i} + \sum_{i=1}^{m} CF_s P_{DGS_i} \le y * \sum_{i=1}^{m} P_{D_i} \tag{3.27}$$

where,

y : The maximum penetration limit as a percentage of the peak load. For the penetration level not to exceed 30%, y equal 0.3.

- Candidate buses:

$$P_{DGSi}, P_{DGWi}, P_{DGDi} = 0 \qquad \forall i \in AB - CB \tag{3.28}$$

where,

AB: All the buses of the distribution system;

CB: The set of the candidate buses.

- Discrete size of DG units:

$$P_{DGW_i} = \text{int}_i \times 1.1\ MW \qquad \forall i \in Can\ buses \tag{3.29}$$

where,

int_i : Integer variables.

3.5 System under study

Figure 3-8 shows a single-line diagram of a practical rural distribution system of 41 buses obtained from a local distribution utility. The system peak load is 16.18 MVA and the substation at bus 1 is used to feed the system with a capacity of 300 A. The system's detailed line and load data can be found in [68]. The voltage at the substation is set to 1.025 p.u.

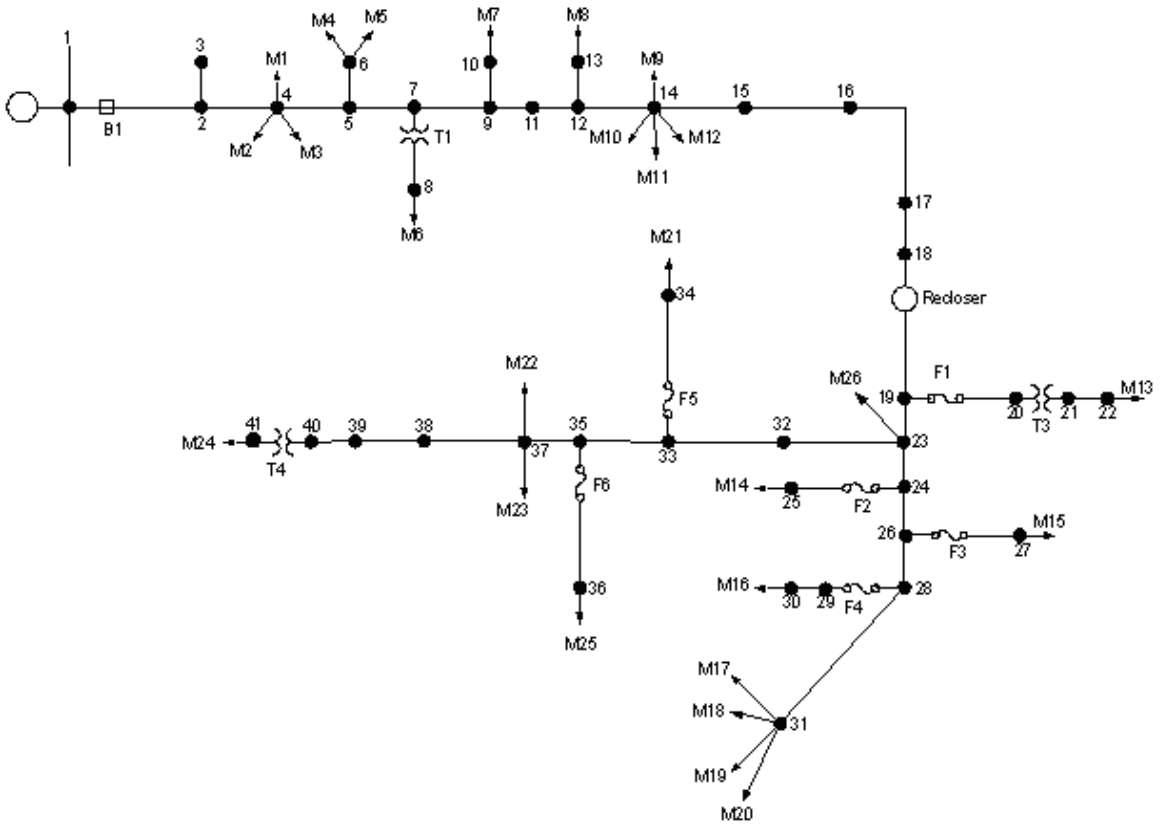

Figure 3- 8: A distribution test system of 41 buses

3.6 Results

This section outlines the results obtained for this study. The results start with the identification of the candidate buses for DG installation obtained by using the sensitivity analysis. This is followed by showing the impact of DG units on voltage stability. Finally, the locations and sizes of the selected DG units are given so as to improve the voltage stability margins.

3.6.1 **Results of Candidate buses for the DG units installation**

In Figure 3-9, the selection is achieved by developing 26 case studies (The cases are equal to the number of the system buses which are located in the main feeders). In each case, a DG unit is installed at a certain bus, and the changes of the system voltages (ΔV) are observed. The installed DG unit is assumed to generate constant power of 4.5 MW at unity power factor (about 30% of the penetration level), and the system load demand is taken at the peak value. In addition, analysis for penetration level of 10% and 20% are shown Figures 3-10 and 3-11.

Figures 3-9 to 3-11 represent the impact of ΔV/ΔP of selected buses: 40, 28, 19, and 4. The x-axis shows the buses' numbers and y-axis shows the changes in ΔV due to the injection of the DG unit. This figure shows that the buses from 19 to 41 can improve the voltage profile better than the buses from 1 to 18. Moreover, the order of the most sensitive buses can be determined using Equation (3.16), and considering the k_i as in Equation (3.19). The most sensitive buses are 40, 39, 38, 37, 35, 33, 32, 23, 24, 19, 26, and 28.

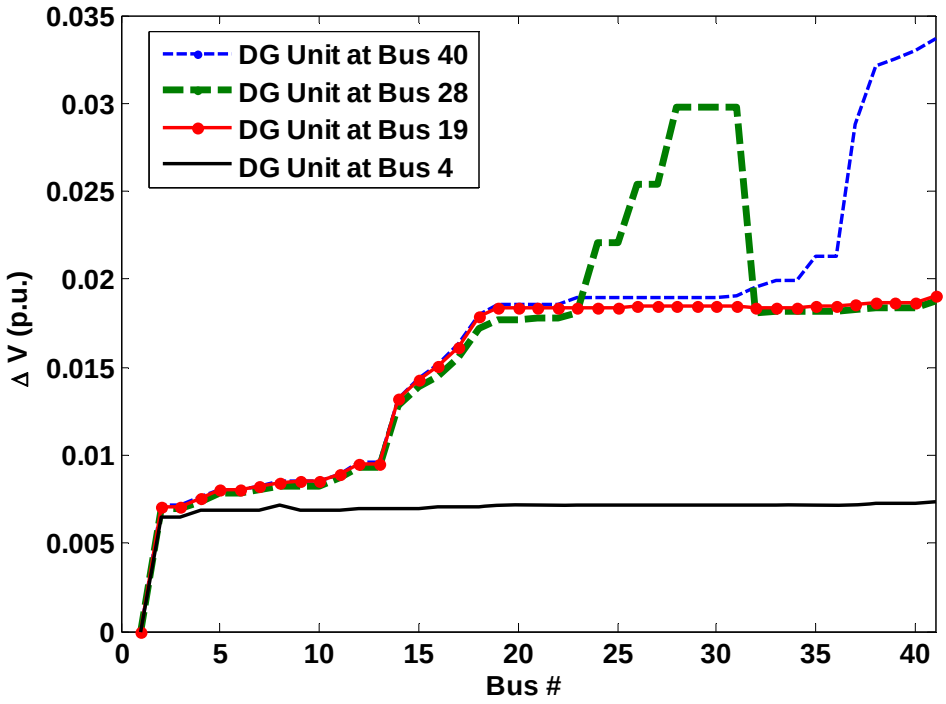

Figure 3- 9: Results of voltage sensitivity analysis (penetration level is 30%)

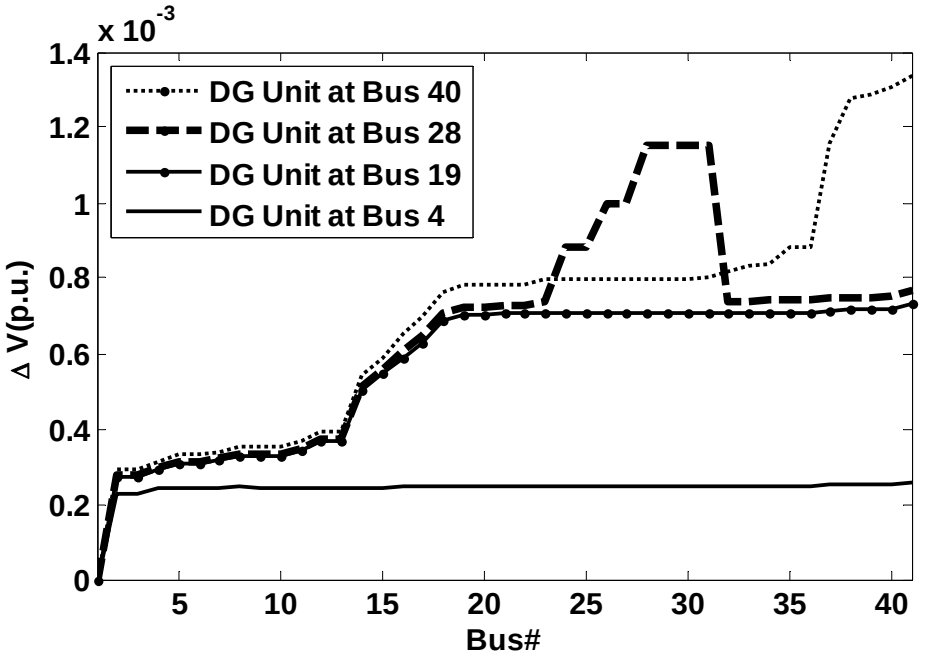

Figure 3- 10: Results of voltage sensitivity analysis (penetration level is 10%)

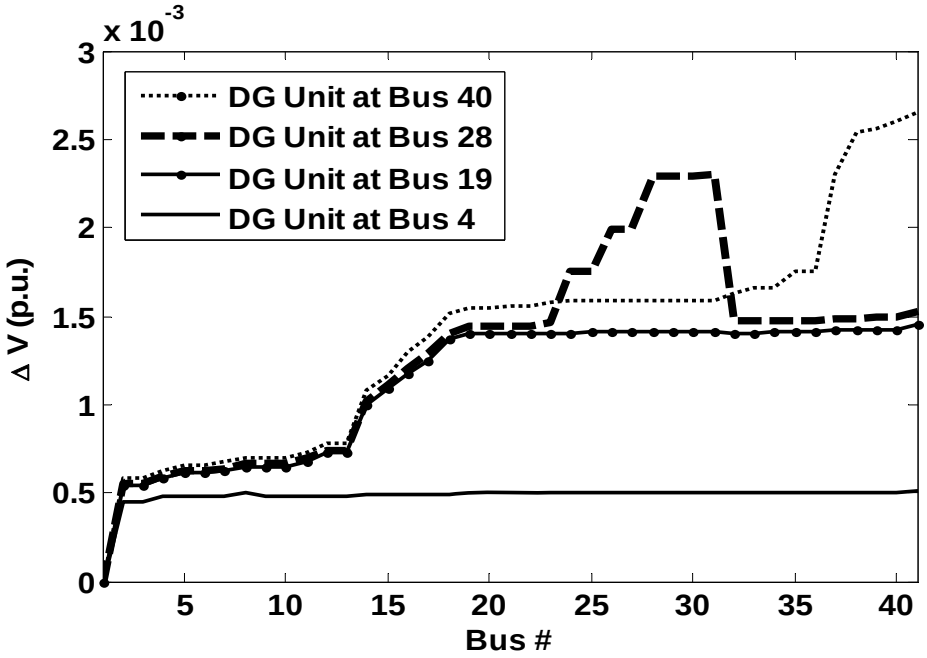

Figure 3- 11: Results of voltage sensitivity analysis (penetration level is 20%)

3.6.2 **Results of the impact of the DG units on voltage stability**

The DG unit is installed at bus 40. This P-V curve (Figure 3-12) represents the voltage stability at bus 41. The load demand in bus 41($P_{o,41}$) is 2.166 MW which corresponds to λ=1. When the DG unit generates 4.4 MW, the voltage moves from V_1 (0.924 p.u) to V_2 (0.959 p.u.), and λ_{max} moves from λ_{max1} (2.71) to λ_{max2} (3.09). Thus the voltage stability margin is improved by 0.82 MW.

Figure 3-12 shows the impact of the DG units on voltage stability margin (V_1 moves to V_2) and the maximum loadability (λ_{max1} moves to λ_{max2}). This result only represents one size and location. However, the size and location can also have an impact on voltage stability.

The rest of this section presents the impact of the size and location of the DG units on both the voltage and the maximum loadability. The study of the impact of the DG size is conducted by installing one DG unit in one of the candidate buses, and then finding the maximum loadability and the voltage of the system. The DG unit is varied from 0 to 16 MW (Note: The DG unit is varied to approximately 100% of the penetration level in order to study the impacts of the DG size on voltage stability margin in different locations. However, for the DG placement and sizing "Section 3.4.2", the penetration level is restricted to Equations (3.26) and (3.27). Then the same method is applied for the other candidate buses.

Alternatively, the impact of the DG location study can be achieved by developing 26 cases (the cases are equal to the number of the system buses which are located in the main feeders). In each case, a DG unit is installed at a certain bus, and the maximum loadability (λmax) is observed. The installed DG unit is assumed to generate constant power of 4.4 MW. In both studies, the DG unit is operated at unity power factor; the system load demand is taken at the peak value. Figures 3-13 and 3-14 show the changes of the maximum loadability of both studies. Placing a DG unit in bus 40 improves the voltage stability margin more than the other candidate buses because the voltage at bus 40 is more sensitive to the real power (Figure 3-9). Also, bus 41 has high load demand, therefore placing the DG unit on bus 40 makes the upper stream feeder gain more capacity for power loading.
However, if the DG unit is placed on bus 28, the feeders will gain less capacity because the load demand downstream is low compared to bus 41. Therefore, when the DG power at bus 28 increases, the current reverses to the upper stream. In this situation, the feeder between bus 23 to 41 will not gain extra capacity for power loading.

Furthermore, Figure 3-13 shows the impact of two DG units. They are placed in bus 40 and 28. Both DG units are varied from 0 to 8 MW; thus, the total of generation for both units is 16 MW (approximately 100% of the penetration level). When the two DG units are added, the downstream feeders (from bus 23 to 31, and from bus 23 to 41), and the upstream feeder (from bus 1 to 23), gain more capacity. Therefore, this capacity is reflected in the increase of the voltage stability margin (λ_{max} =3. 37). However, this result is still lower than that of installing one DG unit at bus 40 (λmax =3. 404). Thus, applying an optimization method can solve the problem of placement and sizing of the DG units to improve the voltage stability margin.

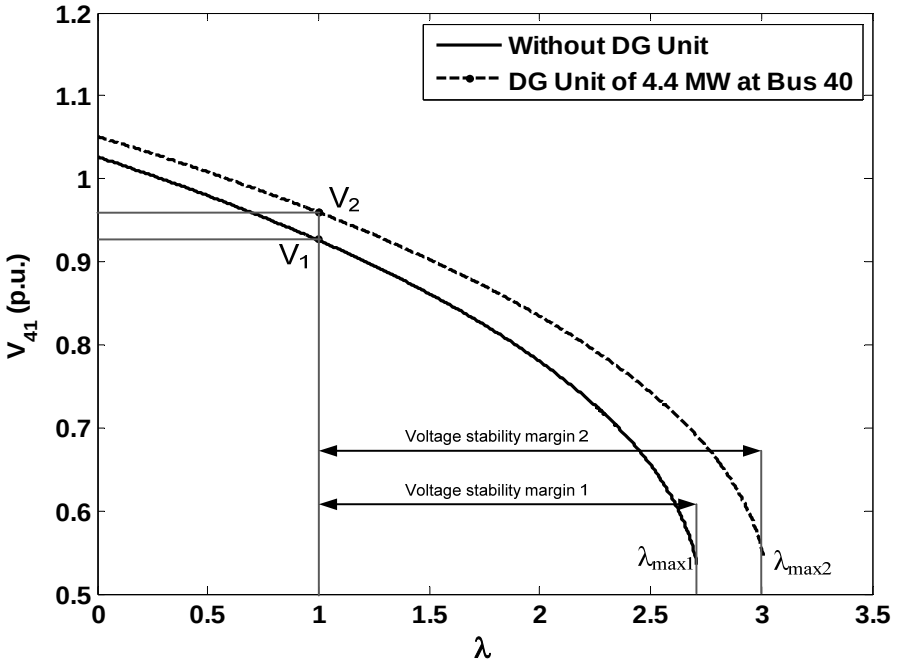

Figure 3- 12: Impact of DG unit on maximum loadability and voltage stability margin at bus 41

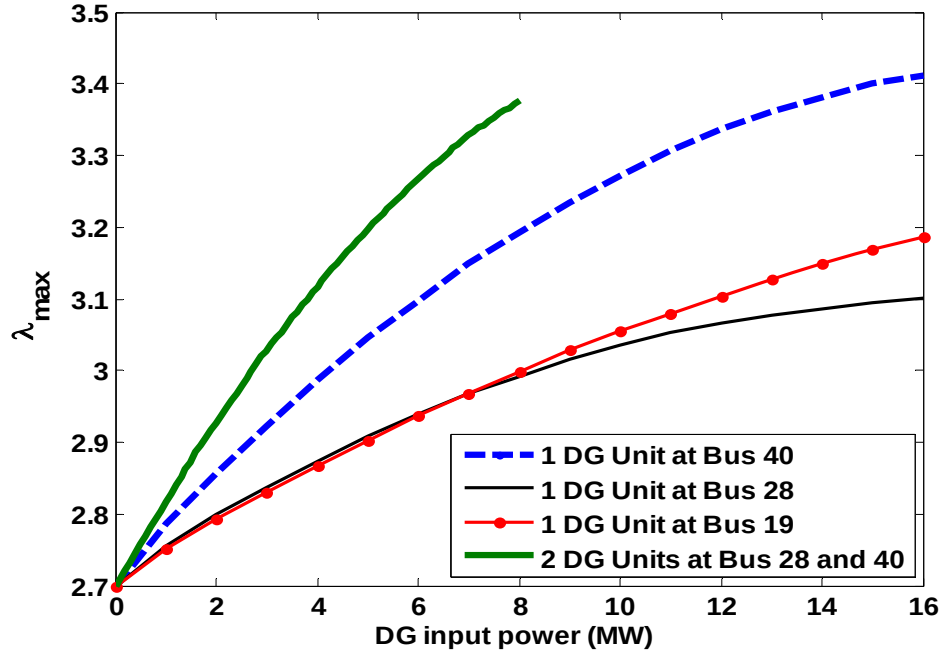

Figure 3- 13: Impact of the size of DG units on maximum loading

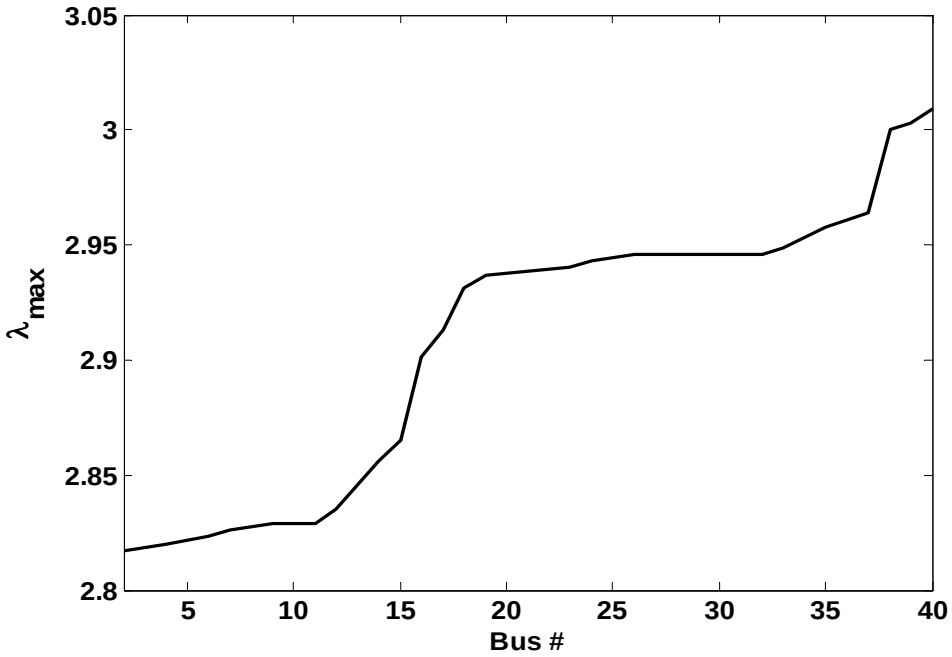

Figure 3- 14: Impact of the location of DG units on maximum loading

3.6.3 **Results of the DG sizes and locations**

The results for the five scenarios which are presented in Section 3.4 are given in Tables 3-2 and 3-4. These results were obtained by the optimization formulation which is proposed in Section 3.4.2. The first column demonstrates the candidate buses for the DG installation. These candidate buses are obtained by the sensitivity analysis in Section 3.3 and 3.6.1. The other columns show the sizing and siting of DG units in each scenario.

Table 3- 2: Results of DG location and size, scenarios (1-4)

Candidate Buses	Scenarios			
	1	2	3	4
19	0	0	0	0
23	0	0	0	0
24	0	0	0	0
26	0	0	0	0
28	0	0	1.1MW	1.55MW
32	0	0	0	0
33	0	0	0	0
35	0	0	0	0
37	0	0	0	0
38	0	0	2.2MW	1.92MW
39	0	0	0	0
40	0	4.5MW	6.6MW	9.47MW
Total size	0	4.5MW	9.9MW	12.94MW

Table 3- 3: Results of DG location and size, scenarios (5)

Candidate Buses	Scenarios		
	5		
	Wind (MW)	Solar (MW)	Dispatchable (MW)
19	0	0	0
23	0	0	0
24	0	0	0
26	0	0	0
28	0	0.87	0
32	0	0	0
33	0	0	0
35	0	0	0
37	0	0	0
38	0	0	0
39	0	0	0
40	3.3	3.38	1.2
Total size	3.3	4.25	1.2

In Tables 3-2 and 3-3, the simulation of the optimization formulation placed and sized the DG units in buses 40, 38, and 28. In all scenarios, the highest DG rating is placed in bus 40. This placement is reasonable, because bus 40 is located at the far end of the distribution system and has low voltage profile. However, if the optimization constraints of the voltage and current are violated, then the second option will be bus 38. Bus 28 is also sensitive to the DG penetration as shown from Figure 3-9. As a result, the simulation has considered this bus (bus 28) for the DG placement and sizing.

The total size of the wind DG units in scenarios 3 and 5 is lower than the solar units in scenarios 4 and 5. This result is logical since the capacity factor of the wind turbine is higher than the solar photovoltaic generator.

Tables I and II show the results when the DG units are operating at unity power factor. On the other hand, the utilities that allow the DG units to operate in fixed power factor mode (0.95 lagging to 0.95 leading) need more elaboration. In this case, the DG units will have more chance to improve the

voltage stability margin if they are operating in leading power factor and supporting the system with reactive power. Sensitivity analysis of ΔV/ΔQ is conducted to test the most sensitive buses as in Equation (2.4). The results show that the most sensitive buses are the same buses as of ΔV/ΔP sensitivity as shown in Figure 3-15 , but with higher magnitude of ΔV due to the high sensitivity of reactive power changes to the voltage profile of the system. In addition, the condition of operating DG units in fixed power factor mode (0.95 lagging to 0.95 leading) should be considered as constraints in the formulation of the placement and sizing of the DG units. In addition, Equation (3.21) should be modified to include the reactive power generation as in Equation (3.30).

$$Q_{G_{n,1}} + C(n,1)*Q_{DGD_i} + C(n,2)*Q_{DGW_i} + C(n,3)*Q_{DGS_i} - C(n,4)*Q_{D_{n,i}} = -\sum_{j=1}^{m} V_{n,i}*V_{n,i}*Y_{ij}*\sin(\theta_{ij} + \delta_{n,j} - \delta_{n,i}) \quad \forall i,n \tag{3.30}$$

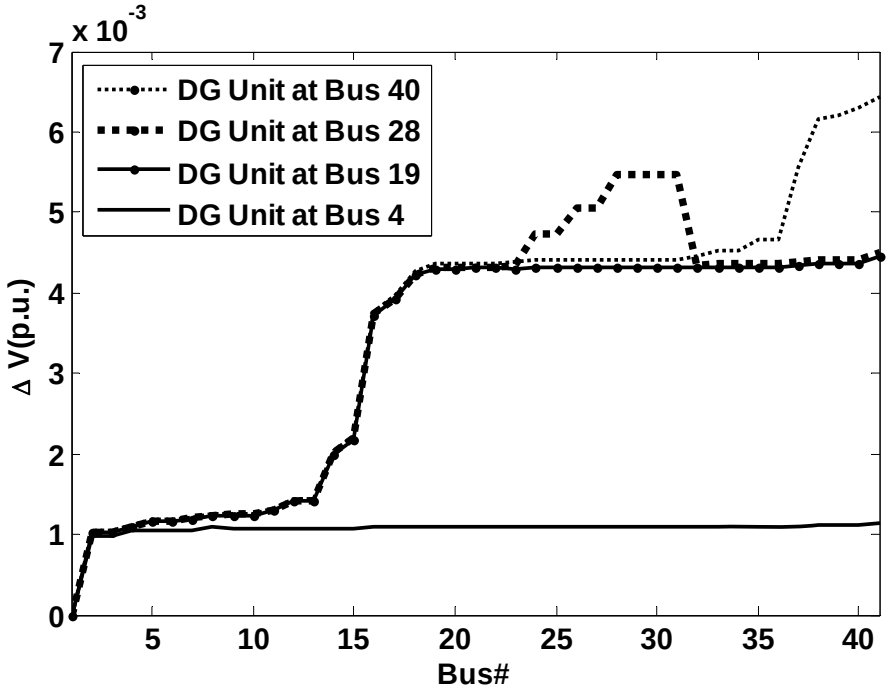

Figure 3- 15: Results of voltage sensitivity analysis ΔV/ΔQ

The simulation results of DG units that operate in fixed power factor mode (0.95 lagging to 0.95 leading) are included in this thesis as given in Table 3-4. These results show that the dispatchable DG units in scenario 1 are placed in bus 40. However, for the wind in scenario 3 and solar in scenario 4, the higher ratings of the DG units are placed in bus 19. The results in (scenario 3 and 4) are

reasonable because the sensitivity analysis shows that bus 19 is less sensitive to the injection of real and reactive power than bus 40. In addition, the voltage is more sensitive to the change in reactive power than real power. As a result, placing a DG unit operating in leading power factor is better upstream, to avoid the violation of the voltage constraints.

In scenario 5 (Table 3-4), all the DG units are operating at 0.95 leading power factor. The renewable DG units are sized and placed in bus 19, while the dispatchable DG unit is sized and sited in bus 40. In this scenario, the ratings of the DG units are smaller compared to the other scenarios, because the dispatchable DG units are operating at constant real and reactive power (their capacity factor equals 1), therefore it improves the voltage stability constantly during the year. Thus, the constant operation of the dispatchable DG unit makes less dependence on renewable energy DG units in improving the voltage stability margin, and hence their ratings are small.

Table 3- 4: Results of DG location and size (DG units operate between 0.95 leading or lagging power factor)

Scenario	Type of DG	Location	Rating MVA	Power factor
1	Base case : No DG installed			
2	dispatchable	Bus 40	4.5	0.95 leading
3	wind	bus 19 bus 40	8.8 1.1	0.95 leading Unity
4	Solar	Bus 19 Bus 28 Bus 40	9.7 1.06 2.38	0.95 leading Unity Unity
5 (mix)	dispatchable wind solar	Bus 40 Bus 19 Bus 19	0.82 3.3 4.2	0.95 leading 0.95 leading 0.95 leading

3.7 Discussion

In this chapter, a method of DG units allocation is proposed. This method targets utilizing the DG units to improve the voltage stability margin. It considers the probabilistic nature of both loads and

renewable DG generation. The load is modeled by the IEEE-RTS system, while the renewable DG resources are modeled by using three years of historical data that have been provided from the site under study. These data are used to model the solar irradiance and wind speed by Beta and Weibull probability distribution functions, respectively. The candidate buses for the DG units' installation are selected based on the sensitivity to the voltage. Simulation results indicate that DG size and location can have positive impacts on the voltage stability margin. Therefore, an optimization method can be used to determine the locations and sizes of the DG units, to achieve the target of improving the voltage stability margin. Furthermore, formulating the problem using an optimization method helps to avoid any violation of the system limits, such as buses' voltage and feeders' current. Simulation shows that placing and sizing DG units is affected by the operating condition of the DG units (unity power factor or between 0.95 lead or lag). When the DG units operate at unity power factor, they are recommended to be placed in the most sensitive voltage buses in order to improve the voltage stability margin with a condition of not violating the system voltage and current limits. However, if the utility allows operating the DG units between 0.95 lead and 0.95 lag, the reactive power during leading power factor could improve the voltage stability margin due to the more sensitivity between $\Delta V/\Delta Q$ than $\Delta V/\Delta P$. Therefore, the DG units with higher rating might be placed in upstream of a radial distribution system to keep the system operating within the allowed limits of voltage and currents.

Chapter 4

Proximity to Voltage Instability Analysis Using Small-Signal Method with high Penetration Level of Distributed Generation

4.1 Introduction

Distributed Generation (DG) units are being increasingly connected at low and medium voltage level in distribution systems. Most of the modern DG units, such as wind, PV, micro-turbines and fuel cells, are equipped with power electronic converters at their terminals. The power electronic converter plays a vital role to match the characteristics of the DG units and the requirements of the grid connections, such as frequency, voltage, control of active and reactive power, and harmonic minimization. A widespread use of these DG units in distribution systems will be seen in the near future. Due to the power electronics interfacing, these DG units have negligible inertia. Thus, they make the system potentially prone to oscillations resulting from the network disturbances. Therefore, one of the ultimate goals of this thesis is to model and analyze the impact of grid connected mode DG units on the proximity of the voltage instability with high penetration level of DG units. This goal is achieved by stressing the system incrementally until it becomes unstable, and at each operating point small-signal analysis and modal analysis are applied.

4.2 Voltage stability analysis and small-signal analysis

Voltage stability analysis has been presented using many techniques, including static and dynamic methods. The static techniques and the impacts of the DG units on voltage stability are discussed in Chapter 3 in Section 3.3. However, static analysis cannot determine the control action and the interactions between the integrated DG units in the system. The proximity to the voltage instability method can be used to determine those issues. This chapter presents this method, and it is accomplished by:

1. Apply static analysis using continuous power flow method. This is achieved by loading the system in steps of λ (as in Equation (2.8)) until the system becomes unstable, or reaches the maximum loadability.

2. Model the system under study using small-signal model. The model includes the DG units, their controllers, system networks and the load.
3. Apply small-signal stability analysis and sensitivity analysis at each loading step.

Small-signal stability

Small-signal stability analysis in power systems is achieved in the frequency domain using eigenvalue analysis. It is carried out by linearizing the mathematical model of the system and then solving the eigenvalues and eigenvectors of the linearized model. This analysis will show the stability of the system with integrated DG units in each operating point (loading step). The system model is presented in the next section.

Sensitivity analysis

In a particular mode of operation, the sensitivity analysis can be achieved by observing the participation factor. The participation factor which is given in Equation (4.1) is a measure of the association between the state variables and the modes. This factor is equal to the sensitivity of the eigenvalue λ_i to the diagonal element of the system state matrix a_{kk} [30].

$$p_{ki} = \frac{\partial \lambda_i}{\partial a_{kk}} = \psi_{ik}\phi_{ji} \tag{4.1}$$

The participation factors can be calculated using left (ψ_{ik}) and right (ϕ_{ji}) eigenvectors.

4.3 System modeling

This part covers small-signal modeling of a distribution system with integrated DG units. The DG units are assumed to be inverter-based. The whole system with DG units is operating in grid-connected mode. Figure 4-1 depicts a block diagram of a complete small-signal model of this system. In grid-connected mode, the DG units act as PQ sources of power, which means they are controlled to supply constant active and reactive power to the network. This study divides the modeling of the system into three main components: the converter and its control, the loads, and the network. Then, all components are combined into one model to form the system model.

The state space equations of the DG units, loads, and the network are represented in the reference frame of the slack bus of the distribution system. The reference frame is considered the common

reference and all other components are translated to this common frame. The transformation technique in Equation (4.2) is presented in [76] and illustrated in Figure 4-2. The next parts of this section present the modeling of each system component.

$$\begin{aligned} \left[f_{DQ}\right] &= \left[T_i\right]\left[f_{dq}\right] \\ \left[T_i\right] &= \begin{bmatrix} \cos(\delta_i) & -\sin(\delta_i) \\ \sin(\delta_i) & \cos(\delta_i) \end{bmatrix} \end{aligned} \tag{4.2}$$

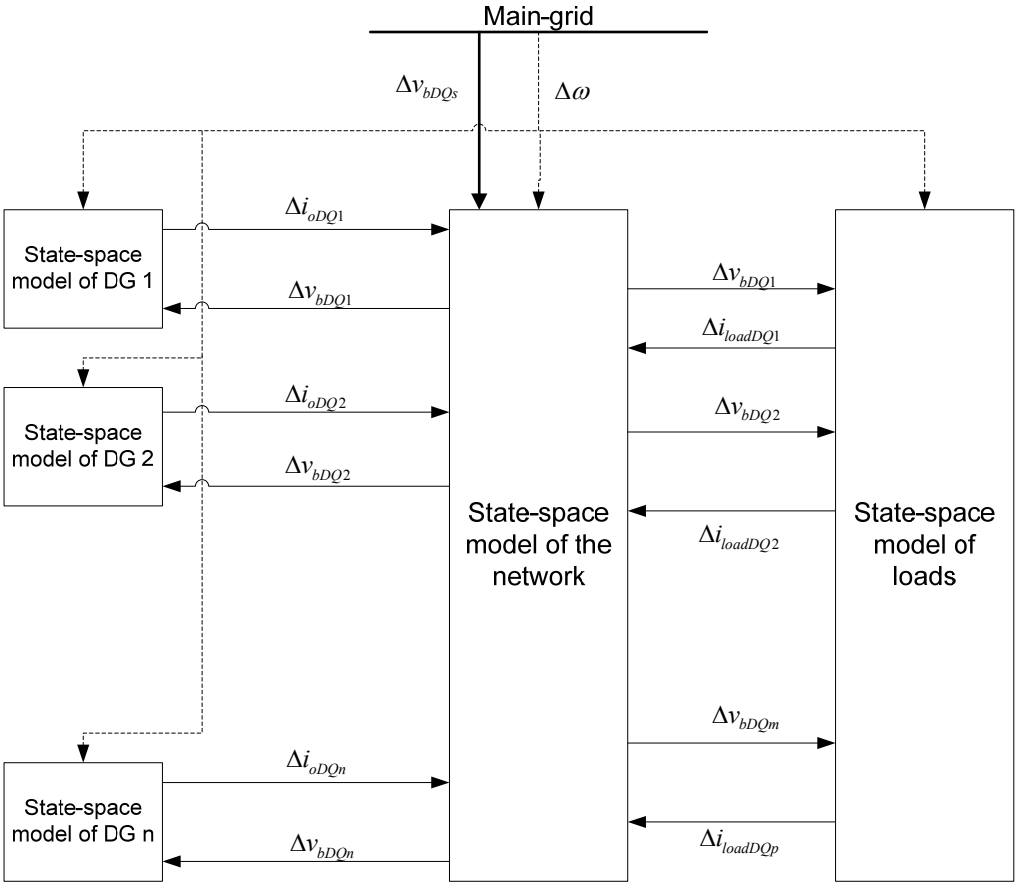

Figure 4- 1: A model of a distribution system with integrated DG units

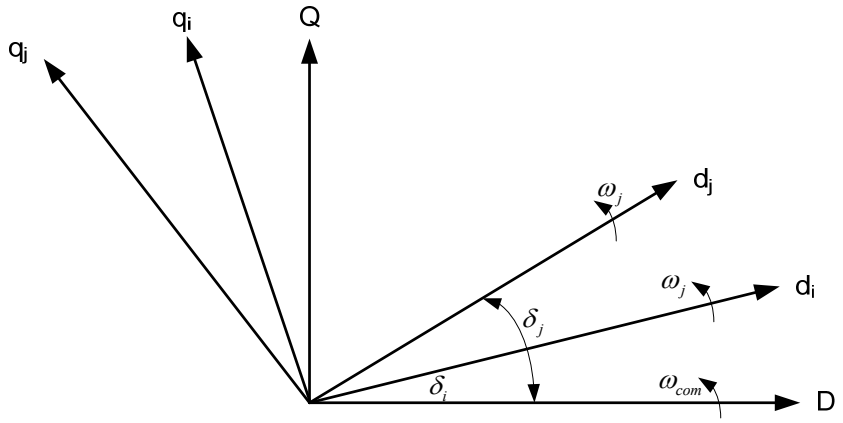

Figure 4- 2: Transformation of reference frame

4.3.1 **DG units modeling**

Figure 4-3 shows a schematic diagram of a DG inverter interface. It is composed of two subsystems: the inverter power circuit and the associated converter control. The DC-side of the converter is represented by a constant voltage (V_{DC}). In this study, the V_{DC} is assumed as an ideal source, so it doesn't introduce dynamic into the converter model. In fact, V_{DC} represents the prime source of the DG units and if the DC-side is not represented by an ideal source, its dynamic can be represented as a part of the converter circuit. The AC-side is represented by series connected R and L elements. R includes the on-state switch resistances, resistance of the series AC-side filter. L represents the inductance of the series filter [56]. The control consists of a power controller and a current controller. This section covers the small-signal model of each subsystem. Then, it combines the subsystems to represent a complete model of the inverter.

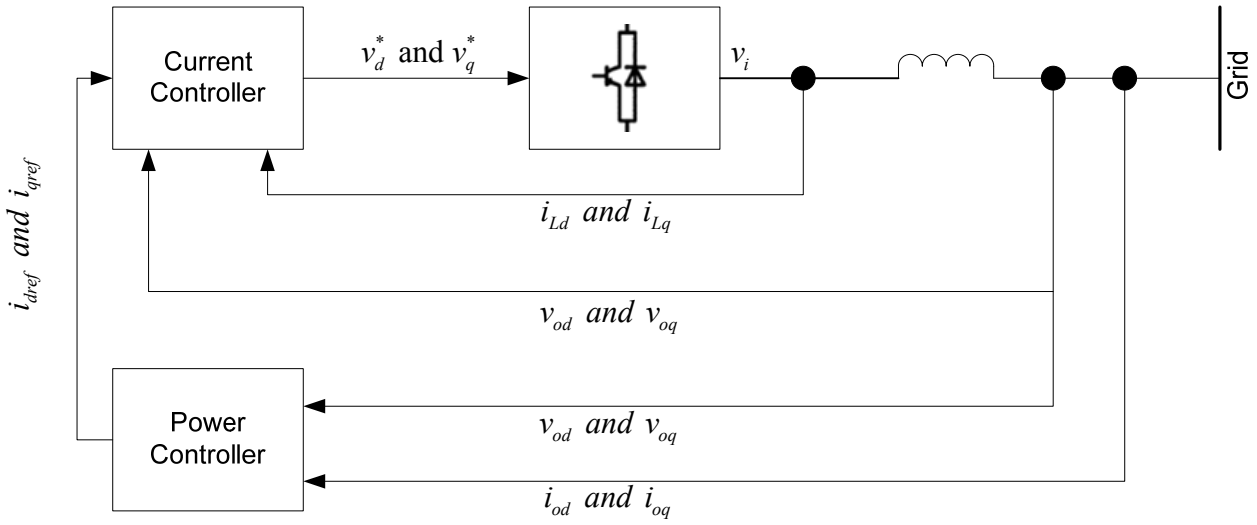

Figure 4- 3: Inverter-based DG unit

4.3.1.1 Power controller

Power controllers are used with DG units to operate in parallel with the utility grid, but they are designed to supply constant real and reactive power, as illustrated in Figure 4-4. They can also supply real and reactive power independently [24]. This technique can be summarized as follows: The instantaneous active (P_{cal}) and reactive (Q_{cal}) power components are calculated using the two-axis theory which is given in Equations (4.3) and (4.4). Then P_{cal} and Q_{cal} are compared to a reference value in order to obtain error signals. Next, the error signals are applied to a PI controller in order to obtain I_{dref} and I_{qref}. Both I_{dref} and I_{qref} are then used as reference signals to the current controller.

$$p_{cal} = \frac{3}{2}(v_{od}i_{od} + v_{oq}i_{oq}) \tag{4.3}$$

$$q_{cal} = \frac{3}{2}(v_{od}i_{oq} - v_{oq}i_{od}) \tag{4.4}$$

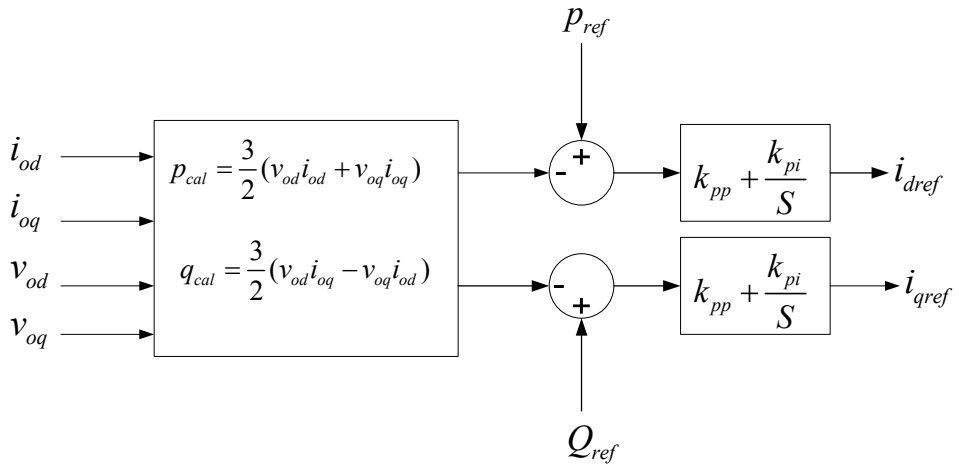

Figure 4- 4: Power controller

The state equations are expressed as follows,

$$\begin{aligned} \frac{d\phi_d}{dt} &= p_{cal} - p_{ref} \\ \frac{d\phi_q}{dt} &= q_{cal} - q_{ref} \end{aligned} \tag{4.5}$$

along with algebraic equations

$$\begin{aligned} I_{dref} &= k_{pp}(p_{cal} - p_{ref}) + k_{pi}\phi_d \\ I_{qref} &= k_{pp}(Q_{cal} - Q_{ref}) + k_{pi}\phi_q \end{aligned} \tag{4.6}$$

In order to model the small-signal state space of the power controller, the instantaneous active (P_{cal}) and reactive (Q_{cal}) power are linearized as follows:

$$\begin{bmatrix} \Delta p_{cal} \\ \Delta q_{cal} \end{bmatrix} = \begin{bmatrix} I_{od} & I_{oq} & V_{od} & V_{oq} \\ I_{oq} & -I_{od} & -V_{oq} & V_{od} \end{bmatrix} \begin{bmatrix} \Delta v_{od} \\ \Delta v_{oq} \\ \Delta i_{od} \\ \Delta i_{oq} \end{bmatrix} \tag{4.7}$$

Equation (4.7) can be extended to Equation (4.8), in order to simplify the inverter modeling.

$$\begin{bmatrix} \Delta p_{cal} \\ \Delta q_{cal} \end{bmatrix} = \begin{bmatrix} B_{p2}^{a} \end{bmatrix} \begin{bmatrix} \Delta v_{od} \\ \Delta v_{oq} \end{bmatrix} + \begin{bmatrix} B_{p2}^{b} \end{bmatrix} \begin{bmatrix} \Delta i_{od} \\ \Delta i_{oq} \end{bmatrix} \tag{4.8}$$

where,

$$B_{p2}^{a} = \begin{bmatrix} I_{od} & I_{oq} \\ I_{oq} & -I_{od} \end{bmatrix}, \; B_{p2}^{b} \begin{bmatrix} V_{od} & V_{oq} \\ -V_{oq} & V_{od} \end{bmatrix}$$

The linearized state space of the power controller is expressed as in Equation (4.9).

$$\begin{aligned} \begin{bmatrix} \Delta \dot{\phi}_d \\ \Delta \dot{\phi}_q \end{bmatrix} &= \begin{bmatrix} A_p \end{bmatrix} \begin{bmatrix} \Delta \phi_d \\ \Delta \phi_q \end{bmatrix} + \begin{bmatrix} B_{p1} \end{bmatrix} \begin{bmatrix} \Delta p_{ref} \\ \Delta Q_{ref} \end{bmatrix} + \begin{bmatrix} B_{p2}^{*} \end{bmatrix} \begin{bmatrix} \Delta p_{cal} \\ \Delta Q_{cal} \end{bmatrix} \\ \begin{bmatrix} \Delta i_{d\,ref} \\ \Delta i_{q\,ref} \end{bmatrix} &= \begin{bmatrix} C_p \end{bmatrix} \begin{bmatrix} \Delta \phi_d \\ \Delta \phi_q \end{bmatrix} + \begin{bmatrix} D_{p1} \end{bmatrix} \begin{bmatrix} \Delta p_{ref} \\ \Delta Q_{ref} \end{bmatrix} + \begin{bmatrix} D_{p2}^{*} \end{bmatrix} \begin{bmatrix} \Delta p_{cal} \\ \Delta Q_{cal} \end{bmatrix} \end{aligned} \tag{4.9}$$

Equation (4.9) can be extended as

$$\begin{bmatrix} \Delta \dot{\phi}_d \\ \Delta \dot{\phi}_q \end{bmatrix} = \begin{bmatrix} A_p \end{bmatrix} \begin{bmatrix} \Delta \phi_d \\ \Delta \phi_q \end{bmatrix} + \begin{bmatrix} B_{p1} \end{bmatrix} \begin{bmatrix} \Delta p_{ref} \\ \Delta Q_{ref} \end{bmatrix} + \begin{bmatrix} B_{p2(1)} \end{bmatrix} \begin{bmatrix} \Delta v_{od} \\ \Delta v_{oq} \end{bmatrix} + \begin{bmatrix} B_{p2(2)} \end{bmatrix} \begin{bmatrix} \Delta i_{od} \\ \Delta i_{oq} \end{bmatrix} \tag{4.10}$$

$$\begin{bmatrix} \Delta i_{d\,ref} \\ \Delta i_{q\,ref} \end{bmatrix} = \begin{bmatrix} C_p \end{bmatrix} \begin{bmatrix} \Delta \phi_d \\ \Delta \phi_q \end{bmatrix} + \begin{bmatrix} D_{p1} \end{bmatrix} \begin{bmatrix} \Delta p_{ref} \\ \Delta Q_{ref} \end{bmatrix} + \begin{bmatrix} D_{p2(1)} \end{bmatrix} \begin{bmatrix} \Delta v_{od} \\ \Delta v_{oq} \end{bmatrix} + \begin{bmatrix} D_{p2(2)} \end{bmatrix} \begin{bmatrix} \Delta i_{od} \\ \Delta i_{oq} \end{bmatrix} \quad (4.11)$$

Where

$$B_{p2(1)} = \begin{bmatrix} B_{p2}^{*} \end{bmatrix} \begin{bmatrix} B_{p2}^{a} \end{bmatrix}, \; B_{p2(2)} = \begin{bmatrix} B_{p2}^{*} \end{bmatrix} \begin{bmatrix} B_{p2}^{b} \end{bmatrix},$$

$$D_{p2(1)} = \begin{bmatrix} D_{p2}^{*} \end{bmatrix} \begin{bmatrix} B_{p2}^{a} \end{bmatrix}, \; D_{p2(2)} = \begin{bmatrix} D_{p2}^{*} \end{bmatrix} \begin{bmatrix} B_{p2}^{b} \end{bmatrix},$$

$$Bp1 = \begin{bmatrix} 1 & 0 \\ 0 & 1 \end{bmatrix}, \; B_{p2}^{*} = \begin{bmatrix} -1 & 0 \\ 0 & -1 \end{bmatrix}, \; D_{p2}^{*} = \begin{bmatrix} -k_{pp} & 0 \\ 0 & -k_{pp} \end{bmatrix},$$

$$B_{p2(1)} = \begin{bmatrix} -I_{od} & -I_{oq} \\ -I_{oq} & I_{od} \end{bmatrix}, \quad B_{p2(2)} = \begin{bmatrix} -V_{od} & -V_{oq} \\ V_{oq} & -V_{od} \end{bmatrix},$$

$$C_p = \begin{bmatrix} k_{pi} & 0 \\ 0 & k_{pi} \end{bmatrix}, \; \mathrm{D_{p1}} = \begin{bmatrix} k_{pp} & 0 \\ 0 & k_{pp} \end{bmatrix},$$

$$D_{p2(1)} = \begin{bmatrix} -k_{pp} I_{od} & -k_{pp} I_{oq} \\ -k_{pp} I_{oq} & k_{pp} I_{od} \end{bmatrix}, \; D_{p2(2)} = \begin{bmatrix} -k_{pp} V_{od} & -k_{pp} V_{oq} \\ k_{pp} V_{oq} & -k_{pp} V_{od} \end{bmatrix}$$

4.3.1.2 Current controller

The current controller is performed in dq frame because of the effectiveness of the PI controllers operating on stationary voltage and current [77]. In this study, the main objectives of the current controller are to ensure accurate current tracking, shorten the transient period as much as possible, and force the VSI to equivalently act as a current source amplifier within the current loop bandwidth [78]. Figure 4-5shows the current controller diagram, where the state equations are:

$$\frac{d\gamma_d}{dt} = i_{dref} - i_d$$
$$\frac{d\gamma_q}{dt} = i_{qref} - i_q \tag{4.12}$$

along with algebraic equations,

$$v_{id} = -\omega_n L_f i_q + k_{pc}(i_{dref} - i_d) + v_d + k_{ci}\gamma_d$$
$$v_{iq} = \omega_n L_f i_d + k_{pc}(i_{qref} - i_q) + v_q + k_{ci}\gamma_q \tag{4.13}$$

The following equations show the linearized small-signal state space from of the current controller

$$\begin{bmatrix} \dot{\Delta\gamma}_d \\ \dot{\Delta\gamma}_q \end{bmatrix} = [A_c]\begin{bmatrix} \Delta\gamma_d \\ \Delta\gamma_q \end{bmatrix} + [B_{c1}]\begin{bmatrix} \Delta i_{dref} \\ \Delta i_{qref} \end{bmatrix} + [B_{c2(1)}]\begin{bmatrix} \Delta v_{od} \\ \Delta v_{oq} \end{bmatrix} + [B_{c2(2)}]\begin{bmatrix} \Delta i_{od} \\ \Delta i_{oq} \end{bmatrix} \tag{4.14}$$

$$\begin{bmatrix} \Delta v_d^* \\ \Delta v_q^* \end{bmatrix} = [C_c]\begin{bmatrix} \Delta\phi_d \\ \Delta\phi_q \end{bmatrix} + [D_{c1}]\begin{bmatrix} \Delta i_{dref} \\ \Delta i_{qref} \end{bmatrix} + [D_{c2(1)}]\begin{bmatrix} \Delta v_{od} \\ \Delta v_{oq} \end{bmatrix} + [D_{c2(2)}]\begin{bmatrix} \Delta i_{od} \\ \Delta i_{oq} \end{bmatrix} \tag{4.15}$$

where,

$$B_{c1} = \begin{bmatrix} 1 & 0 \\ 0 & 1 \end{bmatrix},\ B_{c2(1)} = \begin{bmatrix} 0 & 0 \\ 0 & 0 \end{bmatrix},\ B_{c2(2)} = \begin{bmatrix} -1 & 0 \\ 0 & -1 \end{bmatrix}$$

$$\mathrm{C_c} = \begin{bmatrix} k_{ic} & 0 \\ 0 & k_{ic} \end{bmatrix},\ \mathrm{D_{c1}} = \begin{bmatrix} k_{cc} & 0 \\ 0 & k_{cc} \end{bmatrix},\ D_{c2(1)} = \begin{bmatrix} 1 & 0 \\ 0 & 1 \end{bmatrix}$$

$$D_{c2(2)} = \begin{bmatrix} -k_{cc} & -\omega_s L_f \\ \omega_s L_f & -k_{cc} \end{bmatrix}$$

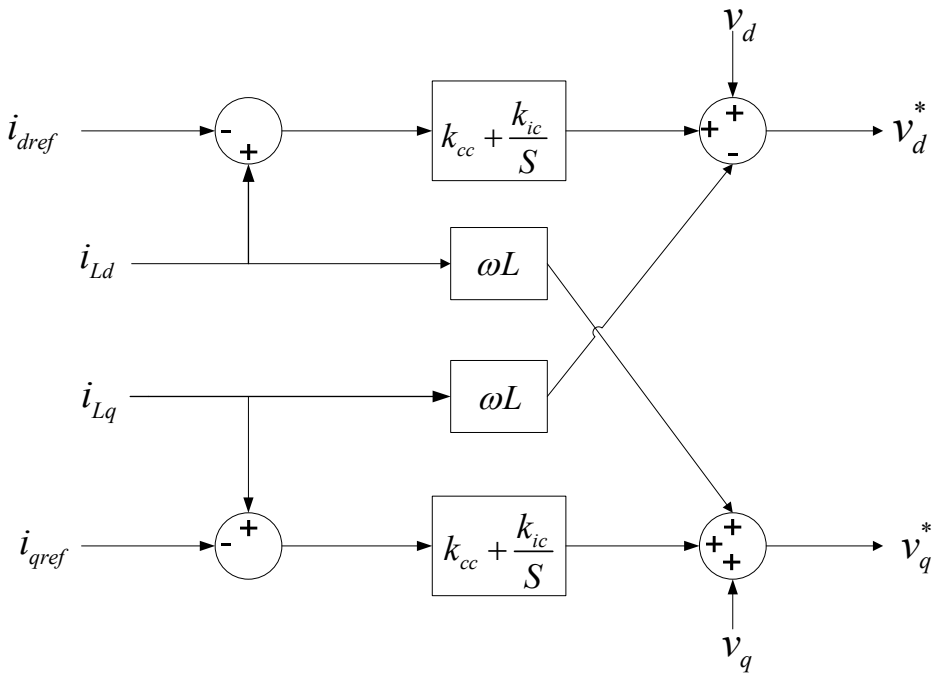

Figure 4- 5: Current controller

4.3.1.3 L-filter

Normally the first order L-filter is used on the AC side of the converter. The main purpose of this filter is to attenuate the current ripples and harmonics which are resulted from the inverter switching. In order to use this filter type, the switching frequency has to be high enough to sufficiently attenuate the inverter harmonics [79]. Therefore, this study is considering the inverter to be operating at high frequency. For the small-signal model, the L-filter and the coupling inductance can be represented by

$$\begin{aligned} \frac{di_d}{dt} &= \frac{-r_f}{L_f} i_d + \omega i_q + \frac{1}{L_f} v_{id} - \frac{1}{L_f} v_{od} \\ \frac{di_q}{dt} &= \frac{-r_f}{L_f} i_q - \omega i_d + \frac{1}{L_f} v_{iq} - \frac{1}{L_f} v_{oq} \end{aligned} \tag{4.16}$$

The linearized small signal state-space form of the L -filter and coupling inductance are given in Equation (4.17).

$$\begin{bmatrix} \Delta \dot{i}_{od} \\ \Delta \dot{i}_{oq} \end{bmatrix} = [A_L] \begin{bmatrix} \Delta i_{od} \\ \Delta i_{oq} \end{bmatrix} + [B_{L1}] \begin{bmatrix} \Delta v_{id} \\ \Delta v_{iq} \end{bmatrix} + [B_{L2}] \begin{bmatrix} \Delta v_{od} \\ \Delta v_{oq} \end{bmatrix} + [B_{L3}][\Delta \omega] \quad (4.17)$$

where,

$$A_L = \begin{bmatrix} \frac{-r_{Lf}}{L_f} & \omega_0 \\ -\omega_0 & \frac{-r_{Lf}}{L_f} \end{bmatrix}, \quad \mathrm{B}_{L1} = \begin{bmatrix} \frac{1}{L_f} & 0 \\ 0 & \frac{1}{L_f} \end{bmatrix}, \quad \mathrm{B}_{L2} = \begin{bmatrix} \frac{-1}{L_f} & 0 \\ 0 & \frac{-1}{L_f} \end{bmatrix}$$

$$B_{L3} = \begin{bmatrix} I_{oq} & -I_{od} \end{bmatrix}^T$$

4.3.1.4 Complete model of the inverter

In this part, the inverter component models are combined together in order to model the inverter. The output variables of the whole system are converted to a common-reference frame. In grid-connected mode, the slack bus (substation bus) is taken as the common-reference frame. The common-reference frame has to provide its common frequency $\Delta\omega_{com}$ to all sub-models and controlling the system voltage. The output of the inverter is the current Δi_{odq} and by using the transformation in Equation (4.2), the output current is transformed to the common reference frame as Δi_{oDQ}. The input signal to the inverter is also transformed to a common reference frame given in Equation (4.2). The state space of the combined model is given by,

$$\begin{bmatrix} \Delta \dot{x}_{invi} \end{bmatrix} = [A_{invi}][\Delta x_{invi}] + [B_{invi}][\Delta v_{bDQi}]$$
$$\begin{bmatrix} \Delta \omega_i \\ \Delta_{ioDQi} \end{bmatrix} = \begin{bmatrix} C_{inv\omega i} \\ C_{invci} \end{bmatrix} [\Delta x_{invi}] \quad (4.18)$$

where,

$$\Delta x_{invi} = [\Delta\phi_{di} \quad \Delta\phi_{qi} \quad \Delta\gamma_{di} \quad \Delta\gamma_{qi} \quad \Delta i_{odi} \quad \Delta i_{oqi}]^T$$

$$A_{invi} = \begin{bmatrix} A_p & 0 & B_{P2(1)} \\ B_{c1}C_{p1} & A_c & B_{c1}D_{P2(2)} + B_{c2(2)} \\ B_{L1}D_{c1}C_{p1} & B_{L1}C_{c1} & H \end{bmatrix}$$

$$H = A_L + B_{L1}D_{c1}D_{P2(2)} + B_{L1}D_{c2(2)}$$

$$B_{invi} = \begin{bmatrix} B_{P2(1)}T_S^{-1} \\ B_{c2(2)}T_S^{-1} \\ \left(B_{L1}D_{c2(1)} + B_{L2} + B_{L1}D_{c1}D_{P2(1)}\right)T_S^{-1} \end{bmatrix}$$

$$C_{invoi} = \begin{bmatrix} 0 & 0 & 0 & 0 & 0 & 0 \end{bmatrix}$$

$$C_{invci} = \begin{bmatrix} [0]_{2\times2} & [0]_{2\times2} & [T_S]_{2\times2} \end{bmatrix}$$

Combine all of the inverters,

$$\begin{bmatrix} \dot{\Delta x}_{INV} \end{bmatrix} = [A_{INV}][\Delta x_{INV}] + [B_{INV}]\begin{bmatrix} \Delta v_{bDQ} \end{bmatrix}$$
$$\begin{bmatrix} \Delta_{ioDQ} \end{bmatrix} = [C_{INVc}][\Delta x_{INV}] \qquad (4.19)$$

where

$$[\Delta x_{INV}] = [\Delta x_{inv1} \ \Delta x_{inv2} \quad \Delta x_{inv3} \ \ldots\ldots\ldots\ldots \ \Delta x_{invs}]^T$$

$$\begin{bmatrix} \Delta v_{bDQ} \end{bmatrix} = \begin{bmatrix} \Delta v_{bDQ1} & \Delta v_{bDQ2} & . & \Delta v_{bDQm} \end{bmatrix}$$

$$A_{INV} = \begin{bmatrix} [A_{inv1}] & 0 & 0 & 0 \\ 0 & [A_{inv2}] & 0 & 0 \\ 0 & 0 & . & 0 \\ 0 & 0 & 0 & [A_{invs}] \end{bmatrix},\ B_{INV} = \begin{bmatrix} B_{inv1} \\ B_{inv2} \\ . \\ B_{invs} \end{bmatrix}$$

$$C_{INVc} = \begin{bmatrix} [C_{invc1}] & 0 & 0 & 0 \\ 0 & [C_{invc2}] & 0 & 0 \\ 0 & 0 & . & 0 \\ 0 & 0 & 0 & [C_{invcs}] \end{bmatrix}$$

4.3.2 **Network Model**

To model the network, the number of lines "n", nodes "m", the load points and inverters connection points should be given. Figure 4-6 illustrates an example of a network with n nodes.

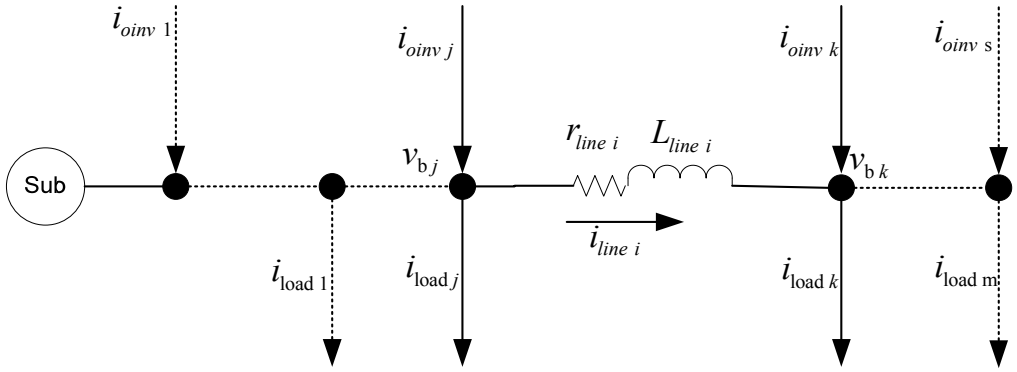

Figure 4- 6: Network model

The state equations of line current of nth line connected between nodes *i* and *j* are,

$$\begin{aligned} \frac{di_{line\ Di}}{dt} &= \frac{-r_{line\ i}}{L_{line\ i}} i_{line\ Di} + \omega i_{line\ Qi} + \frac{1}{L_{line\ i}} v_{bDj} - \frac{1}{L_{line\ i}} v_{bDk} \\ \frac{di_{line\ Qi}}{dt} &= \frac{-r_{line\ i}}{L_{line\ i}} i_{line\ Qi} - \omega i_{line\ Di} + \frac{1}{L_{line\ i}} v_{bQj} - \frac{1}{L_{line\ i}} v_{bQk} \end{aligned} \tag{4.20}$$

From Equation (4.20), the small signal state space model of a network with n[th] lines can be expressed by

$$\left[\dot{\Delta i}_{line\ DQi}\right] = \left[A_{NET}\right]\left[\Delta i_{line\ DQi}\right] + \left[B_{1NET}\right]\left[\Delta v_{bDQ}\right] + \left[B_{2NET}\right]\left[\Delta\omega\right] \tag{4.21}$$

where,

$$A_{NETi} = \begin{bmatrix} \frac{-r_{line\ i}}{L_{line\ i}} & \omega_o \\ -\omega_o & \frac{-r_{line\ i}}{L_{line\ i}} \end{bmatrix}, \quad B_{2NETi} = \begin{bmatrix} i_{line\ Qi} \\ -i_{line\ Di} \end{bmatrix}$$

$$B_{1NETi} = \begin{bmatrix} . & \frac{1}{L_{line\ i}} & 0 & . & \frac{-1}{L_{line\ i}} & 0 & . \\ . & 0 & \frac{1}{L_{line\ i}} & . & 0 & \frac{-1}{L_{line\ i}} & . \end{bmatrix}$$

$$\Delta i_{line\ DQi} = \begin{bmatrix} \Delta i_{line\ DQ1} & \Delta i_{line\ DQ2} & . & . & \Delta i_{line\ DQm} \end{bmatrix}^T$$

$$\Delta\omega = \Delta\omega_{com}$$

$$A_{NET} = \begin{bmatrix} \left[A_{NET1}\right] & 0 & 0 & 0 & 0 \\ 0 & \left[A_{NET2}\right] & 0 & 0 & 0 \\ 0 & 0 & .. & 0 & 0 \\ 0 & 0 & 0 & .. & 0 \\ 0 & 0 & 0 & 0 & \left[A_{NET\ n}\right] \end{bmatrix}$$

$$B_{1NET} = \begin{bmatrix} B_{1NET1} \\ B_{1NET2} \\ .. \\ .. \\ B_{1NET\ n} \end{bmatrix} \quad B_{2NET} = \begin{bmatrix} B_{2NET1} \\ B_{2NET2} \\ .. \\ .. \\ B_{2NET\ n} \end{bmatrix}$$

4.3.3 **Load model**

In this study, the load model is taken as a general RL load model. The state equations of the RL load are connected to j node as in Figure 4-6; this can be expressed by

$$\begin{aligned}\frac{di_{load\ Dj}}{dt} &= \frac{-R_{load\ j}}{L_{load\ j}} i_{load\ Dj} + \omega i_{load\ \mathrm{Qj}} + \frac{1}{L_{load\ j}} v_{bDj} \\ \frac{di_{load\ \mathrm{Qj}}}{dt} &= \frac{-R_{load\ j}}{L_{load\ j}} i_{load\ \mathrm{Qj}} - \omega i_{load\ \mathrm{Dj}} + \frac{1}{L_{load\ j}} v_{bQj}\end{aligned} \tag{4.22}$$

The small-signal state space model of the load is given by

$$\left[\Delta \dot{i}_{load\ DQ}\right] = \left[A_{load}\right]\left[\Delta i_{load\ DQ}\right] + \left[B_{1load}\right]\left[\Delta v_{bDQ}\right] + \left[B_{2load}\right]\left[\Delta \omega\right] \tag{4.23}$$

where,

$$\Delta i_{load\ DQ} = \left[\Delta i_{load\ DQ1} \quad \Delta i_{load\ DQ2} \quad . \quad . \quad \Delta i_{load\ DQ\ P}\right]^T$$

$$A_{load} = \begin{bmatrix} \left[A_{load1}\right] & 0 & 0 & 0 & 0 \\ 0 & \left[A_{load\ 2}\right] & 0 & 0 & 0 \\ 0 & 0 & .. & 0 & 0 \\ 0 & 0 & 0 & .. & 0 \\ 0 & 0 & 0 & 0 & \left[A_{load\ P}\right] \end{bmatrix}$$

$$B_{1load} = \begin{bmatrix} B_{1load1} \\ B_{1load2} \\ .. \\ .. \\ B_{1load\ \mathrm{p}} \end{bmatrix}, B_{2load} = \begin{bmatrix} B_{2load1} \\ B_{2load2} \\ .. \\ .. \\ B_{2load\ \mathrm{p}} \end{bmatrix}$$

$$A_{loadj} = \begin{bmatrix} \dfrac{-R_{load\ j}}{L_{load\ j}} & \omega_o \\ -\omega_o & \dfrac{-R_{load\ j}}{L_{load\ j}} \end{bmatrix},\ B_{2load\ j} = \begin{bmatrix} i_{load\ Qj} \\ -i_{load\ Dj} \end{bmatrix}$$

$$B_{1NETi} = \begin{bmatrix} .. & .. & \dfrac{1}{L_{load\ j}} & 0 & .. & .. & .. \\ .. & .. & 0 & \dfrac{1}{L_{load\ j}} & .. & .. & . \end{bmatrix}$$

4.3.4 **Complete system model**

In Figure 4-6, the node voltages are considered as input to each subsystem. A virtual resistor assumed between each node and the ground is used to define the node voltage. The value of these resistors is chosen to be sufficiently large so as to have minimum influence on the dynamic stability of the system. Therefore, the voltage of the J[th] node is expressed by:

$$\begin{aligned} v_{bDi} &= r_N (i_{oDi} - i_{loadDi} + i_{lineDi,j}) \\ v_{bQi} &= r_N (i_{oQi} - i_{loadQi} + i_{lineQi,j}) \end{aligned} \tag{4.24}$$

$$\left[\Delta v_{bDQ}\right] = R_N (M_{INV}\left[\Delta i_{oDQ}\right] + M_{load}\left[\Delta i_{loadDQ}\right] + M_{NET}\left[\Delta i_{lineDQ}\right]) \tag{4.25}$$

where,

R_N is a $(2m-2)\times(2m-2)$ matrix, whose diagonal elements are equal to r_N.

M_{INV} is a $(2m-2)\times 2s$ matrix that maps the inverter connection points to the network. For example, if the i^{th} inverter is connected at j node, the $M_{INV}(i,j)=1$ and all the other elements in the same row will be equal to 0.

M_{load} is a $(2m-2)\times 2p$ matrix that maps the load connection points to the network. For example, if the i^{th} load is is connected at j node, the $M_{load}(i,j)=-1$ and all the other elements in the same row will be equal to 0.

M_{NET} is $(2m-2)\times 2n$ a matrix that maps the connection of the lines into the network nodes. In this matrix node connection can be either +1 or -1, based on whether the given line current is entering or leaving the node.

The complete small-signal state space model is given by

$$\begin{bmatrix} \dot{\Delta x}_{INV} \\ \dot{\Delta i}_{line\,DQ} \\ \dot{\Delta i}_{load\,DQ} \end{bmatrix} = A_{sys} \begin{bmatrix} \Delta x_{INV} \\ \Delta i_{line\,DQ} \\ \Delta i_{load\,DQ} \end{bmatrix} \tag{4.26}$$

where,

$$A_{sys} = \begin{bmatrix} A_{INV} + B_{INV} R_N M_{INV} C_{INVc} & B_{INV} R_N M_{NET} & B_{INV} R_N M_{load} \\ B_{1NET} R_N M_{INV} C_{INVc} + B_{2NET} C_{IN\omega} & A_{NET} + B_{1NET} R_N M_{NET} & B_{INET} R_N M_{load} \\ B_{1load} R_N M_{INV} C_{INVc} + B_{2load} C_{IN\omega} & B_{1load} R_N M_{NET} & B_{1load} R_N M_{load} \end{bmatrix}$$

4.4 System under study and the proposed scenarios

This study is conducted by using the same system which is presented in chapter 3 in section 3.5. It is a rural distribution system of 41 buses. The single line diagram is given in Figure 3-5. It is demonstrated in five scenarios.

- *Scenario 1: Analyze the impact of DG location on the proximity of the voltage instability*. In this scenario, the system is loaded in steps of λ (from zero to the maximum loadability). In each loading step, the small-signal analysis is applied and the eigenvalues are traced.

- *Scenario 2: Analyze the impact of DG location and size on the small-signal instability.* In this scenario, a DG unit is placed in a certain location and the size of the DG is varied. Then, the DG is placed in other locations and its size is also varied. The eigenvalues are also traced.

- *Scenario 3:Study the impact of injecting reactive power by DG units to the proximity of the voltage instability of the system.* The DG unit is placed at different locations. In each location, the power factor is varied from 1 to 0.95 leading.

- *Scenario 4:Examine the impact of the DG controller setting on the proximity of the voltage instability.*

- *Scenario 5: Investigate the impact of multi-DG units on the proximity of the voltage instability.* Three DG units are installed on the system. The load is varied in the same way as in Scenario 1.

4.4.1 **Results and discussion**

This section outlines the results, presented as follows:

- Scenario 1: Two cases are studied in this scenario. Case 1 , a DG unit of 6.6 MW is placed at bus 40. The size of this DG unit is obtained from the results of a previous study in placement and sizing of the DG units to improve the voltage stability margin of the system [29] and presented in Chapter 3. Case 2, the same DG is placed at bus 4. The DG unit is assumed to operate at unity power factor. In each case, the system is loaded from zero to the maximum loadability. The small-signal analysis is applied at each loading step in both cases; Figure 4-7 shows traces of the system eigenvalues. In addition, to study the eigenvalues, the results of the sensitivity analysis for both cases are shown in Tables 4-1 and 4-2, respectively. The participation factor (columns 3 and 4 in both tables) shows that the most critical eigenvalues are mainly sensitive to the system state variables (network lines and load state variables)

rather than the DG unit state variables. Therefore, the location of the DG units will not affect those values. However, there is a complex conjugate eigenvalue which is affected by the system loadability due to the voltage drop at the point of connection of the DG unit. The sensitivity analysis shows that this eigenvalue is most sensitive to the DG unit (L filter sate variable of the DG unit); therefore these eigenvalues move faster toward the unstable area as the system loading increases. As a result, the system may become unstable before reaching the maximum loadability.

In case 2, Bus 4 is less sensitive to $\Delta V/\Delta P$ and $\Delta V/\Delta Q$, because this bus is located near the substation. The complex conjugate, which is mainly sensitive to the DG L filter sate variable of the unit, moves more slowly than in case 1. As a conclusion, placing a DG unit in the upper stream is more stable than in the lower stream of a distribution system.

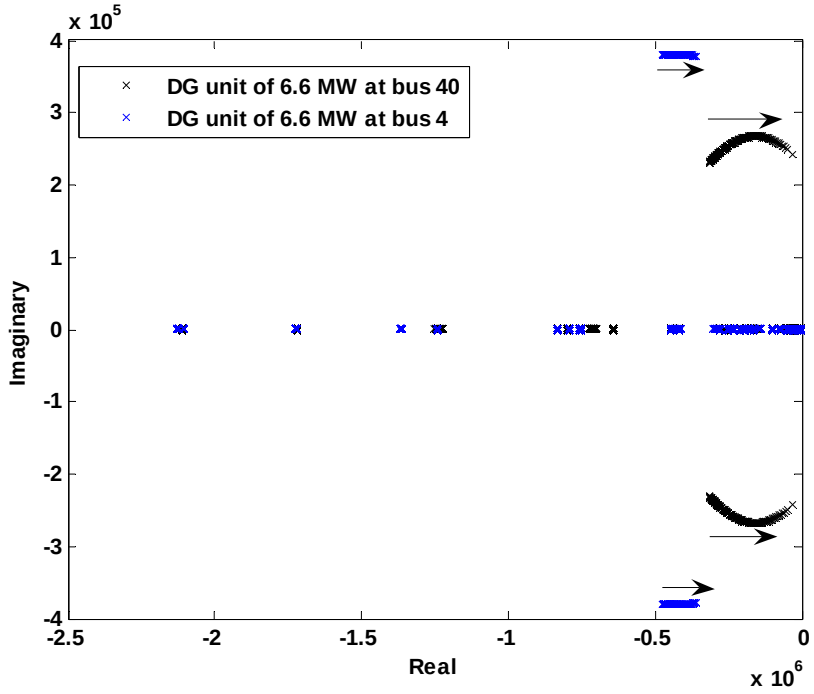

Figure 4- 7: Trace of eigenvalues of the system to study the impact of the DG unit's location of on the proximity to the voltage instability.

Table 4- 1: Results of the sensitivity analysis scenario 1, case1

Real	Imaginary	DG	Network and load
-218.102	376.6397	0.0008	0.9992
-218.102	-376.64	0.0008	0.9992
-421.354	376.9911	0.0000	1.0000
-421.354	-376.991	0.0000	1.0000
-455.143	376.7215	0.0007	0.9993
-455.143	-376.722	0.0007	0.9993
-572.347	376.8669	0.0004	0.9996
-572.347	-376.867	0.0004	0.9996
-659.313	376.989	0.0000	1.0000
-659.313	-376.989	0.0000	1.0000
-32318.4	241638.8	0.5170	0.4830
-32318.4	-241639	0.5170	0.4830

Table 4- 2: Results of the sensitivity analysis scenario 1, case 2

Real	Imaginary	DG	Network and load
-218.623	376.9911	0.0000	1.0000
-218.623	-376.991	0.0000	1.0000
-421.962	376.9911	0.0000	1.0000
-421.962	-376.991	0.0000	1.0000
-456.695	376.9911	0.0000	1.0000
-456.695	-376.991	0.0000	1.0000
-587.428	376.9911	0.0000	1.0000
-587.428	-376.991	0.0000	1.0000
-662.462	376.9911	0.0000	1.0000
-662.462	-376.991	0.0000	1.0000
-607469	70640.71	1.0000	0.0000
-607469	-70640.7	1.0000	0.0000

- In scenario 2, the DG unit is placed in a certain location and the size of the DG is varied. Figure 4-8 shows the trace of eigenvalues of a DG placed in bus 40 and then in bus 4. In both locations, the DG unit is varied from 0 to 10 MW in order to study the impact of the DG size in small-signal stability.
- The participation factor of the sensitivity analysis (see columns 3 and 4 in Table 4-3) shows that the most critical eigenvalues are mainly sensitive to the system network and load state variables, rather than the DG units' state variables; therefore, the size of the DG units will not affect those values. However, there is a complex conjugate eigenvalue which is affected by changing the DG size. The participation factor analysis shows that this eigenvalue is sensitive to the DG unit (L-filter sate variable of the DG unit) with 0.51 and sensitive to the load with 0.49 at bus 40. However, when the DG unit is placed at bus 4 this eigenvalue become more sensitive to the L filter sate variable of the DG unit.

  Bus 4 is less sensitive to $\Delta V/\Delta P$ (the DG operates at unity power factor). The complex conjugate which is mainly sensitive to the state variables of the L-filter of the DG unit, moves slower in case 2 than in case 1. As a conclusion, placing a DG unit in the upper stream is more stable than in the lower stream of a distribution system.

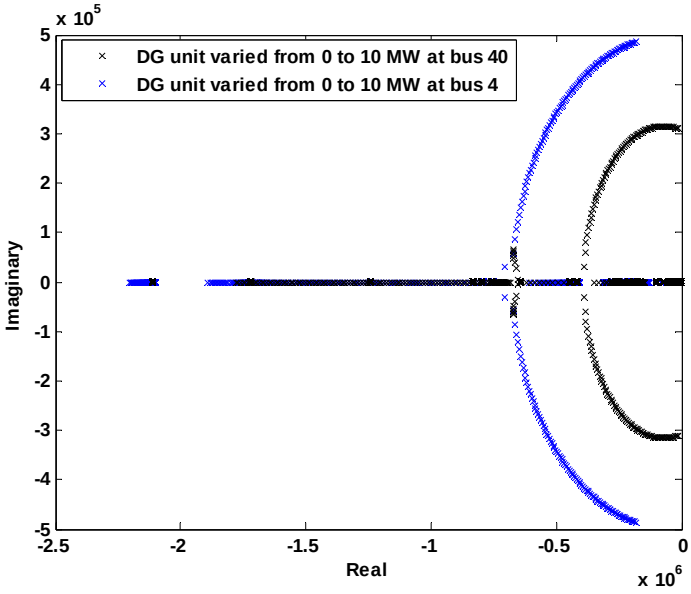

Figure 4- 8: Trace of eigenvalues of the system to study the impact of the size and location of the DG units on small-signal stability

Table 4- 3: Results of the sensitivity analysis scenario 2

Real	Imag	DG	Network and load
-227.458	376.5969	0.0009	0.9991
-227.458	-376.597	0.0009	0.9991
-426.239	376.9911	0.0000	1.0000
-426.239	-376.991	0.0000	1.0000
-473.669	376.5888	0.0011	0.9989
-473.669	-376.589	0.0011	0.9989
-660.737	376.9745	0.0001	0.9999
-660.737	-376.974	0.0001	0.9999
-861.367	376.776	0.0009	0.9991
-861.367	-376.776	0.0009	0.9991
-11843.2	310051.3	0.5133	0.4867
-11843.2	-310051	0.5133	0.4867

- Scenario 3:the aim of this scenario is to study the impact of injecting reactive power by DG units into the system. The DG unit is placed at different locations. This scenario presents the results in two cases. In case 1, a DG unit of 6.6 MVA is placed in bus 40, while in case 2, the same DG is moved to bus 4. In each case, the power factor is varied from 1 to 0.95 leading. Figure 4-9 shows the small-signal trace of case 1 and case 2. In both cases, the complex conjugate eigenvalue, which is sensitive to system network loads and DG unit state variables, moves toward a stable area. However, in case 2 the improvement is less compared to case 1 due to the ΔV/ΔQ sensitivity. The ΔV/ΔQ is more sensitive in low stream buses in radial distribution systems.

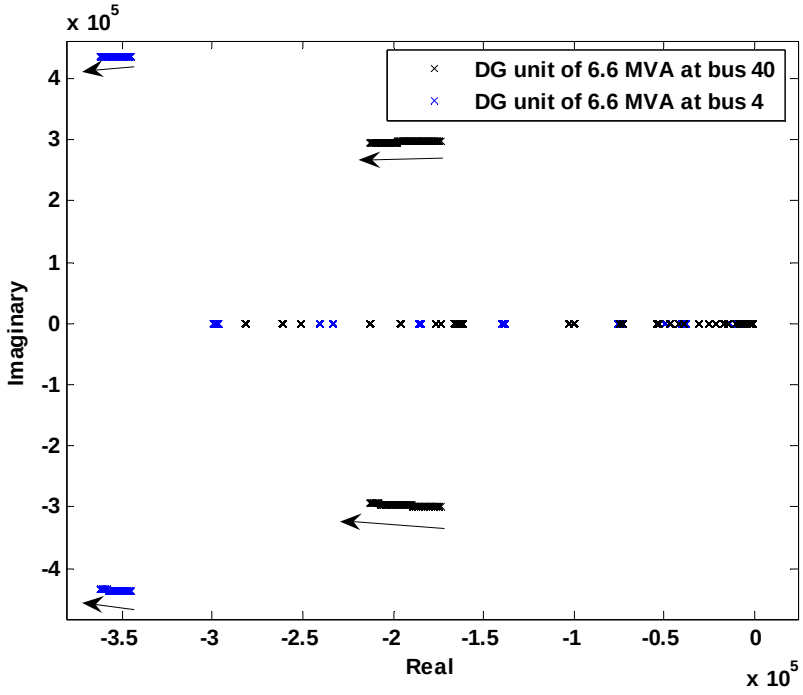

Figure 4- 9: Trace of eigenvalues of the system to study the impact of the DG unit's reactive power generation on small-signal stability

- Scenario #4: by looking at the results of scenarios 1 and 2, the small-signal stability of the system can be affected by the location and size of the DG units. However, the setting of the power controller and current controller could worsen the stability. Thus, the objective of this scenario is to investigate the impact of the DG controller on the small-signal stability of a

distribution system with high penetration of inverter DG units. It is the same as Case 1 in Scenario 1, the DG unit is placed at bus 40 and the system is loaded from zero to maximum loadability. The only difference is that the proportional constant of the power controller (k_{pp}) is changed to 6. Figure 4-10 shows the results, where the system eigenvalues have moved to the unstable area before reaching the maximum loadability of the system, however, in scenario 1 case 1 the system was stable until the maximum loadability of the system, as can be seen in Figure 4-7.

- Scenario 5: the aim of this scenario is to investigate the impact of multi-DG units on small-signal stability. Three DG units are installed in the system. Two cases are presented as shown in Table 4-4. In case 1, the higher DG rating is placed in bus 40 (low stream bus), but in case 2, this DG is changed to be in the upper stream in bus 28. The penetration level of the DG units is kept the same in both cases, and the system load is varied from zero to maximum loadability. Figure 4-12 shows the results of the eigenvalue traces for both cases. As can be noticed from this figure, case 1 is more sensitive to the small-signal stability than case 2, because in case 1, the largest DG unit is placed in the lower stream (bus 40). Thus, bus 40 is more sensitive to $\Delta V/\Delta P$, which affects the system stability.

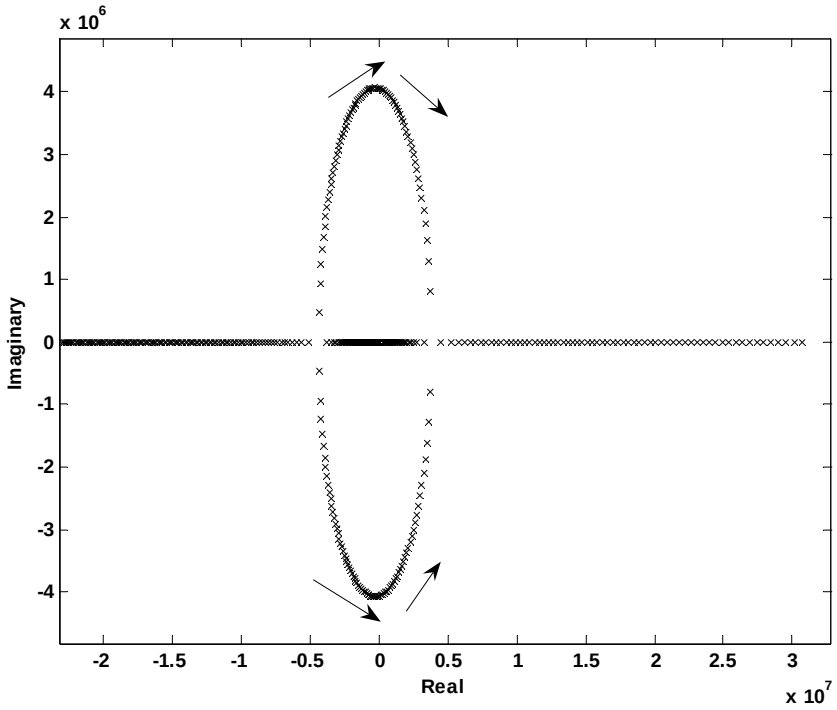

Figure 4- 10: Trace of eigenvalues of the system to study the impact of DG unit's controller settings on small-signal stability

Table 4- 4: Cases under study for scenario 5

	Case 1	Case 2
Bus #	DG rating	DG rating
40	6.6 MW	1.1 MW
38	2.2 MW	2.2 MW
28	1.1 MW	6.6 MW

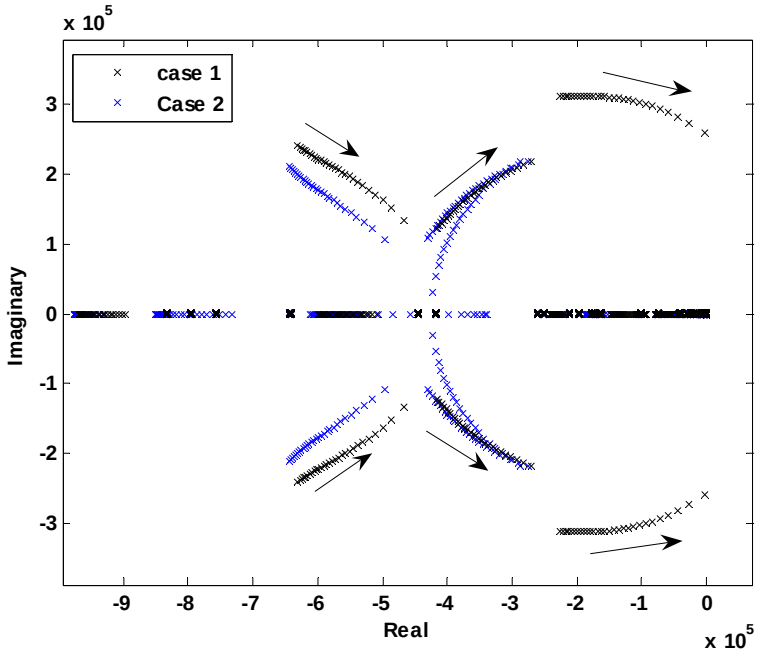

Figure 4- 11: Trace of the system eigenvalues to study the impact of multi-DG units

4.5 Discussion

In this chapter, the impact of DG units on small-signal stability and the proximity to voltage instability was studied. This impact was analyzed based on the location, size, reactive power generation, and controller settings of the DG units. In addition, the impact of integrating multi-DG units into the system has been considered. The study focused on analyzing the inverter-based DG units, because this type of units is expected to be the dominant type in the near future. Moreover, it focused on a system operating in parallel with the grid (grid-connected mode). However, this study can be extended to cover microgrid systems.

As a conclusion, the location can affect the small-signal stability and voltage stability of the system. For example, placing a DG unit in a low stream of a distribution system might make the system unstable before reaching the maximum loadability. The size of the DG unit also affects the stability of the system. It is found that placing a DG unit in the lower stream of a radial distribution system could make the system prone to instability, compared to that of placing the same size of a DG unit in the upper stream.

Some utilities allow the DG units to operate in fixed power factor mode, ranging from 0.95 lagging to 0.95 leading. The lagging power factor mode decreases the voltage stability margin of the system, while the leading mode improves the voltage stability margin. In small-signal analysis, it is found that placing a DG unit that generates reactive power in lower stream buses can move the sensitive eigenvalues toward a stable area faster than if the DG is placed in upper stream, because $\Delta V/\Delta Q$ is more sensitive in low stream buses of a radial distribution system.

Moreover, it is found that the setting of the DG controller parameters could affect the system stability due to the sensitivity of some eigenvalues to DG controller parameters. The eigenvalues could go to the unstable area before reaching the maximum voltage stability margin if the controller is not properly set.

Finally, when more than one DG unit is placed in a radial distribution system, the DG units' size and location can affect the proximity to the voltage instability. It is recommended to place the higher DG ratings in the upper stream of the system, while the DG units with smaller ratings should be in the lower stream, in order to move the eigenvalues of the system toward more stable locations and decrease the effects of $\Delta V/\Delta P$.

Chapter 5
An Investigation on Harmonic Resonance Due to the Integration of Distributed Generation

5.1 Introduction

The main goal of this chapter is to study and analyze the impact of the integration of distributed generation on harmonic resonance by modeling different types of DG units and applying the impedance frequency scan method. The chapter investigates important issues related to the impact of the DG units on harmonic resonance, such as the change of the load demand, lines and DG units disconnections, and the arrangement of the DG units in a wind farm.

Harmonics is one of the power quality problems which is produced in distribution systems due to the presence of some non-linear elements. These elements include power electronic devices, transformers, non-linear loads, and recently distributed generators which are fully or partially interfaced to the grid-network through power electronic inverters. When harmonics exceed a certain level, it impacts negatively the customer equipment as well as the network components. This impact appears as a reduction in the efficiency of network components, and malfunction of the network devices [58]. The level of harmonics is obtained by calculating the voltage and current harmonic distortions and compare it to limits set by standards. These standards are set by IEEE, IEC, EN, and NORSOK [59].

Normally, the distribution system consists of inductive and capacitive elements. The value of these elements depends on the frequency. Thus, the harmonic components affect the system and cause series or parallel resonance phenomena. These phenomena occur when the inductive and the capacitive reactances are equal. In the parallel resonance, the system impedance is high and a small exciting current can develop large voltage. However, in series resonance, the system impedance is low and a small exciting voltage can develop high current [80]. The series and parallel resonance can simply be calculated at a frequency f_r as follows.

$$f_r = \frac{1}{2\pi\sqrt{LC}} \tag{5.1}$$

where,

f_r is the resonance frequency;

C and L are the equivalent capacitance and reactance in a series or parallel network.

5.2 Methods to study harmonic resonance

The resonance phenomenon is an important issue in distribution systems since the system consists of distributed non-linear loads, shunt capacitors, and distributed generation [81]. In the literature, the resonance has been studied in order to design reactive power compensation or filters, and several techniques have been proposed to study the resonance such as using analytical method, conducting harmonic power flow studies, or applying frequency scan method [60, 61].

The analytical method is achieved by using time domain simulation. This simulation can be used to find the magnification of the voltage or current due to the harmonic resonances. The harmonic power flow method starts by conducting a power flow for the fundamental frequency component and then applying the power flow for all the other harmonic components. The details of this method are presented in [82]. The frequency scan technique is achieved by injecting a 1 A constant current at a harmonic source location in the system and sweep over the harmonic frequencies [83]. This study applies the frequency scan method because it is a useful method as it can reveal the resonance frequencies and the associated magnitudes of the system under study.

This research has been conducted to study and analyze the impacts of the DG units' harmonic resonance, thus, it tackles the impacts of the following issues:

1. The load model and changes of the load demand.
2. The DG units size, location and number.
3. The load and line disconnection.
4. The DG units disconnection.
5. The DG units arrangement.

5.3 System Modeling

5.3.1 **Network and load modeling**

Performing a detailed and accurate harmonic resonance analysis in an electrical system is a quite complicated issue, because it involves an accurate model for all system components, including the load, which present high uncertainty. The modeling approach adopted in this chapter is the representation of the system impedance variation at all buses including the DG units. Distribution feeders are modeled by their equivalent impedance including the capacitance for the underground cable or feeders. The proper selection of the load model is very important for correctly assessing the magnitude and the harmonic order of the resonances. In the literature, two main types of load model have been proposed, as shown in Figure 5-1. The series load model is the best for representing individual load and the parallel load model is the best for representing lumped load [59]. In this study modeling both series and parallel will be tested in order to study their impacts before and after adding DG units to the system.

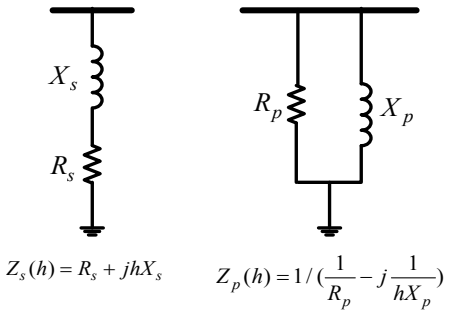

Figure 5- 1: Load models for resonance analysis

5.3.2 **DG units modeling**

The DG units can be either directly connected to the grid or interfaced using power electronic converters. For example, reciprocating internal combustion engine (ICE) and some types of wind DG units are directly connected to the grid using either a synchronous or an induction generator, while photovoltaic (PV) systems, fuel cells, and Micro-turbines are examples of DG units that are connected to the grid through power electronic converters.

Wind turbines are classified into four types, A, B, C and D. These types are explained in detail in [11] and presented in chapter 2. Type A is a fixed speed turbine, directly connected to the grid via conventional induction generator. Type B is a variable speed drive, directly connected to the grid via a wound rotor induction generator with variable rotor resistance. Type C is a doubly-fed induction generator with a wound rotor induction generator and partial scale frequency converter. Type D is a wound rotor synchronous generator, connected to the grid via full converter interface.

For resonance studies, the directly connected DG units such as wind type A, B, and C can be modeled with the equivalent circuit of the induction or synchronous generator. However, it is difficult to model type D as a synchronous generator, because the converter operates as a buffer between the generator and the grid. The modeling of the inverter is dependent on its control. If the inverter-based DG unit is controlled by PQ or current controllers, it can be modeled as a current source. If the DG units is controlled by PV controller, it can be modeled as a voltage source. The IEEE P1547 Standard [5] specified that the DG units should not regulate distribution system voltages. An attempt by a DG units to regulate distribution system voltage can conflict with existing voltage regulation schemes applied by the utility to regulate the same or a nearby point to a different voltage [64]. Thus, DG with PV controller is not recommended. In addition, the inverter grid-connected DG units can interact with other DG converters, system impedance, and the load. Further yet, the uncertainties of load can affect the DG units' stability and resonance. Therefore, many researchers such as [84] have focused on designing a high-bandwidth current controller in order to facilitate the DG units controller to damp the higher frequency disturbances and mitigate the resonance. This research will tackle the impacts of the issues which are stated in section 5.2.

5.4 System under study

This chapter is also conducted by using the same system which is presented in chapter 3 in section 3.5. Figure 3-5 illustrates the single diagram of the rural distribution system.

The selected DG units are 1.1 MW. The ratings and characteristics are obtained from [68]. The penetration of the DG units can be a multiple number of the selected rating. For example, if the result shows the penetration level at a certain bus is 6.6 MW, it means six DG units of 1.1 MW are recommended to be installed in this bus. The size of DG units is obtained from results of previous study in placement and sizing of the DG units to improve the voltage stability margin of the system [29] and presented in chapter 3.

In order to study the impacts of the DG units on harmonic resonance, the following scenarios are proposed.

Scenario 1: study the impact of the changes of the load demand on the harmonic resonance in a distribution system with highly integrated DG units;
Scenario 2: examine the impacts of DG units' size, location and number;
Scenario 3: investigate the impact of the load and line disconnection;
Scenario 4: tackle the impact of the DG units' disconnection;
Scenario 5: study and compare the effects of the DG units arrangement on harmonic resonance.

5.5 Results

5.5.1 **Scenario 1: The impact of the load model and changes of the load demand**

Before studying the impacts of the DG units, the load model of the system under study (Figure 3-5) is analyzed. The impedance variations of the load demand models (both series and parallel models) are shown in Figure 5-2. In order to study this impact, the maximum and the minimum load demand are both considered. The peak load demand of the presented distribution system occurs in summer at 16.18 MVA. The lowest load demand occurs in winter; it is equal to 34.22% of the peak demand. A and B in this figure are points where the load models begin to deviate in magnitude. After the installation of DG units, if the resonance occurs before these points the difference in the magnitude of the resonance between the series and the parallel model is low. However, if the resonance occurs beyond these points the impact will be high. Table 5-1 presents the cases to show these impacts and Figure 5-3 illustrates the results. Cases 1 and 3 represent the impact of the load model before point B and cases 2 and 4 represent the impact after B. In comparison between cases (1 and 3) and cases (2 and 4), the former cases, have lower impact in the magnitude than the latter cases. As a result, the load models, whether series or parallel, can affect the resonance magnitude. In addition, the uncertainty of load demand can also affect the harmonic resonance as in Figure 5-3.

Table 5- 1: Cases under study

	Size of the DG unit	Load model	Load demand	DG location
Case 1	6.6 MW	parallel	minimum load	Bus 40
Case 2	1.1 MW	parallel		
Case 3	6.6 MW	series		
Case 4	1.1 MW	series		

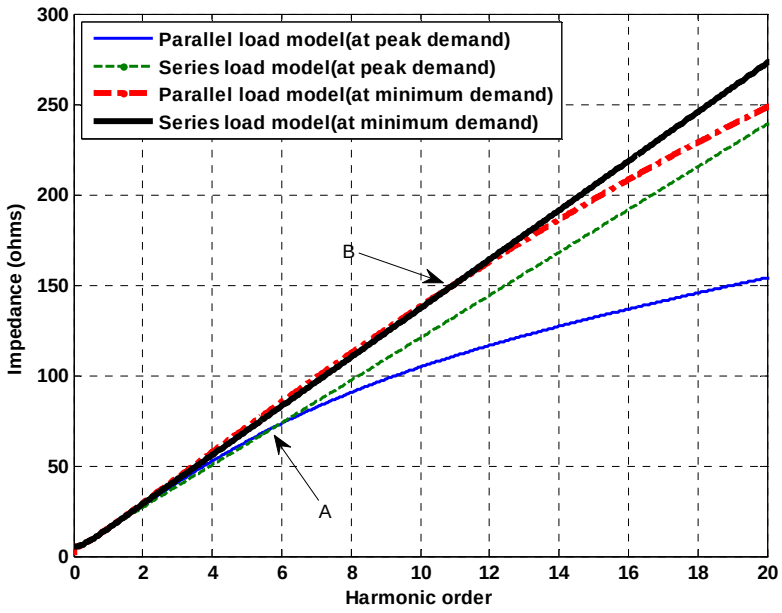

Figure 5- 2: Impedance variations of load demand models before the installation of DG units

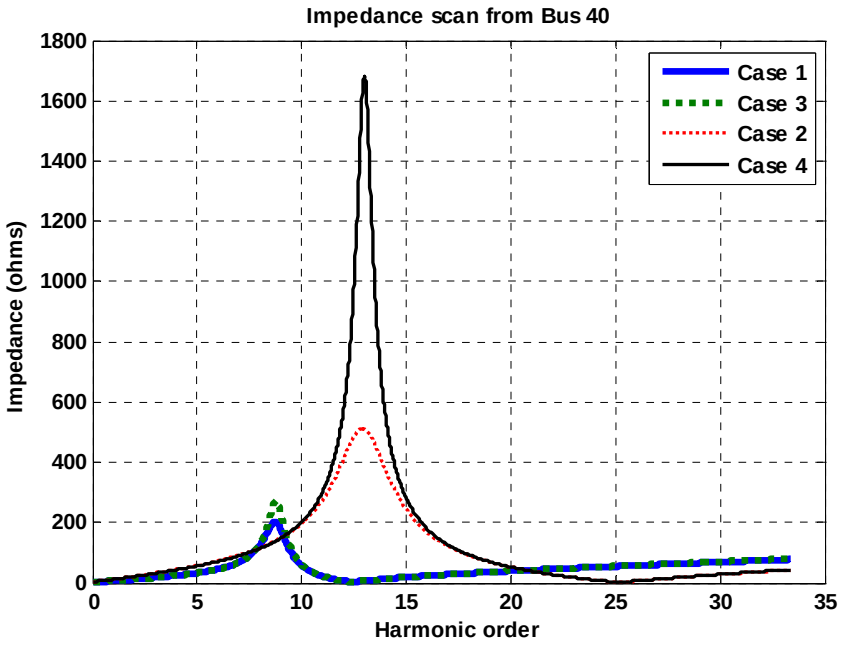

Figure 5- 3: Different cases to study the impacts of the load model on harmonic resonance

5.5.2 **Scenario 2: The impacts of DG units' size, location and number**

This study analyzes the impact of the changes in DG units' size, location and number on the harmonic resonance in a distribution system. The simulation is conducted in four cases as in Table 5-2. The results are shown in Figures 5-4 to 5-7.

Table 5- 2: The impact of DG units size and number on harmonic resonance

	Size of the DG unit	DG units location
Case 1	6.6 MW	40
Case 2	2.2 MW	38
Case 3	1.1 MW	28
Case 4	All DG units (6.6, 2.2, and 1.1MW)	40, 38 , and 28, respectively

The following comments can be noticed:

- In the harmonic order between 0 and 8, as the penetration level of the DG units increases, the total system impedance decreases. Thus, if there is a current harmonic source injecting harmonics less than the 8^{th}, the total harmonic distortion might decrease and hence the power quality improves.
- The peak value of the resonances at light load is higher than those of peak load demand. Thus, the DG units, impact more in the light load demand.
- In comparison between cases 1 to 3 and case 4, the magnitude of the resonance peak is lower when the DG penetration increases.

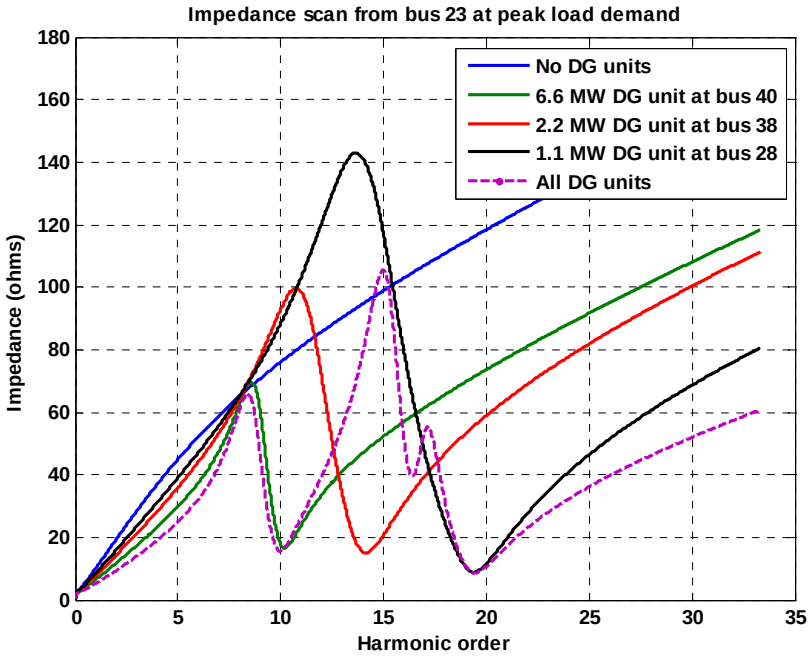

Figure 5- 4: Frequency scans from bus 23 at peak load demand and with different DG penetration

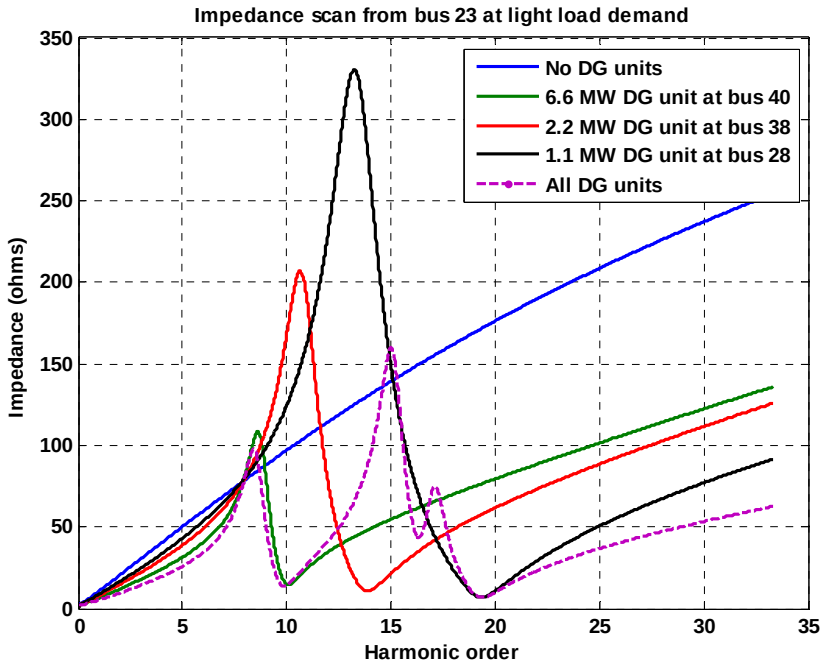

Figure 5- 5: Frequency scans from bus 23 at light load demand and with different DG penetration

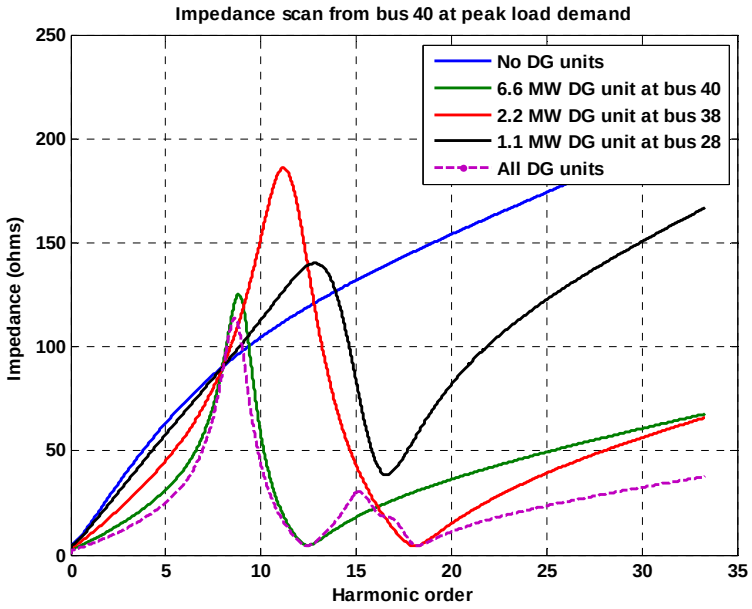

Figure 5- 6: Frequency scans from bus 40 at peak load demand and with different DG penetration

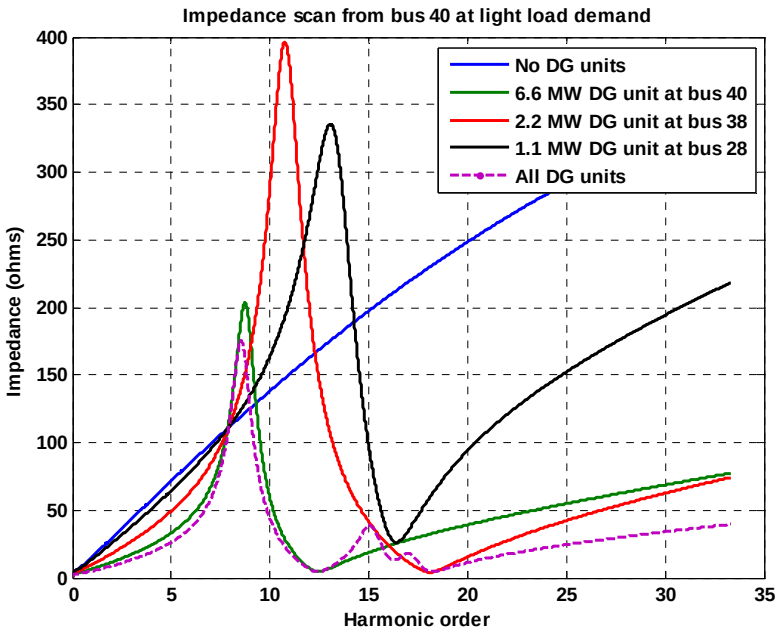

Figure 5- 7: Frequency scans from bus 40 at light load demand and with different DG penetration

- Placing more than one DG unit in the system can make more than one resonance peak. In this study, there are three resonance peaks at harmonic order of 8.56, 15.15 and 17.05 as shown in Figures 5-8 and 5-9. The first peak is due to the 6.6 MW DG unit which is placed at bus 40, the second is due to the 2.2 MW DG unit at bus 38 and the third is due to the 1.1 MW DG unit at bus 28. In this system, load demand value affects the magnitude of the resonance peak , but there is no impact on shifting the harmonic resonance peaks to higher or lower harmonic order. In other systems, it might shift the resonance peaks depending on the significant changes of the equivalent impedances.

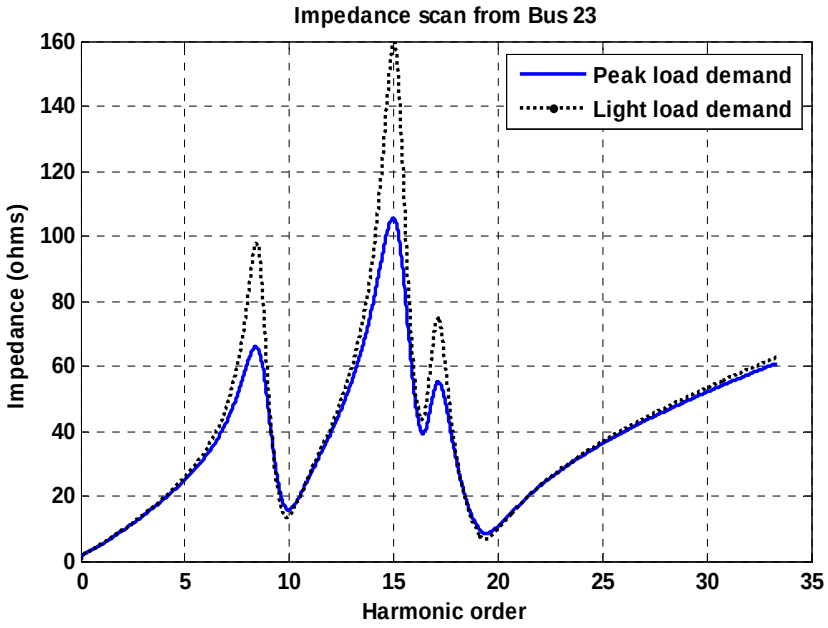

Figure 5- 8: Frequency scans from bus 23 at the peak and light load demand

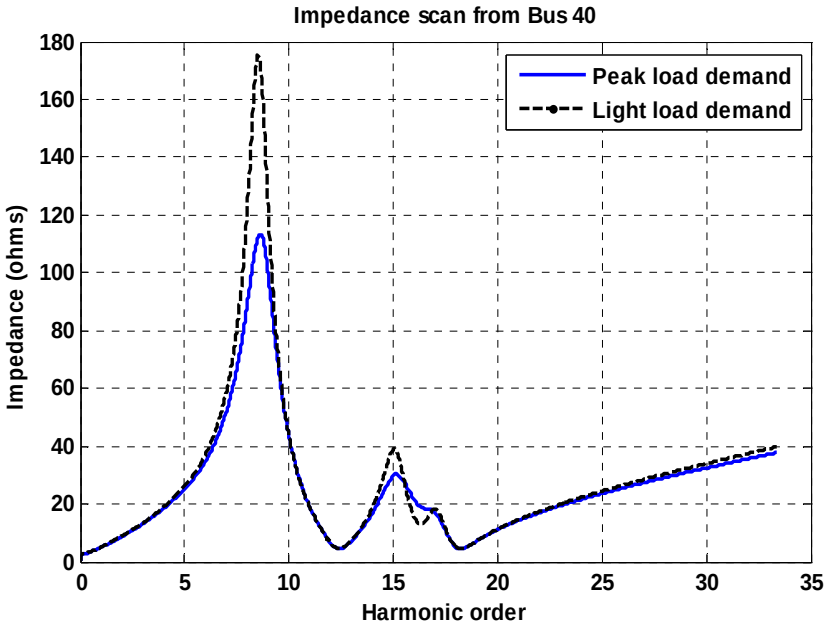

Figure 5- 9: Frequency scans from bus 40 at the peak and light load demand

- The location of the DG unit can change the equivalent impedance of the system, thus it affects the harmonic resonance frequency and magnitude. In order to study this impact, three DG units are installed in the system. Two cases are presented as shown in Table 5-3. In case 1, the higher DG rating is placed in bus 40 (low stream bus), but in case 2, this DG is changed to be in the upper stream in bus 28.

Table 5- 3: Cases to study the impact of DG units location on harmonic resonance

	Case 1	Case 2
Bus #	DG rating	DG rating
40	6.6 MW	1.1 MW
38	2.2 MW	2.2 MW
28	1.1 MW	6.6 MW

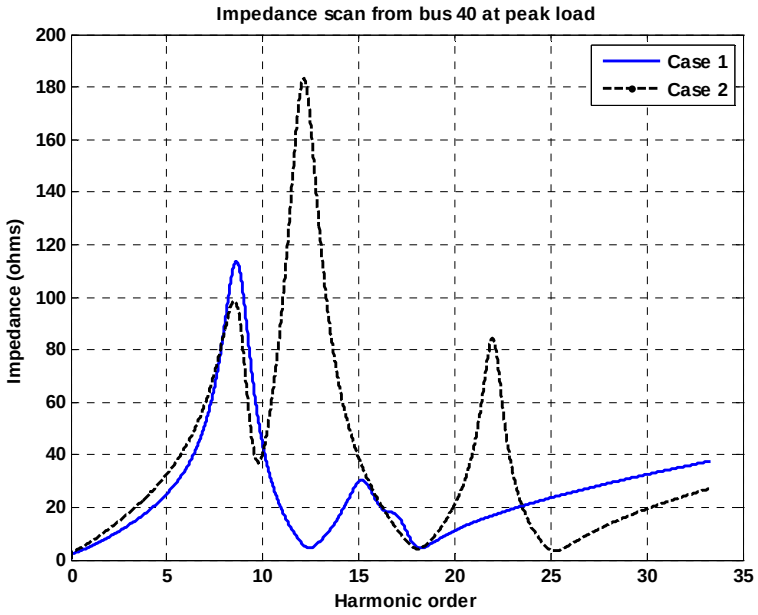

Figure 5- 10: Impedance scan from bus 40 to study the impact of DG units location on harmonic resonance

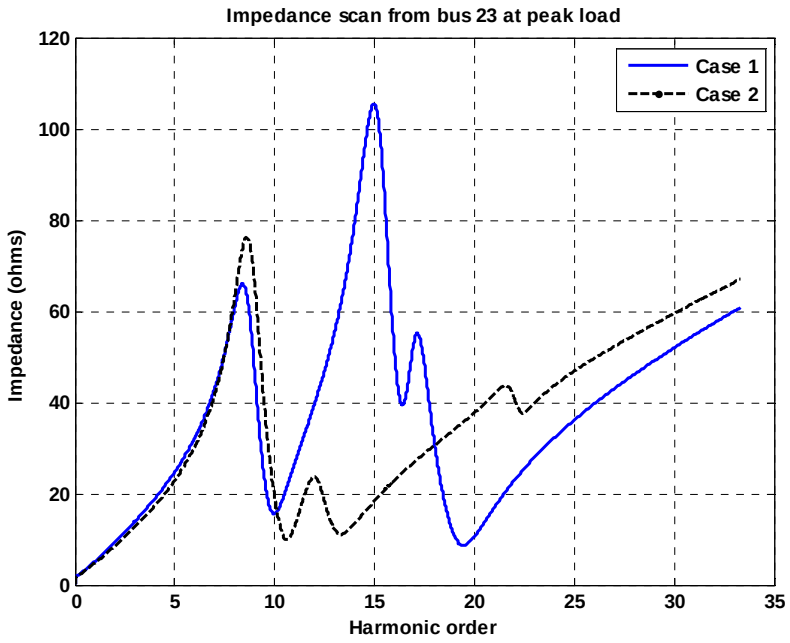

Figure 5- 11: Impedance scan from bus 23 to study the impact of DG units location on harmonic resonance

As resulted from Figures 5-10 and 5-11:

- The location of the DG unit affects the harmonic resonance, for example: when the DG unit of 6.6 MW is placed at bus 28 it shifts the second peak of resonance to lower harmonic order (as in Figure 5-10), however; the impact on bus 23 is minor.
- Due to the equivalent impedance that can be seen from both locations (as in Figure 5-2), the impact of the first peak is minor compared to the second and third peaks of the harmonic resonance.

5.6 Scenario 3: the impact of the load and line disconnection

The lines of the distribution system could be disconnected, either planned or unplanned. This disconnection can affect the equivalent impedance of the system and hence change the resonance frequency of the system. Therefore, this part tackles this issue by disconnecting line 24 of the system as an example. Figures 5-12 and 5-13 show the frequency scans at bus 23 and 40. Each figure compares the system resonance before and after the disconnection of line 24. Since there is a DG unit

located at the downstream of line 24 at bus 28, the resonance peaks decrease from three to two peaks. In both figures, the magnitude and harmonic order change due to the disconnection of line 24. The impact of this disconnection on harmonic resonance is different at each bus on the system depending on the locations of the buses. For example, the impact on bus 23 is different than bus 40. In bus 23, The magnitude of the second resonance decreases. However, in bus 40 the magnitude of this resonance increases. As a result, the disconnection of this line can have more impact on voltage stability at bus 40 than at bus 23.

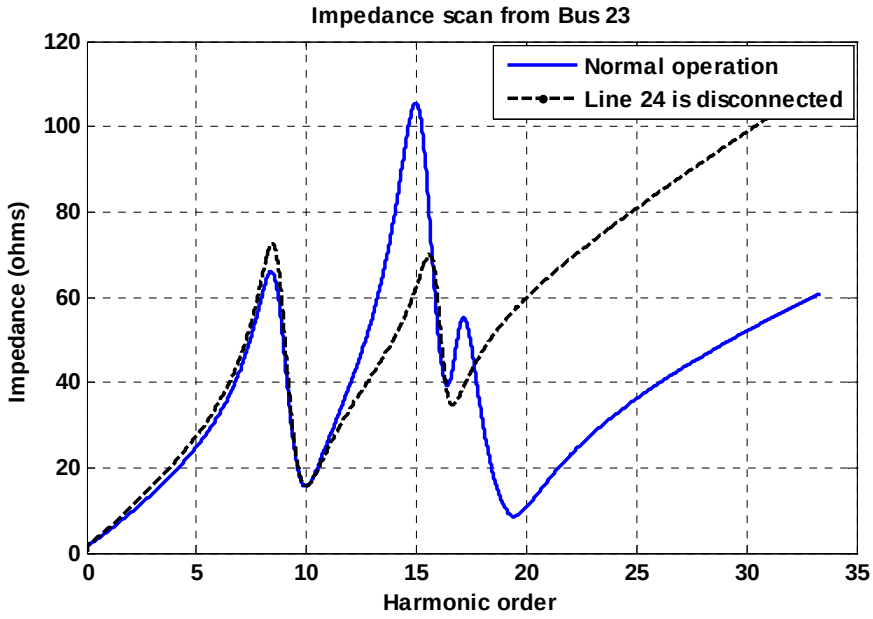

Figure 5- 12: Frequency scans from bus 23 before and after the disconnection of line 24

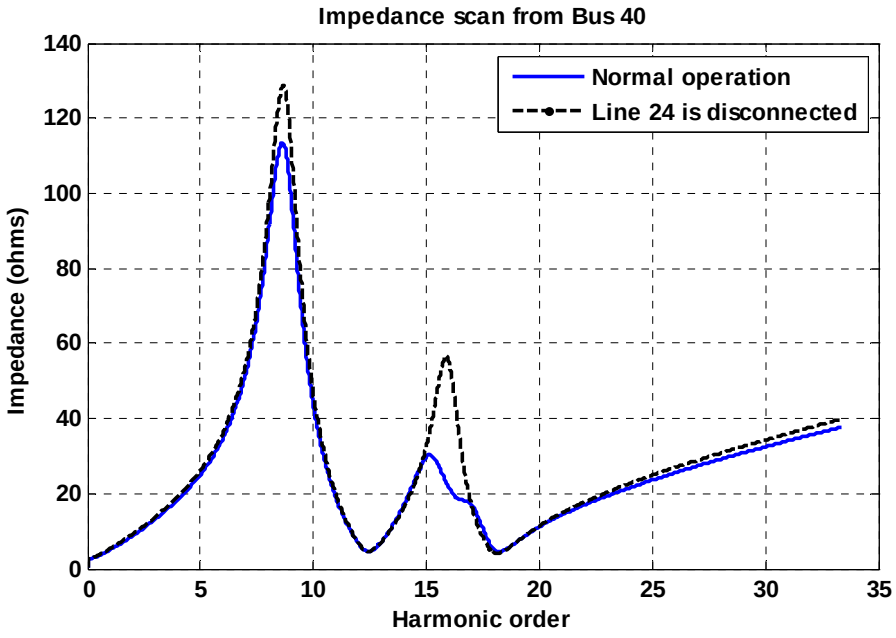

Figure 5- 13: Frequency scans from bus 40 before and after the disconnection of line 24

5.7 Scenario 4: the impact of the DG units disconnection

Like the system loads, DG units could be disconnected, either planned or unplanned. The disconnection of the DG units can affect the equivalent impedance of the system which can cause the harmonic resonance to shift from a harmonic order number to another. In this section, four DG units from bus 40 are disconnected. The system is left with 2.2 MW at bus 40 , 2.2 MW at bus 38, and 1.1 MW at bus 28. After the disconnection of the DG units, the reactive power compensator of the DG units (the capacitor bank see Figure 5-16) is assumed to take few seconds to minutes to change from stage to another due to the disconnection of the DG Units. The frequency scan results in Figures 5-14 and 5-15 depict the resonance before the capacitor switches to a new stage. The results show that the resonance peak is shifted to a lower harmonic order. The first resonance peak shifts from 9^{th} harmonic order to 7^{th} harmonic order. This shift can cause voltage stability problem if there is harmonic filter which is tuned to filter the 9^{th} harmonic. As a result, this shift will magnify the voltage due to the resonance at the 7^{th} harmonic order.

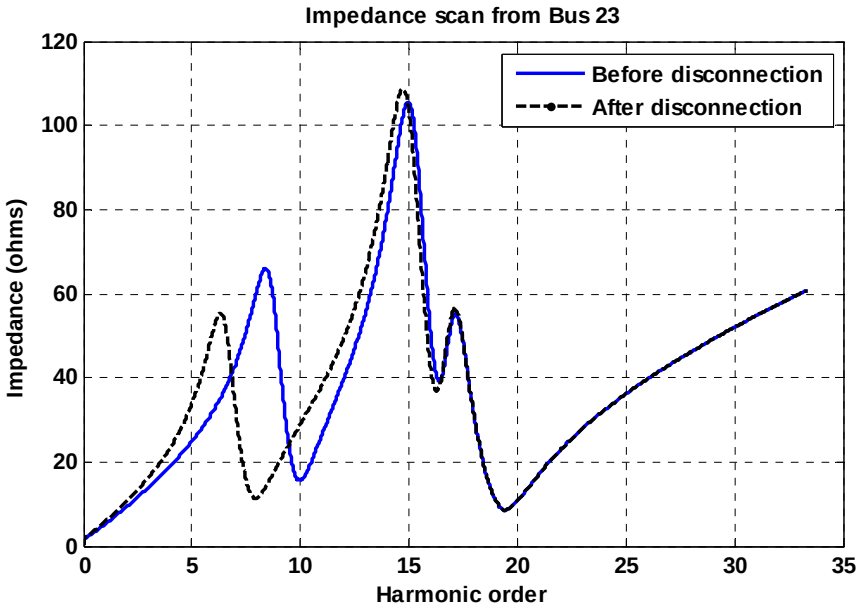

Figure 5-14: Frequency scans from bus 23 before and after the disconnection of 4 DG units from bus 40

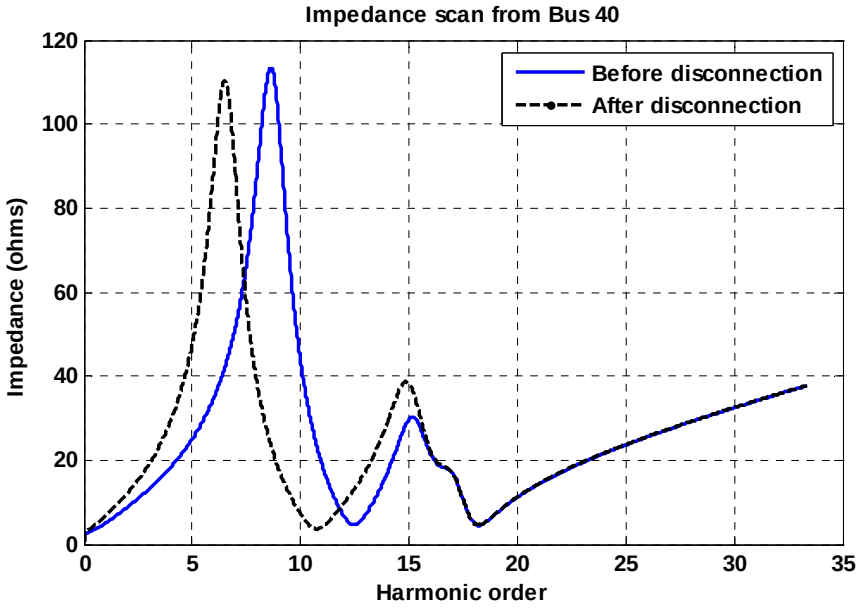

Figure 5- 15: Frequency scans from bus 40 before and after the disconnection of 4 DG units from bus 40

5.8 Scenario 5: the impact of the DG units arrangement

This part studied the impact of the capacitance of the cable due to the wind DG arrangement. Two cases are presented: case 1 assumes the DG units are operating without reactive power compensator such as Type C wind generators see [11], and case 2, the reactive power compensator is included such as Type A and B. Three configurations are conducted to study the impact of DG units arrangement:

1. Arranged in three rows and two columns (Figure 5-16).
2. Arranged in one row (Figure 5-17).
3. Arranged in one column (Figure 5-18).

The distance between the DG units of rows and columns are obtained from [58]. The DG units are assumed equal in size and type, and their ratings are 1.1 MVA. The rating of the DG units is given in [68].

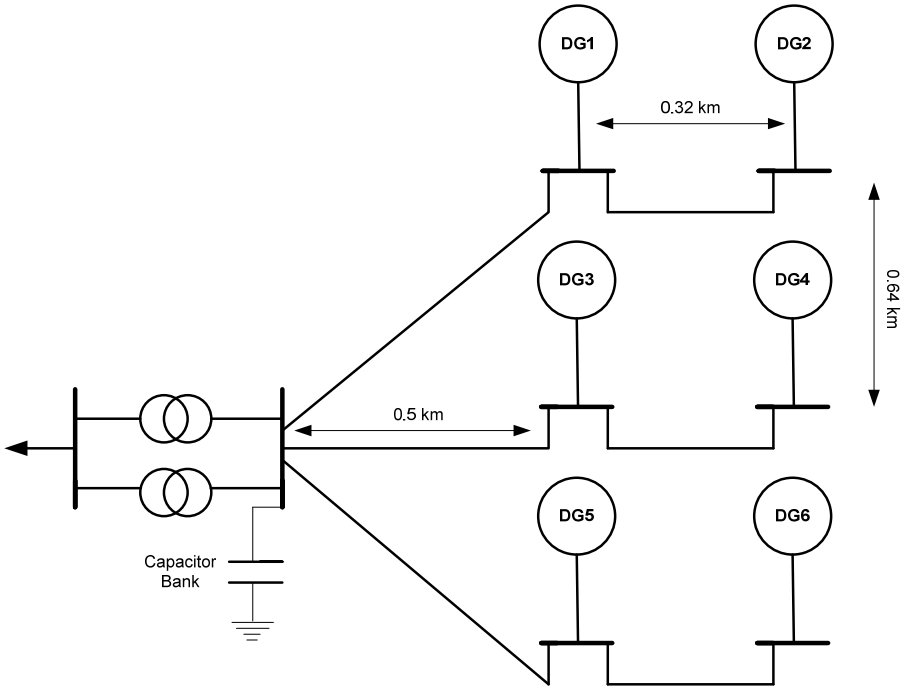

Figure 5- 16: Wind DG units arrangement 1

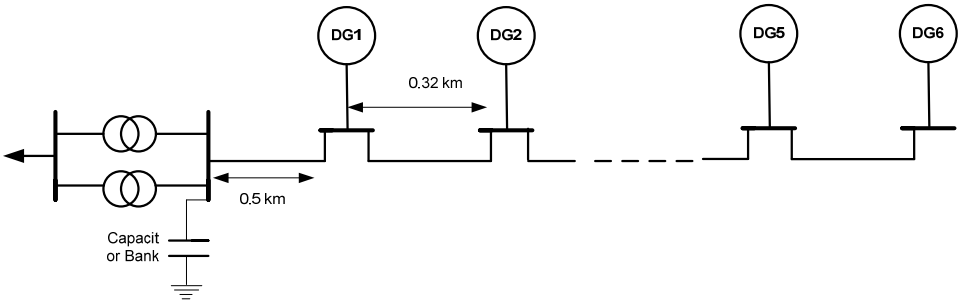

Figure 5- 17: Wind DG units arrangement 2.

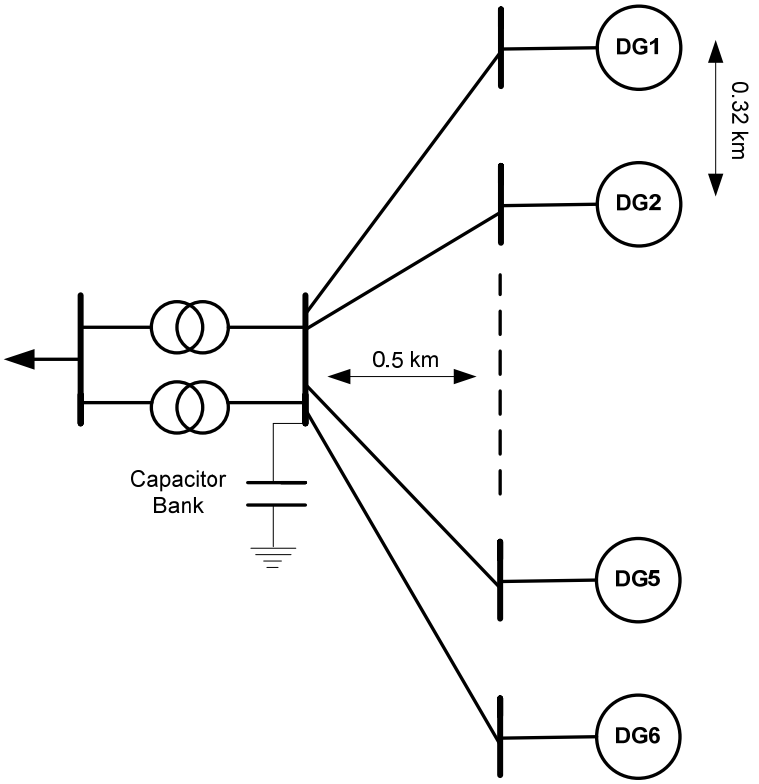

Figure 5- 18: Wind DG units arrangement 3

The impedance frequency results for case 1 and case 2 are shown in Figures 5-19 and 5-20 respectively. Figure 5-19 shows the impacts of wind DG units (type C) and Figure 5-20 shows the impact of Type A and B. Wind DG units (Type C) create harmonic resonace at higher harmonic order than wind DG units (type A and B), because in Type A and B, reactive power compensators are

installed at the terminal of these DG units. However, in type C, the partial scale frequency converter performs the reactive power. Thus, wind DG units of Type C do not require reactive power compensators at their terminal. As a result, Type A and B shifts the harmonic resonace to lower harmonic orders and could cause higher impacts to the voltage stability.

In these both figures, the DG units' arrangement can have an impact on both harmonic order and the resonance value. Arrangement 2, shifts the resonance toward higher harmonic order and arrangement 3 shifts the resonance toward lower harmonic order. Therefore, the arrangement of the DG units could improve or worsen the system resonance and harmonic distortion depending on the spectrum location of the system harmonic components and the system resonance. For example, arrangement 2, in Figure 5-20, shifts the resonance to harmonic order 9 which could match with 9^{th} harmonic component if there is any harmonic source injects this harmonic order in the system. Therefore, The arrangement of the wind DG units could cause the voltage stability problem due to shifts on harmonic resonance.

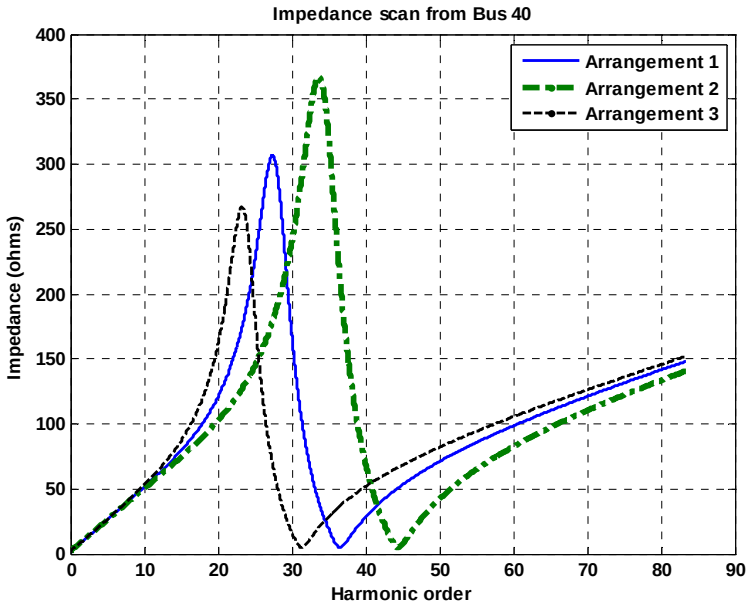

Figure 5- 19:Frequency scan from bus 40 with different arrangement of wind DG units (Type C)

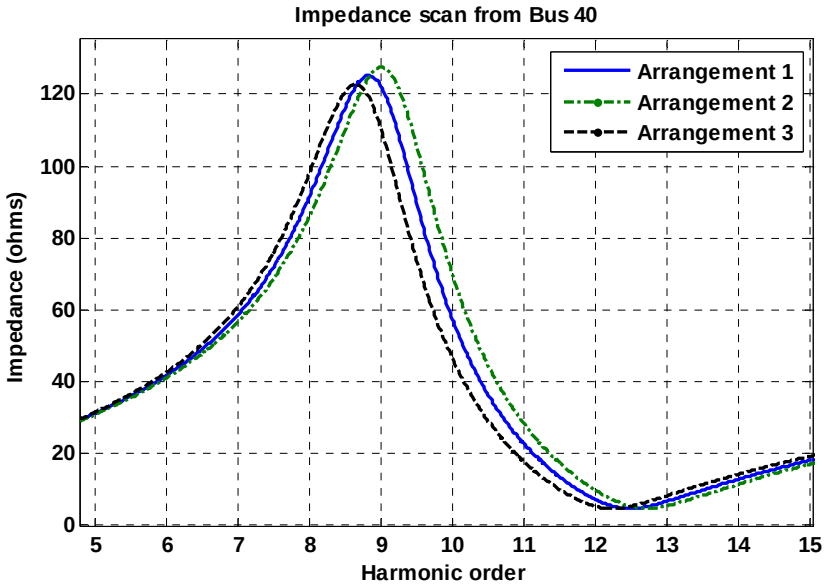

Figure 5- 20: Frequency scan from bus 40with different arrangement of wind DG units (Type A and B).

5.9 Discussion

In this chapter, the impact of the DG units on harmonic resonance has been studied. As a conclusion, the interfacing plays a role in the impact of the DG unit on harmonic resonance. The directly grid-connected DG units affect the harmonic resonance because the equivalent impedance of the rotary machine is included in the system equivalent circuit. In addition, the reactive power compensator, which is equal to one third of the DG unit rating, can have an impact on harmonic resonance. The location, the size, the number of the DG units, the changes of the load, and the disconnection of lines can impact on the harmonic resonance. Moreover, the wind DG units in wind farm are arranged in rows and columns with a distance between the rows and columns in order to decrease the wake effect. This distance is reflected on harmonic resonance due to the change of the underground cable capacitance.

Chapter 6
Conclusions and Contributions

6.1 Conclusions

This thesis tackled the voltage stability problem in distribution systems in the context of the integration of distributed generation of both types, renewable and non-renewable. This research focused on the voltage stability problem from different perspectives, namely the probabilistic nature of the load, DG units' generation, the small signal stability, and harmonic resonance. Chapter 1 introduced the problem of the impact of DG units on voltage stability. Chapter 2 provided background about the distributed generation types and system stability, and then provided a literature survey about the voltage stability problems in distribution system. Chapter 3 utilized the DG units to improve the voltage stability margin by proposing a method to locate and size the DG units. Chapter 4 modeled the system with the DG units to study impact of the DG units to the proximity to the voltage instability. Chapter 5 presented the impacts of the DG units on the harmonic resonance. The following points summarize the work presented in this thesis:

1. Placing DG units in distribution system can improve or worsen the voltage stability margin of the system. The DG units that consume reactive power can worsen the margin. However, the DG units which can be controlled to operate at unity power factor or leading power factor have the ability to improve the voltage stability margin of the system. For this reason, chapter 3 is presented to introduce a guide to utilize the DG units to improve the voltage stability margin. The proposed method tackled the probabilistic nature of the load demand and of the DG units which are fueled by renewable energy resources. The proposed method started by selecting candidate buses based on most sensitive buses to the voltage. An optimization technique was formulated to locate and size the DG units within the candidate buses. This formulation has considered the limits of distribution system such as voltage profile, feeder capacity, the penetration level and the maximum penetration at each bus. The proposed method is applied with different scenarios to consider different types of DG units such as renewable and non-renewable DG units. The method succeeded in placing and sizing the DG units based on their types and their probabilistic nature. Moreover, the study conducted and formulated two cases: the first case when the DG units operate at unity power factor, and the second when they are allowed to operate in a fixed

power factor mode (0.95 lagging to 0.95 leading). In addition this study concluded that when the DG units operate at unity power factor, they are recommended to be placed in the most sensitive voltage buses. However, if the utility allows operating the DG units between 0.95 lead and 0.95 lag, the reactive power during leading power factor could improve the voltage stability margin due to the greater sensitivity between $\Delta V/\Delta Q$ than $\Delta V/\Delta P$. Therefore, the DG units with higher rating might be placed in the upper stream of a radial distribution system in order to keep the system operating within the allowed limits of voltage and currents.

2. Proximity to voltage instability analysis using Small signal method with high penetration level of distributed generation is presented in chapter 4 of this thesis. This study can be considered as a continuous work to the results in chapter 3. It investigated the impacts of the DG to the proximity to voltage instability. The proximity to voltage stability is conducted by stressing the system incrementally until it becomes unstable, and at each operating point small-signal analysis and modal analysis are applied. This impact was studied based on the location, size, reactive power generation, and controller settings of the DG units. Furthermore, the impact of integrating multi-DG units into the system has been considered. This study concluded the following:
    - Location and size can affect the small signal stability and voltage stability of the system.
    - It is found that placing a DG unit that generates reactive power in lower stream buses can move the sensitive eigenvalues toward a stable area faster than if the DG is placed in upper stream, because $\Delta V/\Delta Q$ is more sensitive in low stream buses of a radial distribution system.
    - The setting of the DG controller parameters could affect the system stability due to the sensitivity of some eigenvalues to DG controller parameters. The eigenvalues could go to the unstable area before reaching the maximum voltage stability margin if the controller is not properly set.
    - It is recommended to place the higher DG ratings in the upper stream of the system, while the DG units with smaller ratings should be in the lower stream, in order to

move the eigenvalues of the system toward more stable locations and decrease the effects of $\Delta V/\Delta P$.

3. Harmonic resonance due to the integration of distributed generation is studied in chapter 5. This chapter investigates important issues related to the impact of the DG units on harmonic resonance, such as the change of the load demand, DG units' disconnections, and the arrangement of the DG units in a wind farm. These impacts were tackled in different scenarios. The reason for this investigation is that the harmonic resonance can have an impact on voltage stability, due to the high voltage in parallel resonance or due to the high current in series resonance. This study concluded that the directly gird-connected DG units affect the harmonic resonance more than inverter-based DG units, because the equivalent impedance of the rotary machine is included in the system equivalent circuit. In addition, the reactive power compensator which is equal to one third of the DG unit rating can have an impact on harmonic resonance. The location, size, number of the DG units, changes of the load and the disconnection of lines can impact on the harmonic resonance. Moreover, the wind DG units in wind farms are arranged in rows and columns with a distance between the rows and columns in order to decrease the wake effect. This distance is reflected on harmonic resonance due to the change in the underground cable capacitance.

6.2 Contributions

The main contributions of this thesis can be highlighted as follows:

1. Developed a method to place and size the DG units to improve the voltage stability margin. The method considers the probabilistic nature of the load and the DG units which are fueled by renewable energy sources.
2. Developed a study in proximity to voltage instability in a distribution system with integrated DG units. This study is conducted by using continuous power flow and small-signal analysis methods.
3. Investigated the impacts of the DG units on harmonic resonance.

Appendix A: Assessment of the Effect of Fixed-Speed Wind DG Units on Voltage Stability

A.1 Introduction

The objective of this study is to investigate the impact of wind DG units on system voltage stability using the static method. A fixed-speed wind turbine with a squirrel-cage induction generator (SCIG) will be used. Voltage stability will be explored using a power flow calculation in order to determine the P-V curve, as follows:

This study is arranged as follows:

- Section A.1: Brief description of the system used for the study
- Section A.2 : Description of the fixed-speed wind DG units and their impact on the voltage stability of the system
- Section A.3: Presentation of a simulation to illustrate the impact of these types of DG units on voltage stability

A.2 Description of the System Used for the Study

Figure A-1 shows the system used to investigate the impact of wind DG units on voltage stability. The configuration was extracted from the benchmark system of the IEEE Standard 399-1997 [85], and it has been modified in order to assess the voltage stability of the system. The system is composed of three feeders (13.8 kV) of a radial distribution system, which is connected to a system network of 69 kV. The 13.8kV substation busbar is radially connected to the network through the substation transformer and a 69 kV line. The 69 kV line consists of three buses (1-3) that represent the 69 kV system and 21 buses (4-24) that represent the 13.8 kV and 480 V distribution system. The DG units are connected to bus 5 and bus 15.

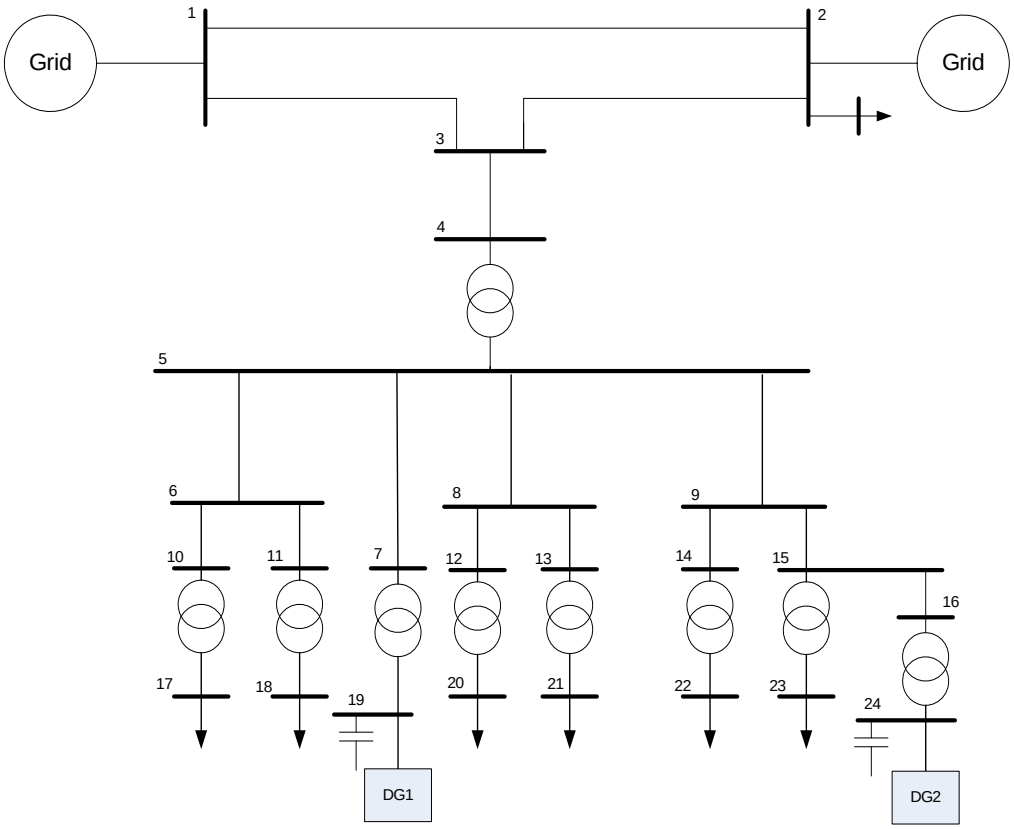

Figure A- 1: Single-line diagram of the system used for the study

The DG units are fixed-speed wind turbine generating units, and each unit is equipped with a squirrel-cage induction generator (SCIG). The input power of the wind is assumed to be constant power injected directly into the induction motor. The reactive power absorbed by the SCIGs is partly compensated by capacitor banks connected at each DG unit's low voltage buses. The capacitors are connected at bus 19 (400 kavr) and 24 (700 kavr), as shown in Figure A-1. Table A-1 provides the specifications of the squirrel-cage induction generator. Table A-2 shows the operation of the DG units.

Table A- 1: Squirrel-cage induction generator specifications

S_{base}= 3MVA , V_{base} = 575V			
R_s =0.004843 (p.u)	Xs = 0.1248 (p.u)	X_m = 6.77 (p.u)	F = 0.01 (p.u)
R_r =0.004377 (p.u)	X_r = 0.1248 (p.u)	H = 5.04 (s)	No. poles = 6

Table A- 2: Proposed scenarios

Scenario #	DG units	Location of the DG unit	Input mechanical power.
1	No DG unit	-	-
2	One DG unit	Bus 5	0.6 p.u
3	Two DG units	Bus 5 and 9	0.6 p.u "both units"
4	One DG unit	Bus 5	0.7 p.u

A.3 Fixed-Speed Wind Turbine Generating Units

A fixed-speed unit (Figure A-2) operates at a speed that is almost constant and may vary by only 2% – 4% from no load to full load [40]. This feature means that regardless of the wind speed, the wind turbine's rotor speed is fixed and is determined by the frequency of the supply grid, the gear ratio, and the design of the generator. The turbine is normally equipped with a squirrel-cage induction generator, which is connected directly to the grid, with a soft-starter and a capacitor bank for reducing reactive power compensation [4].

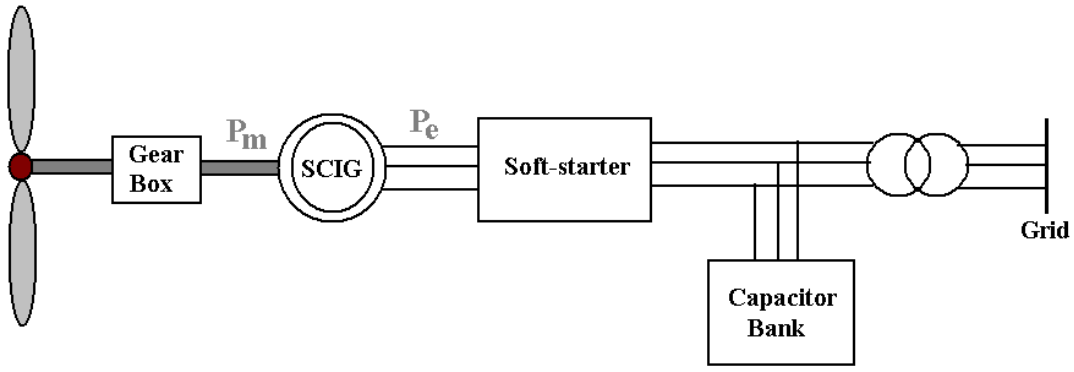

Figure A- 2: Fixed-speed wind turbine

A.3.1 Modeling of Squirrel-Cage Induction Generator

An induction generator consists of a stator and an armature winding (normally a squirrel-cage type) and is connected to the system via a transformer. The steady-state equivalent circuit of this generator is shown in Figure A-3.

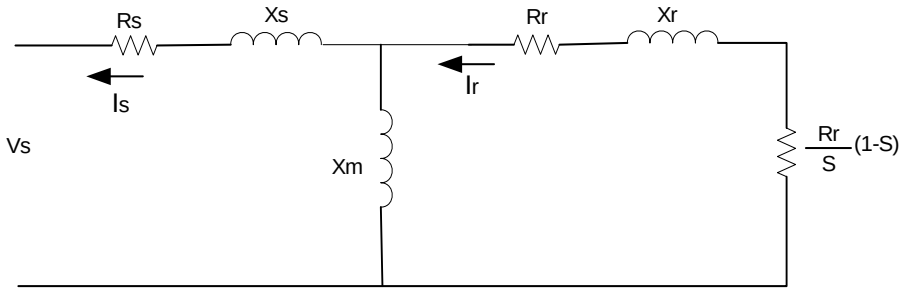

Figure A- 3: Induction generator equivalent circuit

The parameters shown in Figure A-3 are as follows:

V_s = per-phase terminal voltage

R_s = stator winding resistance

X_s = stator leakage reactance

X_m = stator magnetizing reactance

R_r = rotor resistance (referred to the stator)

X_r = per-phase rotor leakage reactance (referred to the stator)

S = slip, $S = \dfrac{n_s - n_m}{n_s}$

Where, n_m = the rotor speed;

n_s = is the synchronous speed;

S is negative for generator operation.

The equivalent circuit is usually simplified by either an approximate equivalent circuit or by using the Thevenin transform [46]. The approximate equivalent circuit is achieved by moving the magnetizing branch X_m to the terminal of the circuit. Therefore, I_r can be expressed as in Equation (A.1):

$$I_r = \frac{V_s}{(R_s + jX_s) + (\frac{R_r}{S} + jX_r)} \tag{A.1}$$

The induction generator delivers real power (P_e) to the network and absorbs reactive power (Q_e) from the network. P_e and $Q_e$can be derived by using the equivalent circuit

$$P_e = P_m - P_{loss} \tag{A.2}$$

Where,

P_{loss}= the stator and rotor losses, $P_{loss} = I_r^2[R_1 + R_2]$

P_m = input mechanical power, which can be expressed electrically by using the equivalent circuit or mechanically as a function of speed and torque, as follows:

$$P_m = T_m\omega_m = I_r^2[\frac{R_2}{S}(1-S)] \tag{A.3}$$

$$P_e = I_r^2[\frac{R_2}{S}(1-S)] - I_r^2[R_1 + R_2] = I_r^2[\frac{R_2}{S} + R_1] \tag{A.4}$$

$$Q_e = I_r^2(X_s + X_r) + \frac{V_s}{X_m} \qquad \text{(A.5)}$$

Both $P_e$and Q_e are functions of the terminal voltage V_s and the slip S.

A.3.2 Real and Reactive Power Characteristics of an Induction Generator

The operation of an induction generator can be described in terms of real and reactive power [46]. For example, the P-Q characteristics of the induction generator (3MVA: Table A-1) is depicted as in Figure A-4. This figure shows that as the generated power increases, the generator imports more reactive power from the system. At zero input power (P_m), the induction generator imports 480 kVar as the excitation reactive power (Figure A-5). As the P_m increases, the power generated increases and the DG unit imports more reactive power from the system, as shown in FigureA-4. The power factor (*pf*) therefore decreases as the power generated increases. To improve the *pf,* a power factor correction capacitor is installed at the generator terminal. The capacitor shifts the reactive power imported from the network to lower values. For example, when a 400 kVAR capacitor is connected at the terminal of the 3 MVA induction generator, the imported reactive power shifts down by 400 kVar, as shown in FigureA-4.

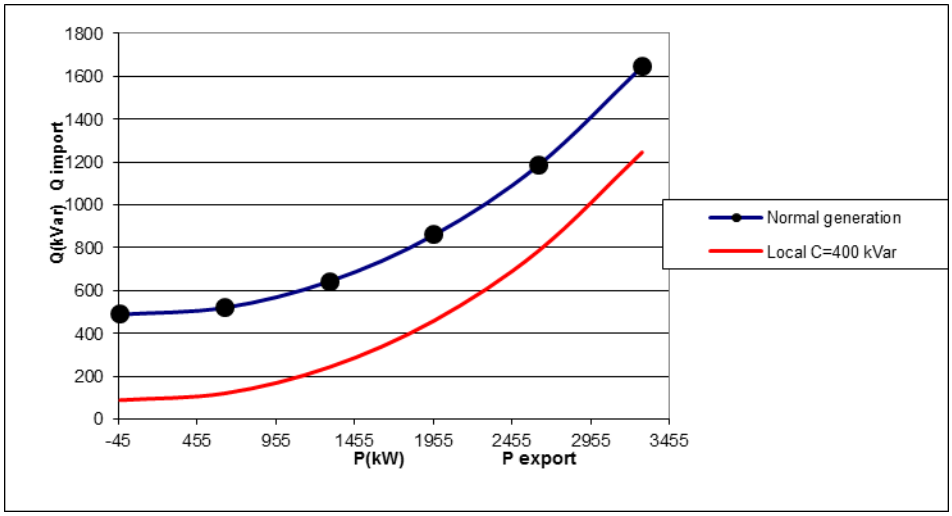

Figure A- 4: P-Q relation of an induction generator

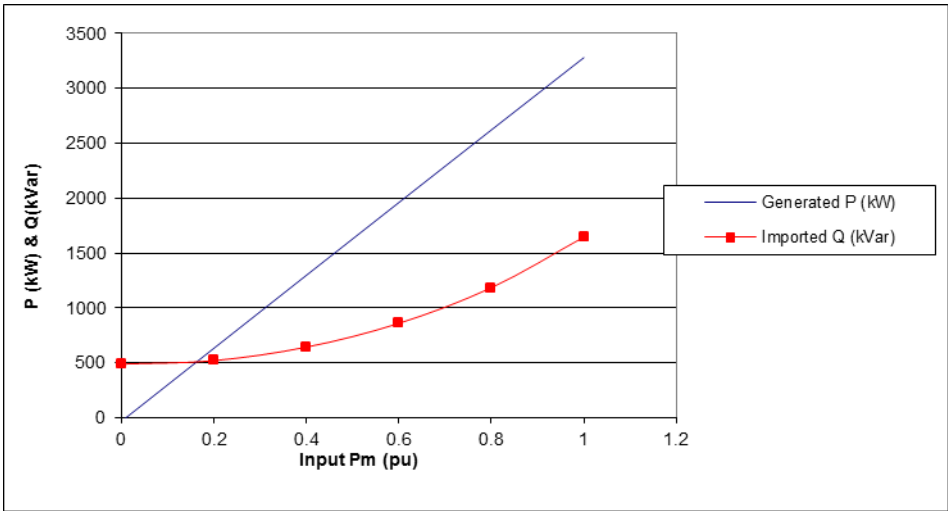

Figure A- 5:The relation between the P_m- (P&Q)

A.3.3 Impact of the Power Factor Capacitor on Voltage Stability

The capacitor delivers reactive power to the generator or to the network, depending on capacitor capacity and the voltage across its terminal as in equation (A.6). If the voltage decreases, the reactive power delivered by the capacitor decreases. For example, if the voltage drops by 10%, the reactive power delivered drops by 19%. However, as the voltage decreases, the reactive power demanded by the DG unit increases, as shown in Figure A-6. Therefore, in the case of a voltage drop due to a fault in the network system, the DG unit absorbs more reactive power and, at the same time, the capacitor delivers smaller reactive power. Consequently, the DG unit absorbs reactive power from the network, as shown in FigureA-6. This process might cause a problem with voltage stability.

$$Q_C = \frac{V_C^2}{X_C} \qquad \text{(A.6)}$$

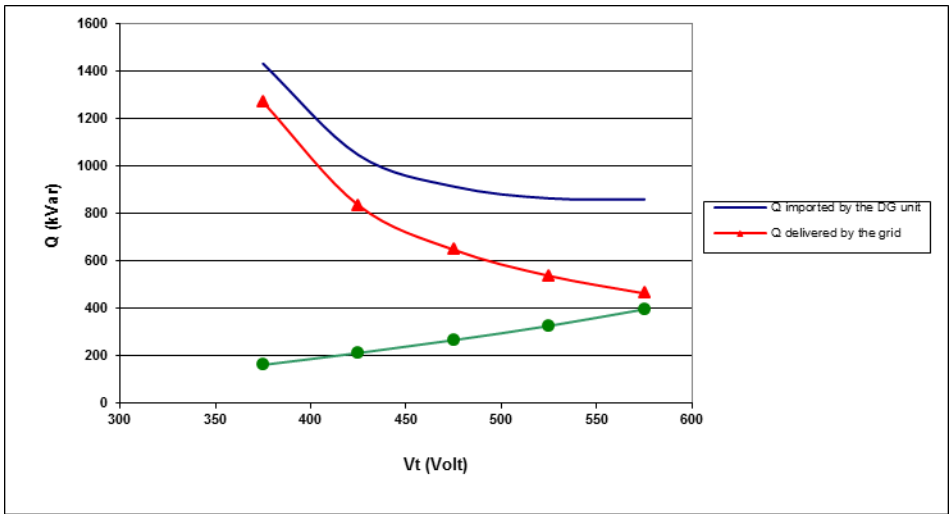

Figure A- 6: V-Q relation at the induction generator terminal and the local *pf* corrector

A.4 Impact of DG units on voltage stability

To investigate the impact of fixed-speed wind DG units on voltage stability, the MATLAB/SIMULINK software package has been used to develop a model of the system to be used for the study (Figure A-1). The investigation was conducted for the following proposed scenarios, as listed in Table A-2:

1. No DG units are installed in the distribution system network.
2. One DG unit is installed at bus 5 of the distribution system network.
3. Two DG units are installed in the system at buses 19 and 24.
4. One DG unit is installed at bus 19 of the distribution system network, with a wind speed different from that in scenario 2.

The Impact at Bus 4

Figure A-7 illustrates the P-V "nose curve" at bus 4. The curve depicts scenarios 1-3. It can be seen that this type of wind DG unit can have an impact on the voltage stability of the system. The power margin decreases as the penetration level of the DG units increases, and the critical point of maximum power delivered ($P_{critical}$) shifts to the left, as shown in Figure A-7. For example, at no DG, the maximum power delivered is 19.16 MW, but when one DG unit is installed at bus 19, the maximum power decreases to 17.13 MW. It then declines to 14.03 MW when the second DG unit is installed at bus 15.

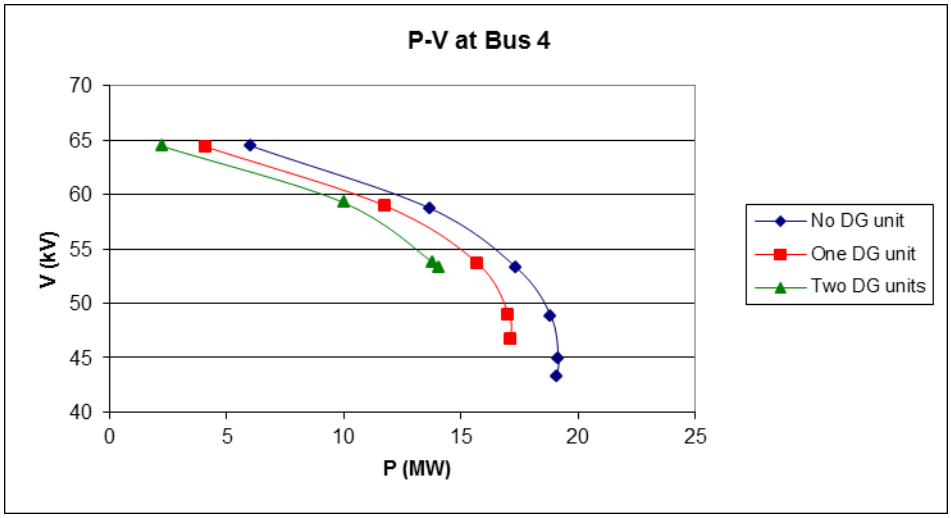

Figure A- 7: P-V curves at bus 4 for scenarios 1-3

Figure A-8 shows the relation between the real and reactive power at bus 4. As the real power demand increases, the reactive power demands increases. However, the DG units shift the reactive power demand to a higher level because the DG units absorb more reactive power.

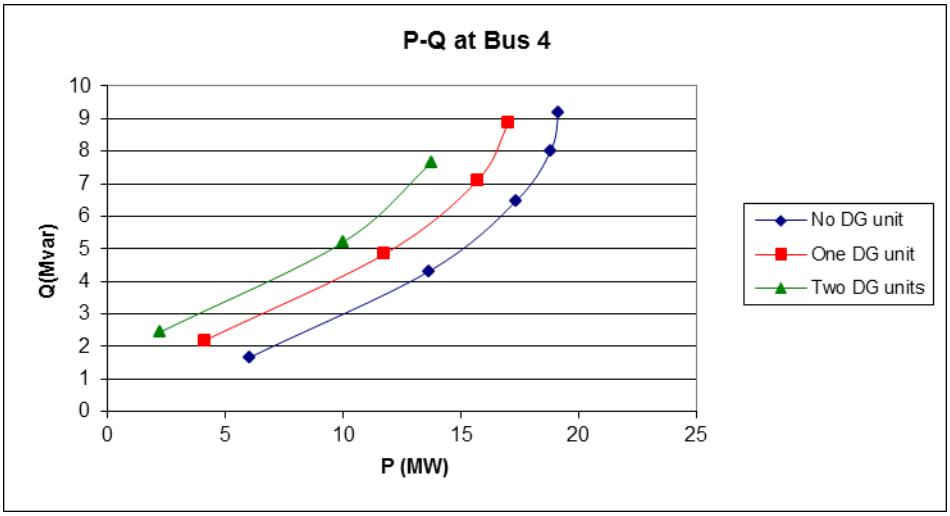

Figure A- 8: P-Q relations at bus 4 for scenarios 1-3

Appendix B: Renewable Energy DG Units

Tables A-3 and A-4 show the characteristics of the wind turbine and solar modules which are used in this study

Table A- 3: Wind turbine characteristics

Features	Wind Turbine
Rated power (MW)	1.1
Cut-in speed (m/s)	4
Rated speed (m/s)	14
Cut-out speed (m/s)	24

Table A- 4: Solar module characteristics

Features	
Watt peak (W)	75
Open circuit voltage (V)	21.98
Short circuit current (A)	5.32
Voltage at maximum power (V)	17.32
Current at maximum power (A)	4.76
Voltage temperature coefficient (mV/^{o}C)	14.4
Current temperature coefficient (mA/^{o}C)	1.22
Nominal cell operating temperature (^{o}C)	43

Appendix C: Impact of the DG Units' Number and their Locations on Harmonic Resonance

This study is proposed to study the impacts of the DG units' number and their locations on harmonic resonance. Table A- 5 reveals this study. A DG unit 1.1MW is installed at bus 40 and then increased to 6.6 MW as in cases 1 to 3. On the other hand 6.6 MW is divided into two buses (bus 40 and bus 28) as in case 4.

Table A- 5: Presents cases to study the impacts of the DG units' number and their locations on harmonic resonance.

Case #	DG units size	location
Case 1	1.1 MW	Bus 40
Case 2	2.2 MW	Bus 40
Case 3	6.6 MW	Bus 40
Case 4	3.3 MW and 3.3 MW	Bus 40 and 28

Figure A-9 shows the results of this study and the following comments can be noticed:

- As the DG number increases at the same bus, the harmonic resonance shifts to lower harmonic order.
- In cases 1 to 3, the DG units create one resonance peak because the compensator capacitors of each DG units are located near each other. However, if the DG units are located in 2 different buses (as in case 4), they create two resonance peaks because the compensator capacitors of each DG unit are located far from each other.

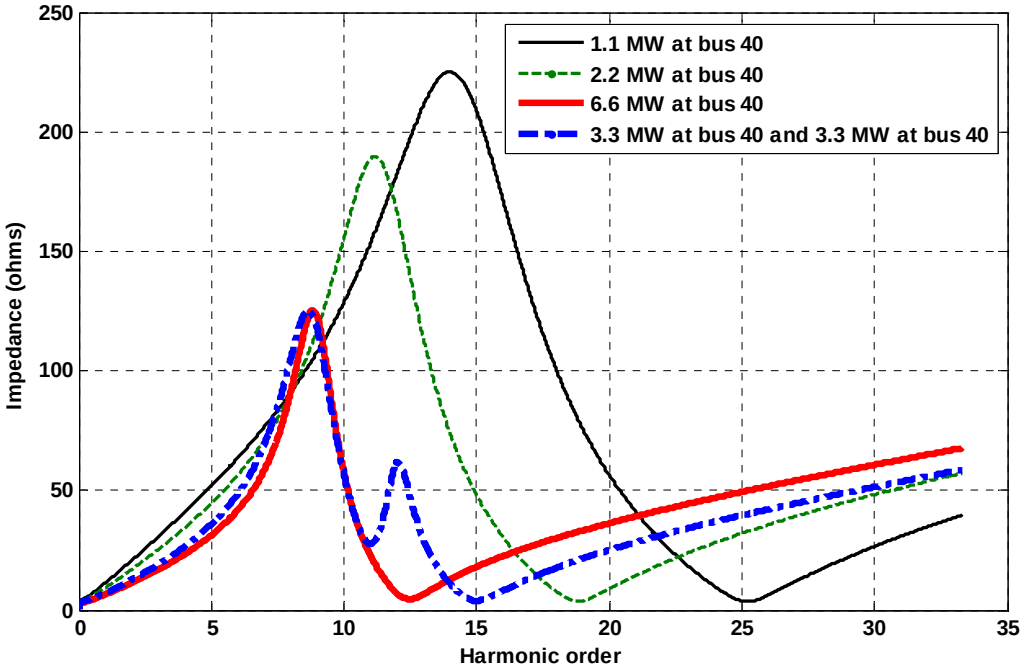

Figure A- 9: Impacts of the DG units' number and their locations on harmonic resonance

Bibliography

[1] H. H. Zeineldin, E. F. El-Saadany, and M. M. A. Salama, "Impact of DG interface control on islanding detection and nondetection zones," *IEEE Trans. Power Del.,* vol. 21, pp. 1515-1523, 2006.

[2] M. N. Marwali, J. Jin-Woo, and A. Keyhani, "Control of distributed generation systems - Part II: Load sharing control," *IEEE Trans. Power Electron.,* vol. 19, pp. 1551-1561, 2004.

[3] Y. Mohamed and E. F. El-Saadany, "Adaptive decentralized droop controller to preserve power sharing stability of paralleled inverters in distributed generation microgrids," *IEEE Trans. Power Electron.,* vol. 23, pp. 2806-2816, 2008.

[4] T. Ackermann, G. Andersson, and L. Sder, "Distributed generation: a definition," *Electr. Power Syst. Res.,* vol. 57, pp. 195-204, 2001.

[5] *IEEE Std 1547-2003,* "IEEE Standard for Interconnecting Distributed Resources with Electric Power Systems,", 2003.

[6] "CIGRE, International Council on Large Electricity Systems, http://www.cigre.org."

[7] "CIRED, International Conference of Electricity Distributors, http://www.cired.be."

[8] A. Chambers, B. Schnoor, and S. Hamilton, *Distributed Generation: A Nontechnical Guide*: PennWell, 2001.

[9] P. Dondi, D. Bayoumi, C. Haederli, D. Julian, and M. Suter, "Network integration of distributed power generation," *J. Power Sources,* vol. 106, pp. 1-9, 2002.

[10] Enercon, "http://www.enercon.de/en/_home.htm or http://www.metaefficient.com/news/new-record-worlds-largest-wind-turbine-7-megawatts.html," Enercon Energy for the World

[11] T. Ackermann, *Wind Power in Power Systems*: John Wiley & Sons, 2005.

[12] T. Markvart, *Solar Electricity*, 2nd ed.: John Wiley & Sons, 1997.

[13] K. Emery, "The rating of photovoltaic performance," *IEEE Trans. Electron Devices,* vol. 46, pp. 1928-1931, 1999.

[14] F. Blaabjerg, C. Zhe, and S. B. Kjaer, "Power electronics as efficient interface in dispersed power generation systems," *IEEE Trans. Power Electron.,* vol. 19, pp. 1184-1194, 2004.

[15] L. Li-Shiang, H. Wen-Chieh, F. Ya-Tsung, and C. Yu-An, "Novel grid-connected photovoltaic generation system," in *Electric Utility Deregulation and Restructuring and Power Technologies (DRPT)* 2008, pp. 2536-2541.

[16] T. Esram and P. L. Chapman, "Comparison of photovoltaic array maximum power point tracking techniques," *IEEE Trans. Energy Convers.,* vol. 22, pp. 439-449, 2007.

[17] D. M. Ali, "A simplified dynamic simulation model (prototype) for a stand-alone Polymer Electrolyte Membrane (PEM) fuel cell stack," in Proc. *International Middle-East*, *Power System Conference, MEPCON,* pp. 480-485, 2008.

[18] B. Cook, "Introduction to fuel cells and hydrogen technology," *Engineering Science and Education Journal,* vol. 11, pp. 205-216, 2002.

[19] M. A. Laughton, "Fuel cells," *Engineering Science and Education Journal,* vol. 11, pp. 7-16, 2002.

[20] R. C. Dugan and M. F. McGranaghan, *Electrical Power Systems Quality*, 2nd ed. New York: McGraw-Hill, 2002.

[21] P. Fu-Sheng and H. Shyh-Jier, "Design and operation of power converter for microturbine powered distributed generator with capacity expansion capability," *IEEE Trans. Energy Convers.,* vol. 23, pp. 110-118, 2008.

[22] M. Uzunoglu, O. Onar, M. Y. El-Sharkh, N. S. Sisworahardjo, A. Rahman, and M. S. Alam, "Parallel operation characteristics of PEM fuel cell and microturbine power plants," *J. Power Sources,* vol. 168, pp. 469-476, 2007.

[23] P. F. Ribeiro, B. K. Johnson, M. L. Crow, A. Arsoy, and Y. Liu, "Energy storage systems for advanced power applications," *Proceedings of the IEEE,* vol. 89, pp. 1744-1756, 2001.

[24] R. S. Alabri and E. F. El-Saadany, "Interfacing control of inverter-based DG units," in *Proc. International Conference on Communication, Computer and Power (ICCCP'09)*. SQU, Oman, 2009.

[25] N. Hadjsaid, J. F. Canard, and F. Dumas, "Dispersed generation impact on distribution networks," *IEEE Comput. Appl. Power,* vol. 12, pp. 22-28, 1999.

[26] T. K. Abdel-Galil, E. F. El-Saadany, and M. M. A. Salama, "Online tracking of voltage flicker utilizing energy operator and Hilbert transform," *IEEE Trans. Power Del.,* vol. 19, pp. 861-867, 2004.

[27] Y. M. Atwa and E. F. El-Saadany, "Probabilistic approach for optimal allocation of wind-based distributed generation in distribution systems," *IET Renew. Power Gener.,* vol. 5, pp. 79-88, 2011.

[28] H. E. Farag and E. F. El-Saadany, "Voltage regulation in distribution feeders with high DG penetration: From traditional to smart," in *Proc. IEEE PES General Meeting*, 2011, pp.

[29] R. S. A. Abri, E. F. El-Saadany, and Y. M. Atwa, "Distributed Generation placement and sizing method to improve the voltage stability margin in a distribution system," in *Proc. Electric Power and Energy Conversion Systems (EPECS)*. 2011.

[30] P. Kundur, N. J. Balu, and M. G. Lauby, *Power System Stability and Control*: McGraw-Hill Professional, 1994.

[31] J. J. Grainger and W. D. Stevenson, *Power System Analysis*: McGraw-Hill Inc., 1968.

[32] P. Kundur, J. Paserba, V. Ajjarapu, G. Andersson, A. Bose, C. Canizares, N. Hatziargyriou, D. Hill, A. Stankovic, C. Taylor, T. Van Cutsem, and V. Vittal, "Definition and classification of power system stability IEEE/CIGRE joint task force on stability terms and definitions," *IEEE Trans. Power Syst.,* vol. 19, pp. 1387-1401, 2004.

[33] CIGRE, "CIGRE Technical Brochure on Modeling New Forms of Generation and Storage," CIGRE TF 38.01.10, November 2000.

[34] N. Jayawarna, X. Wu, Y. Zhang, N. Jenkins, and M. Barnes, "Stability of a MicroGrid," in *IET International Conference, Power Electronics, Machines and Drives, 2006.* , 2006, pp. 316-320.

[35] M. Reza, P. H. Schavemaker, J. G. Slootweg, W. L. A. K. W. L. Kling, and L. A. v. d. S. L. van der Sluis, "Impacts of distributed generation penetration levels on power systems transient stability," in *Proc. IEEE PES General Meeting*, Vol.2, pp. 2150-2155, 2004.

[36] J. G. Slootweg and W. L. Kling, "Impacts of distributed generation on power system transient stability," in *Proc. IEEE PES Summer Meeting*, vol.2, pp. 862-867, 2002.

[37] F. Katiraei, M. R. Iravani, and P. W. Lehn, "Micro-grid autonomous operation during and subsequent to islanding process," *IEEE Trans. Power Del.,* vol. 20, pp. 248-257, 2005.

[38] C. Hsiao-Dong and R. Jean-Jumeau, "Toward a practical performance index for predicting voltage collapse in electric power systems," *IEEE Trans. Power Syst.,* vol. 10, pp. 584-592, 1995.

[39] C. A. Cañizares, *Voltage Stability Assessment: Concepts, Practices and Tools,* IEEE/FES Power System Stability Subcommittee Aug. 2002.

[40] J. Machowski, J. W. Bialek, and J. R. Bumby, *Power System Dynamics: Stability and Control* Second ed. John Wiley & Sons, 2008.

[41] L. L. Grigsby, *The electric power engineering handbook*. Boca Raton, FL: CRC Press/IEEE Press, 2001.

[42] R. B. Prada and L. J. Souza, "Voltage stability and thermal limit: constraints on the maximum loading of electrical energy distribution feeders," *in Proc. IEEE Generation, Transmission and Distribution,* vol. 145, pp. 573-577, 1998.

[43] C. Haiyan, C. Jinfu, S. Dongyuan, and D. Xianzhong, "Power flow study and voltage stability analysis for distribution systems with distributed generation," in *Proc. IEEE PES General Meeting*, p. 8, 2006 .

[44] W. Freitas, L. C. P. DaSilva, and A. Morelato, "Small-disturbance voltage stability of distribution systems with induction generators," *IEEE Trans. Power Syst.,* vol. 20, pp. 1653-1654, 2005.

[45] W. Freitas, J. C. M. Vieira, L. C. P. da Suva, C. M. Affonso, and A. Morelato, "Long-term voltage stability of distribution systems with induction generators," in *Proc. IEEE PES General Meeting*, Vol. 3, pp. 2910-2913, 2005.

[46] N. Jenkins, R. Allan, P. Crossley, D. Kirschen, and a. G. Strb, *Embedded Generation*: IET, 2000.

[47] W. Freitas, A. Morelato, X. Wilsun, and F. Sato, "Impacts of AC Generators and DSTATCOM devices on the dynamic performance of distribution systems," *IEEE Trans. Power Del.,* vol. 20, pp. 1493-1501, 2005.

[48] R. R. Londero, C. M. Affonso, and M. V. A. Nunes, "Impact of distributed generation in steady state, voltage and transient stability — Real case," in *Proc. IEEE Power Tech, in Bucharest*, pp. 1-6, 2009.

[49] S. Kotamarty, S. Khushalani, and N. Schulz, "Impact of distributed generation on distribution contingency analysis," *Electr. Power Syst. Res.,* vol. 78, pp. 1537-1545, 2008.

[50] N. G. A. Hemdan and M. Kurrat, "Distributed generation location and capacity effect on voltage stability of distribution networks," in *Proc. IEEE Annual Conference*, pp. 1-5, 2008.

[51] H. Hedayati, S. A. Nabaviniaki, and A. Akbarimajd, "A method for placement of DG units in distribution networks," *IEEE Trans. Power Del.,* vol. 23, pp. 1620-1628, 2008.

[52] M. Alonso and H. Amaris, "Voltage stability in distribution networks with DG," in *Proc. IEEE PowerTech, in Bucharest*, pp. 1-6, 2009.

[53] N. L. Soultanis, S. A. Papathanasiou, and N. D. Hatziargyriou, "A stability algorithm for the dynamic analysis of inverter dominated unbalanced LV microgrids," *IEEE Trans. Power Syst.,* vol. 22, pp. 294-304, 2007.

[54] C. A. Canizares and F. L. Alvarado, "Point of collapse and continuation methods for large AC/DC systems," *IEEE Trans. Power Syst.,* vol. 8, pp. 1-8, 1993.

[55] N. Pogaku, M. Prodanovic, and T. C. Green, "Modeling, analysis and testing of autonomous operation of an inverter-based microgrid," *IEEE Trans. Power Electron.,* vol. 22, pp. 613-625, 2007.

[56] F. Katiraei, M. R. Iravani, and P. W. Lehn, "Small-signal dynamic model of a micro-grid including conventional and electronically interfaced distributed resources," *IET Gener. Transm. Distrib.,* vol. 1, pp. 369-378, 2007.

[57] F. Katiraei and M. R. Iravani, "Power management strategies for a microgrid with multiple distributed generation units," *IEEE Trans. Power Syst.,* vol. 21, pp. 1821-1831, 2006.

[58] Z. Ruimin, M. H. J. Bollen, and Z. Jin, "Harmonic resonances due to a grid-connected wind farm," in proc. *International Conference in Harmonics and Quality of Power* , pp. 1-7, 2010.

[59] G. J. Wakileh, *Power systems harmonics : fundamentals, analysis, and filter design*. Berlin ; New York: Springer, 2001.

[60] J. J. Mesas and L. Sainz, "Stochastic assessment of distribution system resonance frequencies with capacitors or shunt filters," *Electr. Power Syst. Res.,* vol. 81, pp. 35-42, 2010.

[61] T. E. Grebe, "Application of distribution system capacitor banks and their impact on power quality," *IEEE Trans. Ind. Appl.,* vol. 32, pp. 714-719, 1996.

[62] S. A. Papathanassiou and M. P. Papadopoulos, "Harmonic analysis in a power system with wind generation," *IEEE Trans. Power Del.,* vol. 21, pp. 2006-2016, 2006.

[63] D. Patel, R. K. Varma, R. Seethapathy, and M. Dang, "Impact of wind turbine generators on network resonance and harmonic distortion," in proc. *Canadian Conference, Electrical and Computer Engineering*, pp. 1-6, 2010.

[64] R. A. Walling, R. Saint, R. C. Dugan, J. Burke, and L. A. Kojovic, "Summary of Distributed Resources Impact on Power Delivery Systems," *IEEE Trans. Power Del.,* vol. 23, pp. 1636-1644, 2008.

[65] H. H. Zeineldin, E. F. El-Saadany, and M. M. A. Salama, "Distributed generation micro-grid operation: control and protection," in *Power Systems Conference: Advanced Metering, Protection, Control, Communication, and Distributed Resources*, pp. 105-111, 2006.

[66] T. Ackermann, *Wind Power in Power Systems*. Chichester, West Sussex, England ; Hoboken, John Wiley: NJ, 2005.

[67] "Ontario Power Authority , http://www.powerauthority.on.ca/."

[68] Y. M. Atwa, E. F. El-Saadany, M. M. A. Salama, and R. Seethapathy, "Optimal renewable resources mix for distribution system energy loss minimization," *IEEE Trans. Power Syst.,* vol. 25, pp. 360-370, 2010.

[69] C. Grigg, P. Wong, P. Albrecht, R. Allan, M. Bhavaraju, R. Billinton, Q. Chen, C. Fong, S. Haddad, S. Kuruganty, W. Li, R. Mukerji, D. Patton, N. Rau, D. Reppen, A. Schneider, M. Shahidehpour, and C. Singh, "The IEEE Reliability Test System-1996. A report prepared by the Reliability Test System Task Force of the Application of Probability Methods Subcommittee," *IEEE Trans. Power Syst.,* vol. 14, pp. 1010-1020, 1999.

[70] Y. M. Atwa, E. F. El-Saadany, M. Salama, and R. Seethapathy, "Distribution system loss minimization using optimal DG mix," in *Proc. IEEE PES General Meeting*, 2009.

[71] Z. M. Salameh, B. S. Borowy, and A. R. A. Amin, "Photovoltaic module-site matching based on the capacity factors," *IEEE Trans. Energy Convers.,* vol. 10, pp. 326-332, 1995.

[72] M. H. Albadi and E. F. El-Saadany, "Novel method for estimating the CF of variable speed wind turbines," in *Proc. IEEE PES General Meeting*, 2009.

[73] M. H. Albadi and E. F. El-Saadany, "Wind turbines capacity factor modeling- a novel Approach," *IEEE Trans. Power Syst.,* vol. 24, pp. 1637-1638, 2009.

[74] A. M. Borbely and J. F. Kreider, *Distributed Generation : The Power Paradigm For The New Millennium*. Boca Raton: CRC Press, 2001.

[75] P. Chiradeja and R. Ramakumar, "An approach to quantify the technical benefits of distributed generation," *IEEE Trans. Energy Convers.,* vol. 19, pp. 764-773, 2004.

[76] J. M. Uudrill, "Dynamic stability calculations for an arbitrary number of interconnected synchronous machines," *IEEE Trans. Power App. Syst,* vol. 87, pp. 835-844, 1968.

[77] M. Prodanovi, "Power quality and control aspects of parallel connected inverters in distributed generation." vol. Ph.D. dissertation, University of London, UK, 2004.

[78] Y. A.-R. I. Mohamed, "New control algorithms for the distributed generation interface in grid-connected and micro-grid systems." Ph.D. dissertation, University of Waterloo, Canada, 2009.

[79] K. Jalili and S. Bernet, "Design of LCL Filters of Active-Front-End Two-Level Voltage-Source Converters," *IEEE Trans. Ind. Electron.,* vol. 56, pp. 1674-1689, 2009.

[80] J. H. R. Enslin, W. T. J. Hulshorst, A. M. S. Atmadji, P. J. M. Heskes, A. Kotsopoulos, J. F. G. Cobben, and P. Van der Sluijs, "Harmonic interaction between large numbers of

photovoltaic inverters and the distribution network," in *Proc. IEEE Power Tech Conference, in Bologna*, Vol.3, p. 6 , 2003.

[81] A. Xin, L. Zhili, and C. Mingyong, "A novel assessment method for harmonic environment in Microgrid," in proc. *International Conference, Critical Infrastructure,* , pp. 1-7, 2010.

[82] W. Xu, "Status and future directions of power system harmonic analysis," in *Proc. IEEE PES General Meeting*, Vol. 2, p. 1184, 2003.

[83] Y. Tang and A. A. Mahmoud, "Evaluation and reduction of harmonic distortion in power systems," *Electr. Power Syst. Res.,* vol. 17, pp. 41-48, 1989.

[84] Y. A. R. I. Mohamed, "Mitigation of converter-grid resonance, grid-induced distortion, and parametric instabilities in converter-based distributed generation," *IEEE Trans. Power Electron.,* vol. 26, pp. 983-996, 2011.

[85] *IEEE Std 399-1997,* "IEEE Recommended Practice for Industrial and Commercial Power Systems Analysis", 1998.